National Park Service
Cooperative Agreement # H1200040001

HYDROLOGY AND GEOMORPHOLOGY OF THE SNAKE RIVER IN GRAND TETON NATIONAL PARK, WYOMING

FINAL REPORT

by

Nicholas C. Nelson and John C. Schmidt

Department of Watershed Sciences
Utah State University
Logan, Utah

2007

ABSTRACT

Hydrology and Geomorphology of the Snake River,

Grand Teton National Park, Wyoming

The influence of significant tributaries that join the Snake River within 10 km of Jackson Lake Dam (JLD) mitigate some impacts resulting from nearly 100 years of flow regulation in Grand Teton National Park. I analyzed measured and estimated unregulated flow data for all segments of the study area by accounting for tributary flows. The magnitude of the 2-yr recurrence flood immediately downstream from JLD decreased 45% since 1958 relative to estimated unregulated flows, whereas that downstream from Buffalo Fork, the largest tributary, decreased 36%.

There has been no long-term progressive geomorphic change on the Snake River resulting from dam regulation. I mapped the bankfull channel on four series of aerial photographs taken in 1945, 1969, 1990/1991, and 2002 and analyzed channel change in a geographic information system. Periods of low-magnitude floods (1945 to 1969) resulted in widespread deposition whereas periods of high-magnitude floods (1969 to 1990/1991 and 1990/1991 to 2002) resulted in widespread erosion; channels narrowed and widened by as much as 31%.

I mapped three distinct deposits within the Holocene alluvial valley. The lower floodplain covers 3.5% of the mapped area in the form of abandoned channel and inset, channel-margin facies and has inundating recurrence intervals of one to two years. The upper floodplain covers 36% of the mapped area, is composed of abandoned channels and bars, is higher in elevation than the lower floodplain, and is inundated by floods with recurrence intervals greater than 10 years. The lowest Holocene terrace covers 35% of the mapped area and is approximately 1 m higher in elevation than the upper floodplain. Though the lowest terrace has not been inundated or built since 1945, the two floodplain deposits have been developing since before 1945.

Flood magnitudes have decreased throughout the study area as a result of regulation, but these decreases are mitigated downstream from tributaries. Dam operations have not resulted in long-term progressive channel change or the development and abandonment of floodplain deposits. However, channel change is now dependant on the frequency of high-magnitude floods, and the frequency with which the two floodplains are inundated has been reduced.

(126 pages)

LIST OF TABLES

Chapter 2

Chapter 3

Table Page

LIST OF FIGURES

Chapter 2

Chapter 3

CONTENTS

APPENDICES

CHAPTER 1

INTRODUCTION

The Snake River in Grand Teton National Park (GTNP) is a steep, gravel-bed river that alternates between single-thread channels where the valley is narrow and multi-thread channels where the valley is wide. The Snake River flows for more than 43 km from Jackson Lake Dam (JLD) to Moose and five tributaries contribute to its watershed: Pacific Creek and Buffalo Fork join within 10 km of JLD, Spread Creek joins at 16 km downstream from JLD, Cottonwood Creek at 40 km, and Ditch Creek at 42 km.

JLD was originally built in 1908 and rebuilt to its current size and structure in 1916, raising the water level of Jackson Lake, a pre-existing lake formed by Pleistocene moraines and glacial scour (Love et al., 2003). Regulation of JLD resulted in a change in flow regime, but no change to the sediment flux, because Jackson Lake historically acted as a sediment trap. One of the changes to the flow regime was a decrease in flood magnitudes. Decreased flood magnitudes and no change in the sediment supply necessarily results in sediment surplus downstream from tributaries and other sediment inputs, but the degree of this surplus is unknown. The water stored by JLD served the irrigation needs of Idaho from 1916 to 1958. In 1958, Palisades Dam was built on the Snake River downstream in Idaho and became the primary storage facility for irrigation. The resultant increased flexibility in the timing and magnitude of releases at JLD caused a substantial flow regime change following 1958.

The impacts of dam regulation on single-thread, fine-grained rivers are well documented (Williams and Wolman, 1984; Andrews, 1986; Everitt, 1993; Schmidt et al., 1995; Grams and Schmidt, 2002, 2005), whereas those on multi-thread, gravel-bed rivers have received relatively little attention (Johnson, 1994, 1998; Surian, 1999). The primary objective of this study was to identify and characterize geomorphic changes resulting from changes in the regulated flow regime along a braided, gravel-bed river in sediment surplus.

Chapter 2 focuses on the analysis of flow data, channel change based on four series of aerial photographs, and the mobility of the channel bed. I analyzed measured and estimated unregulated flow data for the Snake River below JLD and measured data for Pacific Creek, Buffalo Fork, and the Snake River at Moose to describe the flow regime for the entire study area. I mapped the bankfull channel on aerial photographs taken in 1945, 1969, 1990/1991, and 2002 and analyzed changes in channel width and braid index for 19 reaches. By overlaying these maps, I determined areas of erosion and deposition and calculated the channel activity and net channel change between photograph series in each reach. Tracer rocks were placed at five locations in the Snake River channel to evaluate the ability of the current flow regime to mobilize the bed.

One paradigm of geomorphology is that the bankfull discharge is exceeded relatively frequently with recurrence intervals of approximately one to two years (Wolman and Leopold, 1957; Wolman and Miller, 1960). Though this may be the case for some river systems, the recurrence intervals of bankfull discharges have also been shown to be highly variable (Pickup and Warner, 1976; Williams, 1978; Nash, 1994). Braided rivers are complex systems that may have multiple floodplain levels with different inundation discharges (Williams and Rust, 1969). Floodplains along braided rivers are built by the lateral accretion of point bars, vertical accretion of abandoned channels and bars, and incision of the main channel (Miall, 1977; Reinfelds and Nanson, 1993; Brierley and Fryirs, 2005).

Chapter 3 focuses on identifying and describing two distinct floodplains and a low terrace. I mapped the extent of these three deposits, surveyed cross-sections of the channel and these deposits, and developed one-dimensional flow models to determine the flows necessary to inundate each deposit. I compared the magnitude of these flows with the measured and estimated unregulated flow regimes to determine their recurrence intervals and periods of inundation. I also overlaid the map of the alluvial deposits with the channel change maps to evaluate the style of deposition and determine the time period in which each deposit formed.

REFERENCES

Andrews, E.D., 1986. Downstream Effects of Flaming Gorge Reservoir on the Green River, Colorado and Utah. Geological Society of America Bulletin 97, 1012-1023.

Brierley, G.J. and Fryiers, K.A., 2005. Geomorphology and River Management: Applications of the River Styles Framework. Blackwell Publishing, Malden, MA. 398pp.

Everitt, B., 1993. Channel Responses to Declining Flow on the Rio Grande between Ft. Quitman and Presidio, Texas. Geomorphology 6, 225-242.

Grams, P.E. and Schmidt, J.C., 2002. Streamflow Regulation and Multi-Level Flood Plain Formation: Channel Narrowing on the Aggrading Green River in the Eastern Uinta Mountains, Colorado and Utah. Geomorphology 44, 337-360.

Grams, P.E. and Schmidt, J.C., 2005. Equilibrium or Indeterminate? Where Sediment Budgets Fail: Sediment Mass Balance and Adjustment of Channel Form, Green River Downstream from Flaming Gorge Dam, Utah and Colorado. Geomorphology 71, 156-181.

Johnson, W.C., 1994. Woodland Expansion in the Platte River, Nebraska: Patterns and Causes. Ecological Monographs 64 (1), 45-84.

Johnson, W.C., 1998. Adjustment of Riparian Vegetation to River Regulation in the Great Plains, USA. Wetlands 18 (4) 608-618.

Love, D.L., Reed, J.C., and Pierce, K.L., 2003. Creation of the Teton Landscape: A Geological Chronicle of Jackson Hole and The Teton Range. Grand Teton Natural History Association. Moose, WY. 132 pp.

Miall, A.D., 1977. A Review of the Braided-River Depositional Environment. Earth-Science Reviews 13, 1-62.

Nash, D.B., 1994. Effective Sediment-Transporting Discharge from Magnitude-Frequency Analysis. The Journal of Geology 102, 79-95.

Pickup, G. and Warner, R.F., 1976. Effects of Hydrologic Regime on Magnitude and Frequency of Dominant Discharge. Journal of Hydrology 29, 51-75.

Reinfelds, I. and Nanson, G., 1993. Formation of Braided River Floodplains, Waimakariri River, New Zealand. Sedimentology 40, 1113-1127.

Schmidt, J.C., Grams, P.E., and Webb, R.H., 1995. Comparison of the Magnitude of Erosion Along Two Large Regulated Rivers. Water Resources Bulletin 31 (4), 617-631.

Surian, N., 1999. Channel Changes Due to River Regulation: the Case of the Piave River, Italy. Earth Surface Processes and Landforms 24, 1135-1151.

Williams, G.P., 1978. Bank-Full Discharge of Rivers. Water Resources Research 14 (6), 1141-1154.

Williams, P.F. and Rust, B.R., 1969. The Sedimentology of a Braided River. Journal of Sedimentary Petrology 39 (2), 649-679.

Williams, G.P. and Wolman, M.G., 1984. Downstream Effects of Dams on Alluvial Rivers. U.S. Geological Survey Professional Paper, 1286, pp. 83.

Wolman, M.G. and Leopold, L.B., 1957. River Flood Plains: Some Observations on their Formation. U.S. Geological Survey Professional Paper, 282-C.

Wolman, M.G. and Miller, J.P., 1960. Magnitude and Frequency of Forces in Geomorphic Processes. Journal of Geology 68 (1), 54-74.

CHAPTER 2

HYDROLOGIC AND GEOMORPHIC CHANGE ON THE SNAKE RIVER IN GRAND TETON NATIONAL PARK, WYOMING: THE INFLUENCE OF DAM REGULATION AND TRIBUTARIES

Abstract

Tributaries mitigate some impacts of nearly 100 years of regulated hydrology on 43 km of the Snake River downstream from Jackson Lake Dam (JLD). We analyzed measured and estimated unregulated flow data for the Snake River immediately below JLD and measured flow data for the two largest tributaries and the Snake River at Moose to accurately estimate flows throughout the study area since the dam was built in 1916. The magnitude of the 2-yr recurrence flood below JLD decreased 45% since 1958 relative to estimated unregulated flows whereas the magnitude of the 2-yr recurrence flood downstream from Buffalo Fork, a tributary to the Snake River 10 km from JLD, decreased 36%. We evaluated the ability of the current flow regime to mobilize the bed of the Snake River by placing tracers on active gravel bars and in the low flow channel and tracking their movement through the high flows of 2005. Portions of gravel bars and the channel bed were fully mobilized downstream from tributaries, but not downstream from JLD.

There was no long-term progressive channel change resulting from flow regulation. We mapped the bankfull channel on four series of aerial photographs taken in 1945, 1969, 1990/1991, and 2002 and analyzed changes in braid index and channel width. We overlaid the photographs to determine areas of deposition and erosion between years and calculate channel activity and net channel change. The majority of

channel activity occurred in the multi-thread reaches in wide alluvial valleys. Widespread deposition and up to 31% channel narrowing occurred during periods of relatively low-magnitude floods (1945 to 1969), whereas erosion and up to 31% channel widening occurred during periods of high-magnitude floods (1969 to 1990/1991 and 1990/1991 to 2002). Channel change occurred throughout the study area, regardless of proximity to tributaries.

1. Introduction

Channel and floodplain form are primarily determined by the flux of water through a reach and the associated transport of sediment delivered from the upstream watershed. One paradigm in fluvial geomorphology is that the size of the bankfull channel and the characteristics of the adjacent floodplain are maintained by the prevalent hydrologic and sediment supply regimes (Wolman and Miller, 1960; Andrews, 1980; Leopold, 1994). The linkages among flow regime, sediment supply, and channel and floodplain form are well illustrated on regulated rivers where the flow regime and sediment supply are altered by dams. Changes in these controlling variables cause evacuation of sediment from the bed and banks under conditions of sediment deficit (Mostafa, 1957; Komura and Simmons, 1967; Galay, 1983; Williams and Wolman, 1984). Farther downstream, near-dam sediment deficit may shift to sediment surplus as tributary sediment influx increases (Stevens, 1938; Andrews, 1986; Grant et al., 2003), although local differences in bed texture, channel organization, and valley confinement affect the magnitude of channel and floodplain change in any specific reach (Stevens, 1938; Lagasse, 1981; Grams and Schmidt, 2002, 2005).

Relatively few studies have described the characteristics of channel change under conditions of sediment surplus, especially where the bed material is coarse. The sequence and magnitude of bed aggradation and narrowing was described by Everitt (1993) for the Rio Grande along the Texas/Mexico border upstream from Presidio, TX, and by Church (1995) for the Peace River in British Columbia and Alberta. A significant length of the Trinity River in California is also in sediment surplus, as described in agency reports (e.g., U.S. Fish and Wildlife Service and Hoopa Valley Tribe, 1999).

The purpose of this paper is to describe patterns of channel and floodplain adjustment downstream from Jackson Lake Dam (JLD), originally constructed in 1908 and rebuilt in 1916. Because this dam increased the water level of an existing, glacially-scoured Pleistocene lake contained by glacial moraines, the dam caused no change in the downstream supply of sediment. Thus, decreased flood magnitudes resulting from dam regulation inevitably led to sediment surplus, although the magnitude of this surplus is unknown. Mills (1991) and Marston et al. (2005) described large-scale changes caused by JLD on the same part of the Snake River described here, but they did not account for tributary inflows that alter the flow regime created by dam releases. Mills (1991) and Marston et al. (2005) analyzed aerial photographs as recent as 1989, and we supplemented their work by analyzing more recent photographs within an improved geographic information system (GIS).

1.1. Study Area

The study area extends more than 43 km between JLD and Moose, WY, and significant changes in stream flow and sediment supply occur over this distance (Figure 2-1). The contributing drainage area more than doubles from 2090 km^2 at the dam to 4343 km^2 at Moose, and much of this increase is related to two large tributaries. Pacific Creek and Buffalo Fork join the Snake River within 10 km of the dam, and their combined watershed area is one-third of the total Snake River watershed upstream from Moose. Thus, these unregulated tributaries likely dampen the influence of dam operations on the flow regime of the Snake River. Three smaller tributaries join the

Snake River farther downstream: Spread Creek at 15.8 km downstream from JLD, Cottonwood Creek at 40.4 km, and Ditch Creek at 41.8 km.

Much of the Snake River is a braided channel and its adjacent floodplains and low terraces are best described as Class B, medium-energy, and non-cohesive, using the classification scheme of Nanson and Croke (1992). Love et al. (2003) divided the study area into three reaches, based on the response of the river to its glacial history and the modern gradient of the Snake River. The most upstream reach extends from JLD to Pacific Creek. The gradient here is 0.0007 (Figure 2-2) and extends through what Love et al. (2003) refer to as the Pacific Creek scour basin that was created during the early Pinedale stage glaciation about 30,000 to 14,000 years ago. Beyond Pacific Creek, the gradient increases to 0.0017 downstream to Deadmans Bar. This reach extends through another Pleistocene scour basin, referred to as the Triangle X basin. Further downstream, the gradient increases from 0.0030 between Deadmans Bar and Schwabachers Landing to 0.0038 from there to Moose.

Marston et al. (2005) described changes in hydrology by creating residual mass curves computed from the measured mean daily flows at the U. S. Geological Survey gaging station immediately downstream from JLD (station number 13011000). They also estimated mean monthly unregulated flows based on changes in end-of-month reservoir storage data (Marston et al., 2005). We used estimated unregulated mean daily discharge values from 1910 to 2005, calculated by the U.S. Bureau of Reclamation for the Snake River downstream from JLD (<http://www.usbr.gov/pn/hydromet/arcread.html>) to more precisely compare measured and estimated unregulated flows throughout the study area.

Mills (1991) and Marston et al. (2005) found that the sinuosity of the Snake River increased during the 20th century, based on analysis of seven topographic map or aerial photograph series between 1899 and 1989. They considered sinuosity to be a surrogate metric of channel stability and concluded that the greatest instability occurred near tributary mouths. They suggested that instability increased near tributaries during periods of high tributary sediment delivery, because the regulated Snake River was unable to transport this load. The channel was more stable during periods of low tributary sediment delivery when the delivered load was presumably transported.

2. Methods

2.1. Hydrology

Instead of characterizing the hydrology of the study area based solely on JLD releases, we estimated the hydrology of four channel segments defined by tributary inputs: JLD to Pacific Creek (Segment 1), Pacific Creek to Buffalo Fork (Segment 2), Buffalo Fork to Ditch Creek (Segment 3), and Ditch Creek to Moose (Segment 4) (Figure 2-3). Gaging stations have directly measured stream flow near the dam since 1903 and at Moose (station number 130136500) since 1995. Elsewhere, and for other periods, main-stem stream flow was estimated by adding measured tributary inflow or by correlation of measured periods and application of that correlation to unmeasured periods. The R^2 values of each regression equation exceeded 0.96 (Table 2-1). We did not analyze flows prior to 1916, because these 13 years of record consisted of five years of natural flows, three years of flows regulated by a log-crib dam, and five years of flows during construction of the larger dam and did not represent a stable flow regime suitable for analysis.

Tributary inflow has been measured at Pacific Creek (station number 13011500) and at Buffalo Fork since 1944, although this gage was moved 7.8 km from the mouth (station number 13012000) to upstream from Lava Creek (station number 13011900) in 1965. We estimated inflow from the entire Buffalo Fork watershed by applying the unit runoff for the upstream gage to the entire watershed area for the post-1965 period:

$$Q_{mouth} = (Q_{above\ LC}/A_{above\ LC})\ A_{mouth} \qquad (1)$$

where Q is mean daily discharge, A is drainage basin area, and the subscripts refer to the location of the gages at the mouth ($_{mouth}$) and upstream from Lava Creek ($_{above\ LC}$). The gage upstream from Lava Creek measured flows from 85% of the total watershed of Buffalo Fork. We did not analyze the sporadic and incomplete inflow data of the smaller tributaries.

Flood frequency was estimated for the maximum mean daily discharge. Calculation of maximum mean daily discharge for each segment provides comparable data not confounded by the addition of instantaneous and mean daily data, because the measured instantaneous annual peak flow immediately downstream from JLD rarely occurred on the same day as the instantaneous annual peak of the tributaries. Estimates of maximum mean daily discharge are also better compared with unregulated conditions, because estimates of annual instantaneous peak flows released from the dam have not been made. The difference between instantaneous and mean daily peak flows was small;

the instantaneous annual peak flow was typically less than 5% greater than the maximum mean daily discharge for the Snake River at the dam and at Moose. Flood recurrences were calculated using a Log-Pearson Type III distribution (Linsley et al., 1982). Because error influenced station estimates of the skew coefficient used in these calculations, especially as the number of observations in the series decreased, we calculated a weighted coefficient of skewness (IACWD, 1982). We obtained the regional skewness factor, -0.1, from generalized skew coefficients for the United States and used the variance in regional skew, 0.302, estimated for the United States (IACWD 1982). The durations of mean daily flows for each segment were also determined.

2.2. Channel Change

Channel location and surface area were mapped on four series of aerial photography and entered into a GIS. Aerial photographs from 1990 and 1991 were combined to obtain complete coverage of the study area; we refer to this photograph series as 1990/1991. We mapped the water surface and also estimated the area of the bankfull channel, because the surface area of the flow is partly dependent on discharges that differed by as much as 55% among dates of photography (Table 2-2). The edge of water was mapped, but isolated bodies of water located on terraces that appeared to have no connection to the channel were not included in calculations of channel area. In multi-thread reaches, we did not consider minor secondary channels, defined as narrow channels bounded on both banks by vegetation in all years of photography, as part of the bankfull channel. These channels were largely inconsequential for channel change analyses and were generally less than 10 m wide, which made the identification of channel banks difficult and imprecise where mature vegetation obscures the channel boundaries. Larger secondary channels located between primary channel threads in braided reaches were considered part of the bankfull channel. We defined the edges of the bankfull channel as the boundary between vegetated surfaces and the water or between vegetated and unvegetated alluvial deposits. Based on field mapping, partially vegetated deposits with less than 10% vegetation were generally below the elevation of the floodplain and were considered part of the bankfull channel (Figure 2-4).

The aerial photographs were georeferenced by matching fixed locations such as road junctions, trees, buildings, and distinct landscape elements common to the aerial photographs. Two main sources of error were inherent in the channel change analyses. First, there was error associated with initial mapping and digitizing of the channel. This error was quantified by calculating the product of the half width of a pencil line (0.15 mm) and the scale of the aerial photograph (Gaeuman et al., 2003). Second, there was error associated with georeferencing the photographs. The root mean square (RMS) error of each fixed location for each photograph in each series was calculated within ArcEdit, the GIS software used to georeference the photographs (Gaeuman et al., 2003; Grams and Schmidt, 2005). Average RMS errors were less than 1 m for each photograph series (Table 2-3). The total linear error inherent in mapping the channel and georeferencing the aerial photographs was determined by calculating the square root of the sum of the squares of each error (Gaeuman et al., 2003). The total linear error associated with overlaying or comparing two photograph series was 9 m, determined by calculating the square root of the sum of the squares of each individual total linear error. This overlay error represents between 6% and 13% of the bankfull channel widths, which ranged from 71 m to 160 m.

We developed several metrics to describe channel change. These metrics included channel activity, net channel change, bankfull channel width, and braid index. These metrics were calculated for 19 reaches whose boundaries were defined primarily by channel organization as well as by the location of tributary inflows (Figure 2-3).

Annual channel activity was defined as the combined area of channel erosion and deposition per unit longitudinal distance of the main channel. Channel activity is an indicator of channel stability and the degree of channel migration over time. Braided rivers are naturally very active, with high rates of scour, avulsions, and bar formation (Leopold and Wolman, 1957; Ashmore, 1991; Brierley and Fryirs, 2005). Changes in the rate of channel activity potentially indicate the response of the channel to changes in the flux of water and sediment through the system. Erosion and deposition were determined by overlay of bankfull channel position maps (Figure 2-5) within the GIS and determining changes from floodplain to bankfull channel (erosion) or from bankfull channel to floodplain (deposition) between years of aerial photography. We assessed the accuracy of each resultant erosion and deposition polygon by comparing the bankfull channel boundaries of each photograph series. Polygons that were created because of the inaccuracy of the overlays were excluded from subsequent analyses. We determined the annual net channel change by calculating the difference between total areas of erosion and deposition and dividing by the length of the main channel.

We calculated the bankfull channel width by dividing the bankfull channel area by the centerline reach length of the main channel at bankfull flow. There was some error associated with these calculations. Van Steeter and Pitlick (1998) determined that the total error in polygon area calculations due to interpretation and mapping of the boundaries (2%), photograph distortion (3%), and differences in discharge (3%), was no more than 8%. Because we estimated bankfull channel area, thus eliminating the error due to differences in discharge, we assumed a 5% maximum error associated with our polygon area calculations. We compared channel lengths measured in a GIS with those measured during detailed field surveys and determined that differences were no more than 1% of the channel length. Therefore, we assumed a 6% maximum error in our bankfull channel width calculations.

Changes in channel width, channel activity, and net channel change are partly dependent on changes in main channel length. Changes in main channel length indicate changes in sinuosity and gradient. We averaged the reach lengths from the four series of aerial photographs to evaluate temporal changes in channel width, channel activity, and net channel change with respect to changes in flow regime.

Comparisons of our maps and those of Mills (1991) indicate that Mills (1991) underestimated channel area (based on edge of water values) by between 8% and 14% (Table 2-4). We estimated the bankfull area from the Mills (1991) maps for 1975 and 1989 for the entire study area from JLD to Moose, although the dimensions of the bankfull channel were not explicitly mapped. Bankfull area was estimated by scaling the Mills (1991) data by the average ratio of water surface to bankfull area for the 1945 and 1990/1991 data in this study (Table 2-4).

The braid index is the ratio of total channel length to main channel length (Mosley, 1981; Church, 1995) and is an indicator of channel complexity. Changes in braid index indicate changes in rates of avulsion, creation of new channels, reactivation of old channels, or mobilization of sediment (Ashmore, 1991; Knighton, 1998; Surian, 1999). We calculated the braid index by dividing the total channel length, including all active secondary channels, by the main channel length based on the centerline of the channels. This was completed for each reach at bankfull flows to eliminate changes in braid index values due to differences in discharge and number of channel-splitting, bare gravel bars between years of aerial photography. We also evaluated the difference in relative stability between reaches close to, and farther from, tributaries. We summed the channel lengths for all reaches proximal to tributaries to obtain single braid index values for each photograph series. This analysis was repeated for the reaches distal to tributaries. We compared the two values for each series to assess temporal trends with regards to the proximity of reaches to tributaries.

2.3. Bed Mobility

We estimated bed mobility of the present channel by marking tracer rocks on gravel bars and determining the flows when these particles moved. Tracers were marked by painting exposed bars or by placing painted rocks on these bars or in the low flow channel prior to the 2005 runoff season. In the latter case, we placed tracers that represented the local D_{16}, D_{50}, and D_{84} into the top layer of clasts on the gravel bar. We expected these tracers to move more readily than those painted in situ because the latter were imbedded in the gravel bar and would necessarily require greater shear stresses to move. The placed tracers were marked with numbers representing their location to distinguish them from the in situ tracers. We placed 264 clasts in clusters on exposed bars and in the low flow channel and otherwise painted more than 3800 clasts in clusters on exposed bars. Tracers were located in each of the four segments (Table 2-5, Figure 2-3).

Repeat photographs and surveys before and after the 2005 floods helped relocate tracers and track changes in topography. Two low-magnitude floods occurred during 2005 with recurrence intervals of less than 1.2 years; one was due to natural flood runoff from the tributaries and the other was due to high dam releases (Table 2-6). We recorded movement before and after both peak flows. After the floods receded and tracers were fully exposed, we identified the locations of the clasts and measured the distance and direction that each had moved. Tracers not found in the vicinity of their original placement were assumed to have moved greater than 1 m as large amounts of deposition, and thus burial, were not recorded near the tracers in 2005. Tracers that were slightly buried were recovered by removing the overlying fine-grained sediments and gravels. The size of tracers painted in situ was unknown prior to the floods; the grain-size distribution of in situ tracers that moved does not include clasts with b-axes less than 22.6 mm in diameter as these were too numerous and difficult to individually identify in pre-flood photographs. We used pre-flood photographs to identify the original location of tracers and then measured the distance moved during the 2005 floods.

We could not determine the exact magnitude of flows that initiated movement because tracers were inaccessible at peak flows and the water was opaque due to suspended sediment. However, because there were two floods in 2005, we could estimate the range of flows that initiated bed movement by comparing the mobility of tracers through each peak flow. To compare tracers that were in different depths of water and were of different sizes we calculated the boundary shear stress (τ_o) and dimensionless shear stress (τ^*) for the tracers:

$$\tau_o = \rho\, g\, h\, S \qquad (2)$$

$$\tau^* = \tau_o / (\rho_s - \rho)\, g\, D_i \qquad (3),$$

where ρ_s, ρ, and g refer to sediment density, water density and gravitational acceleration, respectively, h is the maximum flow depth over the tracers during the observation period, S is the local slope, and D_i is the b-axis diameter of the particles. We calculated the maximum water depth over the tracers by surveying the edge of water in relation to fixed benchmarks near the tracers during flood flows and comparing these surveys with the initial topographic surveys of tracer locations. The local slope was calculated by dividing the difference between the water surface elevations near benchmarks about 135 m upstream and downstream from the tracers by the sum of the mid-channel longitudinal distance from the tracers to these benchmarks.

We calculated the active proportion of the channel bed at each tracer location during the 2005 flood season. The active proportion is the proportion of tracers that moved to the total number of tracers at that location (Haschenburger and Wilcock, 2003). Tracers placed on bars and in the low flow channel were analyzed separately from the tracers marked in situ. The extremes of mobility are of greatest importance in determining the ability of a river to mobilize its bed; thus, active proportions less than 10% were considered immobile, greater than 90% fully mobile, and between 10% and 90% partially mobile (Haschenburger and Wilcock, 2003). We calculated the dimensionless shear stress for each tracer in each mobility category and determined the thresholds of dimensionless shear stress, and thus discharge, necessary for partial and full mobilization.

We compared the values of τ^* during the 2005 floods with those during a 2-yr recurrence flood to estimate the bed mobility during a slightly larger, though still moderately-sized, flood. The stage of the 2-yr flood was estimated using a one-dimensional flow model (Chapter 3 in Nelson, 2007). We used the estimated water surface elevation of the 2-yr recurrence flood to estimate the depth of flow over each tracer and the local slope.

3. Results

3.1. Hydrology

The hydrology of the Snake River during the past century includes five episodes of relatively high runoff. The long-term average runoff between 1904 and 2005 was 41 m^3/s below JLD, and episodes of above average runoff occurred between 1907 and 1918, 1943 and 1956, 1970 and 1976, 1982 and 1986, and between 1996 and 2001. These episodes of high average runoff also occurred throughout the study area, because the cycles of high and low runoff of the tributaries were in phase with the runoff pattern on the Snake River near the dam (Figure 2-6).

The timing or relative magnitude of large floods on the Snake River did not always precisely match that of the tributaries. Between 1954, a year of large floods throughout the system, and 1969, the first year in which aerial photographs were taken after the flow regime change in 1958, there were four years in which peak flows on

Pacific Creek exceeded the magnitude of the 2-yr recurrence flood (Figure 2-7), while there were only three years in which Segment 2 of the Snake River exceeded its 2-yr flood (Figure 2-8). For this same time period, there were five years in which Buffalo Fork exceeded its 2-yr recurrence flood and only three years in which Segment 3 of the Snake River exceeded this recurrence flood. Large tributary floods occurred more frequently from 1969 to 2002 than between 1945 and 1969; flows on Pacific Creek and Buffalo Fork exceeded their 5-yr recurrence floods during eight and 13 years between 1969 and 2002, respectively. In Segments 2 and 3 of the Snake River, the 5-yr recurrence flood was exceeded during seven and eight years respectively. The largest floods on record below Buffalo Fork occurred in 1997.

The magnitude of floods in Segment 1 between 1916 and 1958 was somewhat lower than that estimated for the unregulated flow regime (Figure 2-8A, B) and the timing of the flood was delayed approximately two months (Figure 2-9A) as shown in previous studies (Mills, 1991; Marston et al., 2005); this shift in timing allowed delivery of water downstream to meet summer irrigation needs. The magnitude of the 2-year recurrence flood was 17% less than estimated for the unregulated flow regime, and the magnitude of the 10-year recurrence flood was 14% less than that of the estimated unregulated regime. The mismatch in timing of high dam releases with unregulated floods on tributaries resulted in a 22% reduction in the 2-year recurrence flood downstream from Buffalo Fork (Table 2-7).

The increased flexibility in the release schedule at JLD following the construction of Palisades Dam in 1958 allowed managers of JLD to decrease peak flows, realign the floods with their natural timing, and increase releases throughout the summer to benefit the recreational boating industry (Figure 2-9). Between 1959 and 2005, the 2-yr recurrence flood was reduced, relative to the estimated unregulated flood, by 45% in Segment 1, and by 36% downstream from Buffalo Fork. Thus, the change in operations of JLD that occurred in the late 1950s caused a slightly greater degree of flood reduction immediately downstream from the dam than elsewhere. The magnitude of the 2-yr recurrence flood between 1959 and 2005 was reduced 32% from pre-1958 magnitudes in Segment 1, and only 19% in Segment 3.

The magnitudes of flows that were equaled or exceeded for various periods of time also changed after 1958 and the characteristics of these changes differed near JLD compared to further downstream (Table 2-8). Measured flows were 97% of estimated unregulated flows in Segment 1 prior to 1958, but 64% after 1958. The mismatch in the timing of peak releases and peak tributary flows prior to 1958 resulted in measured flows in Segment 4 that were only 89% of estimated unregulated flows. Measured flows after 1958 in this segment were 68% of estimated unregulated flows, lower than those prior to 1958, but somewhat higher in proportion to estimated unregulated flows than those in Segment 1.

Base flows, which were equaled or exceeded 90% of the year, were minimal in Segment 1 prior to 1958. Tributaries were the primary contributors of flows during this period, increasing measured flows from 3% of estimated unregulated flows in Segment 1 to 61% of estimated unregulated flows in Segment 4. After 1958, base flows were somewhat restored and measured flows increased from 54% to 70% of estimated flows between Segments 1 and 4, respectively.

3.2. Channel Change

3.2.1. Channel Organization

The channel organization of the Snake River is closely linked to the width of the Holocene alluvial valley within high Pleistocene terraces and can be grouped into two main channel types: single-thread reaches where the Holocene alluvial valley is narrow and multi-thread reaches where the valley is wide (Figure 2-10). Between JLD and Pacific Creek, the Holocene alluvial valley is confined by Tertiary and Upper Cretaceous sedimentary rocks, Holocene landslide debris off Signal Mountain, and Pleistocene alluvial deposits (Love et al., 2003). High Pleistocene terraces of alluvial deposits flank the Snake River through most of the study area (Love et al., 2003). In some areas, these deposits restrict channel movement: about 2 km downstream from Buffalo Fork, near Spread Creek, about 2 km downstream from Spread Creek, and near Moose (Love et al., 2003). Debris from the late-Pleistocene Burned Ridge moraine limits movement of the river at Deadmans Bar (Love et al., 2003).

We distinguished 19 reaches within this framework. Single-thread reaches make up 18.4 km of the study area length, which is 43.5 km. The average braid index for most single-thread reaches is approximately 1.0, though stable, densely vegetated islands in Reaches 2 and 3 divide the channel in a few places (Table 2-9). The remaining 58% of the Snake River is multi-thread; some of these reaches are at the mouths of tributaries (Reach 7 near Buffalo Fork and Reach 18 near Cottonwood and Ditch Creeks) and others are far from tributary inflows (Reaches 10, 15, and 17). Reaches 15 and 17 are the longest reaches at 5.9 and 10.4 km, respectively, and make up 38% of the study area length. Braid index averages for the multi-thread reaches generally exceed 1.5 and those of Reaches 8, 15, 17, and 18 exceed 2.0.

We subdivided the channel types. Single-thread channels were identified as either straight or restricted meandering and multi-thread channels were identified as braided or meandering. Straight channels occur in low-gradient reaches in Segment 1 (Reaches 1, 2, 4, and 5) as well as Reaches 9, 11, 12, and 19 further downstream. These are stable channels with occasional vegetated islands. The restricted meandering channels are located at the Oxbow Bend (Reach 3), about 2 km downstream of Spread Creek (Reach 14), and near Deadmans Bar (Reach 16). These channels have a high sinuosity but Holocene or Pleistocene terraces limit large-scale channel migration.

Braided channels are the most active multi-thread channels and occur in Reaches 6 through 8, upstream and downstream from Deadmans Bar (Reaches 15 and 17), and in the very short reach between Cottonwood and Ditch Creeks (Reach 18). Average braid index values in these reaches were generally greater than all other reaches, with Reaches 8 and 18 exceeding a braid index of 3.0. Meandering channels are less active but still experience channel migration and bar formation and are located in Reaches 10 and 13, upstream and downstream from Spread Creek, respectively. The average braid index values of these two reaches were generally greater than the single-thread channels, but less than the braided channels.

3.2.2. Spatial Patterns in Channel Change

Channels in multi-thread reaches were generally wider and more active than those in single-thread reaches (Table 2-9). The bankfull width of braided reaches typically exceeded 140 m, and the width of meandering reaches was between 99 m and 110 m. The straight, single-thread reaches ranged in width from 71 m to 96 m, and the widths of the restricted meandering reaches were between 83 m and 89 m. The average annual channel activity of most multi-thread reaches exceeded 1000 m^2/km, while that of most single-thread reaches were less than 500 m^2/km. Much of the channel activity on the Snake River occurred in the long or highly braided Reaches 15, 17, and 18 where annual values ranged from 4900 to 6200 m^2/km. Channel change in the braided reaches consisted of abandonment and reactivation of secondary channels, frequent avulsions that changed the course of the main channel, and alluvial bar erosion and construction. Main channel migration in meandering reaches occurred by bank erosion and point bar formation, as well as alluvial bar erosion and construction (Figure 2-11).

The annual channel activity in the single-thread reaches was minimal, but was generally greatest at tributary inflows (Reaches 5 and 12) and in the restricted meandering channels (Reaches 14 and 16). Channel change in the restricted meandering reaches consisted of small amounts of bank erosion and point bar construction as well as minor changes to alluvial bars and islands; the least amount of channel change generally occurred in the straight, single-thread reaches and consisted of occasional erosion and deposition of alluvial bars and islands and bank erosion (Figure 2-11).

3.2.3. Temporal Patterns in Channel Change

There was no long-term progressive change in channel width and migration rates over the study period. Periods with few large floods (1945-1969) along the Snake River resulted in net deposition, channel narrowing, and an increase in braid index whereas periods with many large floods (1969-1990/1991, 1990/1991-2002) resulted in net erosion, channel widening, and a decrease in braid index (Figure 2-12). The channel activity remained high in all time periods, particularly in the braided reaches (Figure 2-13a). The relative sinuosity of the Snake River, based on temporal changes in main channel length, did not change with the frequency of large floods (Table 2-10).

Net deposition and channel narrowing occurred in 16 of the 19 reaches between 1945 and 1969 (Tables 2-11 and 2-12, Figures 2-13b and 2-14). During this period of relatively low-magnitude floods on the Snake River and its tributaries, some secondary channels were abandoned. Larger volumes of sediment were deposited in the main channels than could be eroded away, resulting in increased deposition and formation of vegetated islands and a subsequent increase in braid index (Table 2-13). The mismatch in timing of main-stem and tributary floods and the infrequent high-magnitude floods on the main-stem most likely contributed to deposition, channel narrowing, and increased braid index in most of the study area.

The braid index for reaches proximal and distal to tributaries was equal in 1945 (Figure 2-15). By 1969, the braid index was slightly larger for reaches proximal to tributaries, suggesting that the Snake River was incapable of transporting all of the delivered sediment in the period of few large floods prior to 1969, resulting in aggradation and decreased stability downstream from tributaries. The period of many large floods in the 1980s likely reversed this trend, as the braid index for reaches proximal to tributaries was slightly lower than that for reaches far from tributaries in the period since 1990/1991.

Neither the bankfull channel area, length, width, nor braid index of the Snake River from JLD to Moose has changed substantially or progressively over time (Table 2-14). We could not evaluate the length, width, or braid index for 1975 and 1989 as these metrics were based on the channel at bankfull flow and we did not have the aerial photographs to distinguish bare gravels and accurately calculate reach lengths.

3.3. Bed Mobility

The movement of tracers was measured through the 2005 flood season. The 2005 flood season consisted of two relatively low-magnitude floods. The tributaries flooded in late May, causing the first flood on the Snake River downstream from Pacific Creek. One month later, dam releases caused the second, slightly larger flood that ranged from 25% to 37% lower than the magnitude of the 2-yr recurrence interval in Segments 1 and 4 respectively (Table 2-6).

The median bed grain size of the Snake River near the tracers was larger in Segments 3 and 4 than in Segments 1 and 2 (Figure 2-16), corresponding to a downstream increase in channel gradient (Table 2-15). The slope in the immediate vicinity of the tracers at Moose is lower than those in Segments 2 and 3, but the overall slope of the Snake River increases steadily downstream (Figure 2-2).

There was clear evidence of bed movement at all sites. Of the 264 painted clasts placed onto gravel bars or in the low flow channel, 41% moved and 17% moved downstream at least 1 m (Table 2-16). Movement increased substantially downstream. Tracer movement in Segment 1 was always less than 1 m, whereas 81% and 49% of the tracers placed in Segments 3 and 4 respectively moved more than 1 m. Fewer in situ tracers moved, though a downstream increase in mobility also occurred for tracers moving at least 1 m.

There was little difference throughout the study area in the median grain size of tracers that moved, though it was somewhat higher in Segments 3 and 4 and lower in Segment 2 (Table 2-17). The largest tracers that moved were 120 mm, which occurred in Segments 3 and 4 and exceeded the D_{84} in every location but Schwabachers Landing; the largest that moved at least 1 m were 100 mm and 105 mm in Segments 3 and 4, respectively, exceeding the D_{50} in all locations.

Topographic changes at these marked sites further demonstrated bed movement during the 2005 flood season. The most notable changes were scour at Moose EP1 and deposition in Segment 2 and at Moose EP2, though small changes did occur at some locations in Segments 1 and 3 (Appendix A in Nelson, 2007).

A larger proportion of tracers moved during the dam-released flood than the earlier natural flood and there was a general downstream increase in the mobilization of tracer clusters (Table 2-18). During the later, released flood of 2005, 57% of placed tracer clusters in Segment 1 were immobile, whereas none were immobile in Segments 3 and 4. No clusters of tracers were fully mobilized in Segment 1, but 75% and 61% were fully mobilized in Segments 3 and 4 respectively. The larger proportion of movement during the second flood is likely due to a combination of its slightly greater magnitude and its longer duration; in Segment 3, flows exceeded 100 m^3/s for six days and 150 m^3/s for only one day during the first flood, as compared to 25 and 11 days respectively during the second flood.

According to these data, the Snake River is capable of fully mobilizing its bed downstream from Pacific Creek during relatively frequent, low-magnitude floods. The estimated median τ^* of the 2-yr recurrence flood is greater than the median τ^* of the immobile and partially mobile categories for both in situ tracer and placed tracer locations in all segments during both floods (Figure 2-17). This analysis suggests that during fairly frequent but moderate-in-magnitude floods a greater proportion of the channel bed in each segment will be partially or fully mobilized than during the low-magnitude floods of 2005.

4. Discussion

4.1. A General Model of Channel Change of the Snake River in GTNP

Temporal changes in channel and floodplain form are primarily dependant on the relative magnitude of sediment delivered by tributaries and floods that transport the sediment. Thus, before conducting our research, we expected two types of net deposition and channel narrowing throughout the study area between 1945 and 1969. First, we did not expect that the low-magnitude floods between 1945 and 1969 were capable of evacuating the large volumes of sediment delivered by higher-magnitude tributary floods. We expected this to result in deposition, increased channel activity, and overall channel narrowing near tributaries. Second, farther from tributaries we expected net deposition and narrowing in the form of fully or partially abandoned secondary channels and increased stability, as suggested by Marston et al. (2005). The 10-yr recurrence flood was exceeded during 14% of the years from 1969 to 1990/1991 and during 25% of the years from 1990/1991 to 2002, compared to 4% from 1945 to 1969. This increased frequency of high-magnitude floods on the Snake River after 1969 should have been capable of mobilizing more sediment and probably reactivated old, or created new, secondary channels. Therefore, we expected net erosion and channel widening throughout the study area between 1969 and 2002.

Changes in braid index on a multi-thread, gravel-bed river in sediment surplus are difficult to predict. Field studies on a heavily regulated, braided, gravel-bed river in Italy suggested that braid index was positively correlated with discharge (Surian, 1999). The combination of reduced flood magnitudes and the trapping of large volumes of sediment behind dams along the Piave River and its tributaries resulted in secondary channel abandonment, decreased braid index, sediment deficit, incision, and channel narrowing (Surian, 1999). The construction of JLD resulted in decreased flood magnitudes but no change in the sediment supply, thus causing an unknown degree of sediment surplus downstream from tributaries. As on the Piave River, periods of decreased flood magnitudes should have resulted in decreased braid index values because secondary channels would likely be abandoned. In a system in sediment surplus, decreased flood magnitudes may cause some secondary channels to be abandoned, but the accumulation of sediment in the main channel may also result in channel-splitting alluvial bars and vegetated islands. Changes in braid index values on the Snake River result from a combination of these two processes and may cause unexpected responses such as channel narrowing coupled with an increased braid index in the same reach for the same time period (Figure 2-18).

The response of geomorphic change to regulation matched our expectations fairly well. The period of low-magnitude floods following the flow regime change in 1958 resulted in deposition and channel narrowing throughout most of the river between 1945 and 1969. Periods of high-magnitude floods since 1969, particularly in the 1980s and 1990s, coincided with net erosion and channel widening in most reaches of the Snake River. Between 1969 and 1990/1991, the timing and magnitude of floods on Pacific Creek matched those in Segment 2 of the Snake River, while floods on Buffalo Fork exceeded the 5-yr recurrence flood twice as often as those in Segment 3. These tributaries likely delivered large volumes of sediment during this period. The floods in 1983 and 1986, which exceeded the 25-yr recurrence flood in Segment 2 and were substantially greater than the 10-yr recurrence flood in Segment 3, were likely large enough to transport the delivered sediment and erode more of the floodplain than they built. The degree of bar and island erosion was likely greater than the degree of secondary channel reactivation, resulting in decreased braid index values in many of the reaches.

The 25-yr recurrence flood was exceeded in 1996 and the 100-yr recurrence flood exceeded in 1997 in Segments 2 and 3. The floods on the Snake River between 1990/1991 and 2002 corresponded relatively well in magnitude and timing with floods on the tributaries and were thus likely able to transport the sediment presumably delivered by the tributaries. The large floods in 1996 and 1997 and the five additional years in which the 2-yr recurrence flood was exceeded were likely the primary factors driving increased channel activity, net erosion, and channel widening.

The only comparable study of the hydrology and geomorphology of the Snake River in GTNP was that of Marston et al. (2005). These two studies were closely linked as our initial hypotheses were based, in part, on the work of Marston et al. (2005), thereby necessitating a direct comparison of findings.

Many of the results and conclusions of Marston et al. (2005) were based on the premise that the flow regime immediately downstream from JLD describes the hydrology for the entire study area. The gage data for Pacific Creek and Buffalo Fork since 1944 and our estimates of flows below these tributaries based on these data suggested a substantially different flow regime for 79% of the study area. Estimates of mean daily discharge without the dam allowed a detailed comparison of measured and unregulated flows for each segment of the Snake River. Flood magnitudes have decreased throughout the study area due to regulation, as suggested by Marston et al. (2005), but the tributaries provide substantial flows and somewhat mitigate the impacts of JLD.

Marston et al. (2005) completed their fieldwork in 1990, between the large floods in the 1980s and the highest floods on record in the 1990s. Therefore, their findings of progressive channel change, mainly aggradation and decreased stability proximal to tributaries and abandonment of channels and increased stability distal to tributaries, was influenced by the long period of low-magnitude floods between the late 1950s and the early 1980s. From 1945 to 1969, we found channel narrowing throughout the study area and increased braid index proximal to tributaries, similar to Marston et al. (2005). However, we did not find an increase in stability far from tributaries, and in the subsequent period, from 1969 to 2002, we found widespread channel widening and erosion, as well as similar braid index values for reaches proximal and distal to tributaries. Channel activity and net channel change was concentrated within the unstable multi-thread reaches in wide alluvial valleys, particularly in Reaches 15 and 17.

These data suggest that the degree of channel activity and channel change along the Snake River in the study area is primarily dependant on the width of the alluvial valley, and less dependant on proximity to sediment sources such as tributary inflows or high cut banks.

The conclusion that the Snake River was incapable of mobilizing sediment introduced by tributaries (Marston et al., 2005) was also partially refuted by our bed mobility study. We suggest that the bed immediately downstream from JLD is armored, but that the bed for much of the Snake River is active and capable of movement even during low-magnitude floods, such as those of 2005. A complete sediment budget is necessary to fully understand the flux of sediment downstream from tributaries.

4.2. The Snake River in Relation to Other Regulated Rivers

Much of what we know regarding the effects of dam regulation on rivers is from studies of large dams on fine-grained, single-thread rivers (e.g. Williams and Wolman, 1984; Everitt, 1993; Grams and Schmidt, 2002; Topping et al., 2003). These dams generally impact both the flux of water and sediment to varying degrees. Little is known about the mechanics of gravel-bed, multi-thread rivers, less is known about the effects of dams on these types of rivers, and even less is understood about these types of rivers under conditions of sediment surplus.

Similar to other braided rivers (Knighton, 1972; Bridge and Gabel, 1992; Ferguson et al., 1992; Reinfelds and Nanson, 1993), the Snake River has a high gradient, high bed load, erodible banks, and it frequently changes course by channel migration and avulsion through much of the study area. While meandering rivers primarily build floodplains through lateral accretion of point bars and vertical overbank accretion (Wolman and Leopold, 1957), the Snake River has two active floodplain surfaces formed by multiple processes (Chapter 3 in Nelson, 2007).

The changes to the hydrologic regime for most of the Snake River in GTNP were relatively small compared to other large regulated rivers in the western United States. The 2-yr recurrence flood of the Snake River downstream from Buffalo Fork decreased 19% since the flow regime change in 1958 and 36% from estimated unregulated flows. Dam regulation reduced the 1-day maximum flow by an average of 55% on 21 rivers throughout the U.S. (Magilligan and Nislow, 2005), resulted in a 65% decrease of peak flows on the Colorado River (Topping et al., 2003), an approximately 50% decrease of peak flows on the Platte River (Johnson, 1998), a 90% decrease in mean and peak annual discharge on the Rio Grande at Presidio (Everitt, 1993), a 57% decrease in the 2-yr flood on the Green River (Grams and Schmidt, 2002), and a 53% decrease in stream flow on the lower Duchesne River (Gaeuman et al., 2005).

Changes in channel width in our study area ranged from 31% channel narrowing in Reach 17 from 1945 to 1969 to 31% channel widening in the same reach from 1969 to 1990/1991. Reductions in channel areas or widths due to regulation is common: 55% to >90% on the braided Platte River (Johnson, 1994, 1998), 58% to 70% on the braided Piave River (Surian, 1999), 25% to 45% in some reaches of the single-thread lower Duchesne River (Gaeuman et al., 2005), and 11% to 22% in various reaches of the single-thread Green River below the Gates of Lodore (Grams and Schmidt, 2002). Uncommon, however, is channel widening following regulation. The Snake River initially experienced widespread channel narrowing resulting from the flow regime change, but this was followed by periods of channel widening that corresponded to periods of frequent large floods. Channels in 15 reaches became wider by between 1% and 29% from 1945 to 2002 suggesting that the geomorphic impacts of dam regulation not only decreased through time, but also may have been eliminated and reversed. Smaller amounts of channel recovery have been observed in other regulated river systems. In the two decades following the greatest reductions in channel area on the Platte River, recovery of channel area ranged from 1 to 20% (Johnson, 1994 and 1998). Williams and Wolman (1984) also observed recovery in relative change in channel width in some reaches through time.

Erosion, deposition, and changes in channel width in our study area appear to correspond with the frequency of floods larger than the 2-yr recurrence flood. The highly erodible banks of braided rivers result in large amounts of channel change during periods of high stream power, variable or flashy flows, or larger, less frequent floods (Knighton, 1972, 1998; Brierley and Fryirs, 2005). The large floods in 1983, 1986, 1996, and 1997 that exceeded the 10, 25, and 100-year recurrence floods likely resulted in the observed increased channel activity and reversal of negative geomorphic impacts of regulation. This influence of large floods suggests that the channel change associated with the high natural spring runoff, may be as important as the channel change associated with lower-magnitude floods caused by regulation. The effects of these large floods may persist for many years (Knighton, 1998).

The combination of large amounts of channel activity and little change in braid index suggests that the Snake River frequently changes course, as is common in high-gradient, multi-thread river systems, but that the overall channel planform has not been drastically altered. Surian (1999) suggested that the planform of multiple reaches on the Piave River had changed from braided to wandering as a result of dam regulation. We did not observe planform changes in any of the 19 reaches we analyzed.

5. Conclusions

The construction of JLD in 1916 resulted in nearly a century of flow regulation, but essentially no change to the flux of sediment, as Jackson Lake is Pleistocene in age and has historically acted as a sediment trap. The change in operations of JLD after 1958 resulted in a decrease in flood magnitudes throughout the study area. These decreases were somewhat less severe downstream from tributaries due to the influx of unregulated flows.

Net changes to channel and floodplain form in our study area have been minimal despite this flow regulation. Based on analyses of spatial and temporal changes in channel form, our data indicate that the Snake River remains active with no long-term, net change to the overall stability or planform of the channel. Net deposition and channel narrowing between 1945 and 1969 were later replaced by periods of net erosion and channel widening. The channel gradient and width of the alluvial valley are the stable, long-term determinants of the general organization of the channel, whereas localized changes in channel width and net channel change are more sensitive to, and dependant on, the frequency of larger floods at shorter time scales.

The current flow regime is capable of mobilizing the bed material in the Snake River. The proportion of the bed mobilized during the floods of 2005 typically increased downstream and this longitudinal pattern occurred despite a downstream increase in bed-material size. Thus, the downstream increase in flood magnitude and channel gradient more than compensates for the increase in substrate grain size. However, the volume of bed material that the Snake River is capable of mobilizing is unknown; therefore, a sediment budget is necessary to more fully understand the flux of sediment downstream of tributaries.

Our study confirms that different rivers respond differently to different proportioned changes in water and sediment flux. Hypotheses and predictions about impacts of regulation on gravel-bed, braided rivers should not be based on fine-grained, single-thread rivers, or even fine-grained, multi-thread rivers. Our study also emphasizes the importance of analyzing all available flow data for a river and its significant tributaries. Analysis of a single gage may lead to misguided conclusions and management decisions if applied to a large section of river with significant increases in flow downstream from the gage.

REFERENCES

Andrews, E.D., 1980. Effective and Bankfull Discharges in the Yampa River Basin, Colorado and Wyoming. Journal of Hydrology 46: 311-330.

Andrews, E.D., 1986. Downstream Effects of Flaming Gorge Reservoir on the Green River, Colorado and Utah. Geological Society of America Bulletin 97, 1012-1023.

Ashmore, P.E., 1991. Channel Morphology and Bed Load Pulses in Braided, Gravel-Bed Streams. Geografiska Annaler 73A, 37-52.

Brierley, G.J. and Fryirs, K.A., 2005. Geomorphology and River Management: Applications of the River Styles Framework. Blackwell Publishing, Malden, MA. 398 pp.

Bridge, J.S. and Gabel, S.L., 1992. Flow and Sediment Dynamics in a Low Sinuosity, Braided River: Calamus River, Nebraska Sandhills. Sedimentology 39, 125-142.

Church, M., 1995. Geomorphic Response to River Flow Regulation: Case Studies and Time-Scales. Regulated Rivers: Research and Management 11, 3-22.

Everitt, B., 1993. Channel Responses to Declining Flow on the Rio Grande between FT. Quitman and Presidio, Texas. Geomorphology 6, 225-242.

Ferguson, R.I., Ashmore, P.E., Ashworth, P.J., Paola, C., and Prestegaard, K.L., 1992. Measurements in a Braided River Chute and Lobe; 1, Flow Pattern, Sediment Transport, and Channel Change. Water Resources Research 28 (7), 1877-1886.

Gaeuman, D.A., Schmidt, J.C., and Wilcock, P.R., 2003. Evaluation of In-Channel Gravel Storage with Morphology-Based Gravel Budgets Developed from Planimetric Data. Journal of Geophysical Research 108 (F1), 6001, doi:10.1029/2002JF000002).

Gaeuman, D., Schmidt, J.C., and Wilcock, P.R., 2005. Complex Channel Responses to Changes in Stream Flow and Sediment Supply on the Lower Duchesne River, Utah. Geomorphology 64, 185-206.

Galay, V.J., 1983. Causes of Bed Degradation. Water Resources Research 19 (5), 1057-1090.

Grams, P.E. and Schmidt, J.C., 2002. Streamflow Regulation and Multi-Level Flood Plain Formation: Channel Narrowing on the Aggrading Green River in the Eastern Uinta Mountains, Colorado and Utah. Geomorphology 44, 337-360.

Grams, P.E. and Schmidt, J.C., 2005. Equilibrium or Indeterminate? Where Sediment Budgets Fail: Sediment Mass Balance and Adjustment of Channel Form, Green River Downstream from Flaming Gorge Dam, Utah and Colorado. Geomorphology 71, 156-181.

Grant, G.E., Schmidt, J.C., and Lewis, S.L., 2003. A Geological Framework for Interpreting Downstream Effects of Dams on Rivers. In: Grant, G.E., O'Connor, J.E. (Eds.), A Peculiar River: Geology, Geomorphology, and Hydrology of the Deschutes River, Oregon. American Geophysical Union, Washington, DC, pp. 203-219.

Haschenburger, J.K. and Wilcock, P.R., 2003. Partial Transport in a Natural Gravel Bed Channel. Water Resources Research 39 (1), 1020, doi:10.1029/2002WR001532.

Interagency Advisory Committee on Water Data, 1982. Guidelines for Determining Flood Flow Frequency, Bulletin #17B of the Hydrology Subcommittee. U.S. Department of the Interior. Reston, VA.

Johnson, W.C., 1994. Woodland Expansion in the Platte River, Nebraska: Patterns and Causes. Ecological Monographs 64 (1), 45-84.

Johnson, W.C., 1998. Adjustment of Riparian Vegetation to River Regulation in the Great Plains, USA. Wetlands 18 (4) 608-618.

Knighton, A.D., 1972. Changes in a Braided Reach. Geological Society of America Bulletin 83, 3813-3822.

Knighton, A.D., 1998. Fluvial Forms and Processes: A New Perspective. Oxford University Press, Inc., New York, NY. 383 pp.

Komura, S. and Simmons, D.B., 1967. River-bed Degradation Below Dams. Journal of the Hydraulics Division, Proceedings of the American Society of Civil Engineers HY4, 1-14.

Lagasse, P.F., 1981. Geomorphic Response of the Rio Grande to Dam Construction. New Mexico Geological Society, Special Publication 10, 27-46.

Leopold, L.B., 1994. A View of the River. Harvard University Press, Cambridge, MA. 298 pp.

Leopold, L.B. and Wolman, M.G., 1957. River Channel Patterns: Braided, Meandering and Straight. U.S. Geological Survey Professional Paper, 282-B.

Linsley, R.K., Kohler, M.A., and Paulhus, J.L.H., 1982. Hydrology for Engineers. McGraw-Hill, New York, NY. 508 pp.

Love, D.L., Reed, J.C., and Pierce, K.L., 2003. Creation of the Teton Landscape: A Geological Chronicle of Jackson Hole and The Teton Range. Grand Teton Natural History Association, Moose, WY. 132 pp.

Magilligan, F.J. and Nislow, K.H., 2005. Changes in Hydrologic Regime by Dams. Geomorphology 71, 61-78.

Marston, R.A., Mills, J.D., Wrazien, D.R., Bassett, B., and Splinter, D.K., 2005. Effects of Jackson Lake Dam on the Snake River and its floodplain, Grand Teton National Park, Wyoming, USA. Geomorphology 71, 79-98.

Mills, J.D., 1991. Wyoming's Jackson Lake Dam, Horizontal Channel Stability, and Floodplain Vegetation Dynamics. Masters Thesis from the University of Wyoming. Laramie, WY. 54 pp.

Mosley, M.P., 1981. Semi-determinate hydraulic geometry of river channels, South Island, New Zealand. Earth Surfaces, Processes, Landforms 6, 127-137.

Mostafa, M.G., 1957. River-Bed Degradation Below Large-Capacity Reservoirs. American Society of Civil Engineers Transactions, paper no. 2879, 122, 688-704.

Nanson, G.C. and Croke, J.C., 1992. A Genetic Classification of Floodplains. Geomorphology 4, 459-486.

Nelson, N.C., 2007. Hydrology and Geomorphology of the Snake River in Grand Teton National Park, WY. Master's thesis, Utah State University, Logan, UT. 126 pp.

Reinfelds, I. and Nanson, G., 1993. Formation of Braided River Floodplains, Waimakariri River, New Zealand. Sedimentology 40, 1113-1127.

Stevens, J.C., 1938. The Effect of Silt-Removal and Flow-Regulation on the Regimen of Rio Grande and Colorado Rivers. Transactions of the American Geophysical Union, 653-661.

Surian, N., 1999. Channel Changes Due to River Regulation: the Case of the Piave River, Italy. Earth Surface Processes and Landforms 24, 1135-1151.

Topping, D.J., Schmidt, J.C., and Vierra Jr., L.E., 2003. Computation and Analysis of the Instantaneous Discharge Record for the Colorado River at Lees Ferry, Arizona –

May 8, 1921 through September 30, 2000. U.S. Geological Survey Professional Paper, 1677.

U.S. Fish and Wildlife Service and Hoopa Valley Tribe, 1999. Trinity River Flow Evaluation Final Report, 308 pp.

Van Steeter, M.M. and Pitlick, J., 1998. Geomorphology and Endangered Fish Habitats of the Upper Colorado River: Historic Changes in Streamflow, Sediment Load, and Channel Morphology. Water Resources Research 34 (2), 287-302.

Williams, G.P. and Wolman, M.G., 1984. Downstream Effects of Dams on Alluvial Rivers. U.S. Geological Survey Professional Paper, 1286, pp. 83.

Wolman, M.G. and Leopold, L.B., 1957. River Flood Plains: Some Observations on their Formation. U.S. Geological Survey Professional Paper, 282-C, 87-107.

Wolman, M.G. and Miller, J.P., 1960. Magnitude and Frequency of Forces in Geomorphic Processes. Journal of Geology 68 (1), 54-74.

http://www.usbr.gov/pn/hydromet/arcread.html

TABLES

Table 2-1: Linear regressions used to estimate flows for the Snake River in Segments 2-4.

Two data series used to create regression	Regression for Mean Daily Flows (m^3/s)	R^2
Segments 1, 2	y = 1.1083x + 2.98	0.97
Segments 2, 3	y = 1.3005x + 2.60	0.96
Segments 3, 4	y = 1.0987x + 7.96	0.99

Table 2-2: Mean daily discharges in each segment of the Snake River for dates of photograph series.

	Discharge (m^3/s)			
Image Date	Segment 1	Segment 2	Segment 3	Segment 4
July 1, 1945	81	97	136	158
September 8, 1969	74	75	83	99
August 7, 1990	54	56	69	83
July 4, 1991	56	63	122	142
July 10, 2002	70	75	106	127

Table 2-3: Error associated with mapping the channel, georeferencing the aerial photographs, and overlaying or comparing two sets of aerial photographs. RMS = root mean square.

Year of Aerial Photograph	Scale of Photograph	Mapping Error (m)	RMS Error (m)	Total Linear Error (m)	Overlay Error (m)
1945	1:56,000	8	0.9	8	1945-1969: 9
1969	1:16,000	2	0.9	3	1969-1990/91: 9
1990/1991	1:56,000	8	0.7	8	1990/91-2002: 9
2002	1:12,000	2	0.0*	2	

* There was no RMS error for 2002 because these photographs were already orthorectified through physical control points.

Table 2-4: Channel area data from Mills (1991) recalculated to approximate bankfull channel area. "EOW" = edge of water; "BF" = bankfull.

Year of Aerial Photograph	Mills (EOW)	This study (EOW)	This study (BF)	Mills' EOW vs. this study's BF	Mills (recalculated for BF)
	Area (x 10^6 m^2)	Area (x 10^6 m^2)	Area (x 10^6 m^2)	% Difference	Area (x 10^6 m^2)
1945	4.50	5.11	5.93	31.8	5.85
1975	4.32	--	--	--	5.62
1989	4.40	--	--	--	5.72
1990/1991	--	4.77	5.65	28.4	--
Average				30.1	

Table 2-5: Location of tracers marked within the active Snake River channel in 2005.

Segment #	Location of Tracers
1 (Reach 2)	-river left -upstream end of bank-attached gravel bar
2 (Reach 6)	-river left -main channel side of mid-channel gravel bar
3-Deadmans Bar (Reach 16)	-river left -downstream of boat ramp on bank-attached gravel bar -also placed in main channel
3-Schwabachers Landing (Reach 17)	-river left -distributed across mid-channel bar
4-upstream of bridge (Reach 19)	-river left -distributed across mid-channel bar -also placed in main channel and secondary channel
4-downstream of bridge (Reach 19)	-river right -distributed across mid-channel bar -also placed in main channel

Table 2-6: Peak flows in 2005 for each segment of the Snake River based on mean daily discharges. The first flood was natural, the second due to regulation.

Reach of Snake River	Date	Discharge (m^3/s)	Date	Discharge (m^3/s)
Segment 1			June 15	117
Segment 2	May 21	92	June 15	133
Segment 3	May 21	170	June 18	183
Segment 4	May 21	174	June 18	192

Table 2-7: Magnitude of floods (m^3/s) of different recurrence intervals (RI) for the four segments of the Snake River. Estimated unregulated (Est. Unreg.) and measured flow magnitudes are provided for the periods before and after 1958.

	Segment 1		Segment 2		Segment 3		Segment 4	
RI	Est. Unreg.	Measured	Est. Unreg.	Measured	Est. Unreg.	Measured	Est. Unreg.	Measured
1916-1958								
1.25	217	185	263	211	345	282	387	318
2	276	230	334	255	434	340	485	381
5	338	285	409	317	534	419	595	468
10	371	319	449	358	590	472	656	526
1959-2005								
1.25	221	126	264	146	336	215	378	243
2	288	157	349	191	433	276	484	307
5	352	202	426	252	545	361	606	401
10	381	234	460	291	608	418	675	467

Table 2-8: Magnitude of flows (m^3/s) that were equaled or exceeded 1%, 10%, 50%, and 90% of each year in each time period. "Est. Unreg." = estimated unregulated.

	Segment 1		Segment 2		Segment 3		Segment 4	
% of year (# of days)	Est. Unreg.	Measured	Est. Unreg.	Measured	Est. Unreg.	Measured	Est. Unreg.	Measured
1916-1958								
1 (3.65)	264	255	322	287	423	376	472	419
10 (36.5)	111	141	135	157	180	202	206	238
50 (182.5)	17	1	19	17*	26	23*	36	33*
90 (328.5)	9	0.3	9	1*	14	5*	23	14*
1959-2005								
1 (3.65)	286	182	353	221	464	311	518	352
10 (36.5)	140	102	169	119	224	150	253	185
50 (182.5)	23	16	26	21	34	24	46	39
90 (328.5)	13	7	15	9	20	9	30	21

*Based on measured mean daily discharge for below Pacific Creek and Buffalo Fork from 1944 to 1958.

Table 2-9: Average channel change on the Snake River based on the maps of the 1945, 1969, 1990/1991, and 2002 aerial photographs. Reaches with asterisks are unstable, multi-thread reaches; all other reaches are stable and single-thread.

Reach #	Average Length (km)	Average Braid Index	Average Bankfull Width (m)	Average Channel Activity (m^2/km-yr)
1	1.99	1.00	71.4	10
2	1.66	1.94	96.0	280
3	2.39	1.37	99.9	80
4	2.59	1.00	96.1	0
5	0.302	1.00	70.8	550
6*	0.761	1.46	101	850
7*	0.214	1.70	139	1400
8*	1.97	3.14	155	3200
9	0.293	1.00	81.8	0
10*	2.59	1.58	99.0	1000
11	0.826	1.03	76.4	80
12	0.213	1.00	73.7	210
13*	1.81	1.49	110	2600
14	2.15	1.00	88.7	410
15*	5.94	2.18	148	4900
16	4.34	1.13	82.9	300
17*	10.4	2.82	155	6200
18*	1.36	3.10	160	5400
19	1.65	1.17	74.1	60
JLD to Moose	43.5	1.90	119	2800

Table 2-10: Changes in bankfull channel length (L) and area (A) for each reach of the Snake River. The ranges in error are 1% of the length and 5% of the area. Reaches with asterisks are unstable, multi-thread reaches; all other reaches are stable and single-thread.

	1945		1969		1990/1991		2002	
Reach #	L (km)	A (x 10^4 m^2)	L (km)	A (x 10^4 m^2)	L (km)	A (x 10^4 m^2)	L (km)	A (x 10^4 m^2)
1	1.99 ± 0.02	14.0 ± 0.7	1.99 ± 0.02	14.0 ± 0.7	2.00 ± 0.02	14.0 ± 0.7	1.99 ± 0.02	14.8 ± 0.7
2	1.66 ± 0.02	16.1 ± 0.8	1.67 ± 0.02	15.4 ± 0.8	1.66 ± 0.02	15.9 ± 0.8	1.65 ± 0.02	16.3 ± 0.8
3	2.40 ± 0.02	22.6 ± 1	2.40 ± 0.02	22.5 ± 1	2.38 ± 0.02	24.6 ± 1	2.39 ± 0.02	25.7 ± 1
4	2.59 ± 0.03	23.8 ± 1	2.58 ± 0.03	24.2 ± 1	2.59 ± 0.03	25.1 ± 1	2.59 ± 0.03	26.3 ± 1
5	0.305 ± 0.003	2.19 ± 0.1	0.295 ± 0.003	1.92 ± 0.1	0.306 ± 0.003	2.14 ± 0.1	0.303 ± 0.003	2.30 ± 0.1
6*	0.765 ± 0.008	7.55 ± 0.4	0.753 ± 0.008	7.22 ± 0.4	0.760 ± 0.008	7.88 ± 0.4	0.764 ± 0.008	8.13 ± 0.4
7*	0.253 ± 0.003	2.64 ± 0.1	0.234 ± 0.002	2.57 ± 0.1	0.177 ± 0.002	3.30 ± 0.2	0.193 ± 0.002	3.36 ± 0.2
8*	2.00 ± 0.02	31.4 ± 2	2.06 ± 0.02	27.5 ± 1	1.82 ± 0.02	31.1 ± 2	2.00 ± 0.02	32.0 ± 2
9	0.292 ± 0.003	2.43 ± 0.1	0.293 ± 0.003	2.43 ± 0.1	0.294 ± 0.003	2.39 ± 0.1	0.294 ± 0.003	2.34 ± 0.1
10*	2.45 ± 0.02	26.6 ± 1	2.58 ± 0.03	23.9 ± 1	2.62 ± 0.03	24.8 ± 1	2.72 ± 0.03	27.1 ± 1
11	0.827 ± 0.008	6.52 ± 0.3	0.824 ± 0.008	6.20 ± 0.3	0.826 ± 0.008	6.33 ± 0.3	0.825 ± 0.008	6.19 ± 0.3
12	0.213 ± 0.002	1.67 ± 0.08	0.213 ± 0.002	1.52 ± 0.1	0.213 ± 0.002	1.54 ± 0.08	0.212 ± 0.002	1.55 ± 0.08
13*	1.62 ± 0.02	18.4 ± 0.9	1.78 ± 0.02	16.4 ± 0.8	1.87 ± 0.02	21.0 ± 1	1.95 ± 0.02	23.8 ± 1
14	2.12 ± 0.02	19.4 ± 1	2.14 ± 0.02	18.0 ± 0.9	2.15 ± 0.02	18.7 ± 0.9	2.17 ± 0.02	20.2 ± 1
15*	6.23 ± 0.06	87.8 ± 4	5.83 ± 0.06	75.3 ± 4	5.69 ± 0.06	88.0 ± 4	5.99 ± 0.06	99.3 ± 5
16	4.30 ± 0.04	36.2 ± 2	4.35 ± 0.04	33.4 ± 2	4.34 ± 0.04	36.8 ± 2	4.36 ± 0.04	37.5 ± 2
17*	10.4 ± 0.1	173 ± 9	10.7 ± 0.1	120 ± 6	10.1 ± 0.1	157 ± 8	10.5 ± 0.1	196 ± 10
18*	1.32 ± 0.01	19.7 ± 1	1.25 ± 0.01	19.2 ± 1	1.38 ± 0.01	23.6 ± 1	1.48 ± 0.01	24.2 ± 1
19	1.66 ± 0.02	12.7 ± 0.6	1.65 ± 0.02	12.2 ± 0.6	1.65 ± 0.02	11.5 ± 0.6	1.65 ± 0.02	12.5 ± 0.6
JLD to Moose	43.4 ± 0.4	525 ± 30	43.6 ± 0.4	444 ± 20	42.8 ± 0.4	516 ± 30	44.0 ± 0.4	580 ± 30

Table 2-11: Channel activity (CA) and net channel change (NCC) for each reach of the Snake River. Positive NCC means net deposition, negative means net erosion. Ranges in error are based on a 1% error in reach length calculations. Reaches with asterisks are unstable, multi-thread reaches; all other reaches are stable and single-thread.

Reach #	Average Length (km)	1945-1969		1969-1990/1991		1990/1991-2002	
		CA (m^2/km-yr)	NCC (m^2/km-yr)	CA (m^2/km-yr)	NCC (m^2/km-yr)	CA (m^2/km-yr)	NCC (m^2/km-yr)
1	1.99	10	-10	0	0	20	20
2	1.66	160	160	180	-140	510 ± 10	-20
3	2.39	80	10	70	-70	100	50
4	2.59	0	0	0	0	0	0
5	0.302	670 ± 10	670 ± 10	640 ± 10	-350	330	-330
6*	0.761	670 ± 10	240	1300 ± 10	-450	580 ± 10	-480
7*	0.214	2300 ± 20	500 ± 10	1300 ± 10	-1300 ± 10	650 ± 10	130
8*	1.97	2900 ± 30	790 ± 10	2700 ± 30	-680 ± 10	4000 ± 40	-920 ± 10
9	0.293	0	0	0	0	0	0
10*	2.59	960 ± 10	500 ± 10	680 ± 10	-70	1400 ± 10	-830 ± 10
11	0.826	120	120	10	-10	110	-110
12	0.213	280	280	350	-200	0	0
13*	1.81	2500 ± 30	420	2500 ± 30	-1100 ± 10	2900 ± 30	-1500 ± 20
14	2.15	270	270	140	-140	810 ± 10	-740 ± 10
15*	5.94	5000 ± 50	790 ± 10	4500 ± 50	-910 ± 10	5200 ± 50	-1800 ± 20
16	4.34	330	220	210	-120	360	-250
17*	10.4	5000 ± 50	1800 ± 20	4500 ± 50	-1700 ± 20	9200 ± 90	-3100 ± 30
18*	1.36	3000 ± 30	240	5500 ± 60	-1000 ± 10	7800 ± 80	-1100 ± 10
19	1.65	50	50	130	80	0	0
JLD to Moose	43.5	2300 ± 20	710 ± 10	2200 ± 20	-680 ± 10	3800 ± 40	-1300 ± 10

Table 2-12: Change in bankfull channel width (W) of the Snake River by reach. Ranges in error are 6% of the width. Values in bold are changes in width greater than the total error between each series of photographs. Reaches with asterisks are unstable, multi-thread reaches; all other reaches are stable and single-thread.

Reach #	Average Length (km)	1945 W (m)	1969 W (m)	1990/1991 W (m)	2002 W (m)	Change in W (m) 1945 to 1969	Change in W (m) 1969 to 1990/1991	Change in W (m) 1990/1991 to 2002
1	1.99	70.4 ± 4	70.4 ± 4	70.4 ± 4	74.4 ± 4	0 ± 8	0 ± 8	4.0 ± 8
2	1.66	97.0 ± 6	92.8 ± 6	95.8 ± 6	98.2 ± 6	-4.2 ± 12	3.0 ± 12	2.4 ± 12
3	2.39	94.6 ± 6	94.1 ± 6	103 ± 6	108 ± 6	-0.5 ± 12	8.9 ± 12	5.0 ± 12
4	2.59	91.9 ± 6	93.4 ± 6	96.9 ± 6	102 ± 6	1.5 ± 12	3.5 ± 12	5.1 ± 12
5	0.302	72.5 ± 4	63.6 ± 4	70.9 ± 4	76.2 ± 5	**-8.9 ± 8**	7.3 ± 8	5.3 ± 9
6*	0.761	99.2 ± 6	94.9 ± 6	104 ± 6	107 ± 6	-4.3 ± 12	9.1 ± 12	3.0 ± 12
7*	0.214	123 ± 7	120 ± 7	154 ± 9	157 ± 9	-3.0 ± 14	**34.0 ± 16**	3.0 ± 18
8*	1.97	159 ± 10	140 ± 8	158 ± 9	162 ± 10	**-19.0 ± 18**	**18.0 ± 17**	4.0 ± 19
9	0.293	82.9 ± 5	82.9 ± 5	81.6 ± 5	79.9 ± 5	0 ± 10	-1.3 ± 10	-1.7 ± 10
10*	2.59	103 ± 6	92.3 ± 6	95.8 ± 6	105 ± 6	-10.7 ± 12	3.5 ± 12	9.2 ± 12
11	0.826	78.9 ± 5	75.1 ± 5	76.6 ± 5	74.9 ± 4	-3.8 ± 10	1.5 ± 10	-1.7 ± 9
12	0.213	78.4 ± 5	71.4 ± 4	72.3 ± 4	72.8 ± 4	-7.0 ± 9	0.9 ± 8	0.5 ± 8
13*	1.81	102 ± 6	90.6 ± 5	116 ± 7	131 ± 8	**-11.4 ± 11**	**25.4 ± 12**	**15.0 ± 15**
14	2.15	90.2 ± 5	83.7 ± 5	87.0 ± 5	94.0 ± 6	-6.5 ± 10	3.3 ± 10	7.0 ± 11
15*	5.94	148 ± 9	127 ± 8	148 ± 9	167 ± 10	**-21.0 ± 17**	**21.0 ± 17**	**19.0 ± 19**
16	4.34	83.4 ± 5	77.0 ± 5	84.8 ± 5	86.4 ± 5	-6.4 ± 10	7.8 ± 10	1.6 ± 10
17*	10.4	166 ± 10	115 ± 7	151 ± 9	188 ± 11	**-51.0 ± 17**	**36.0 ± 16**	**37.0 ± 20**
18*	1.36	145 ± 9	141 ± 8	174 ± 10	178 ± 11	-4.0 ± 17	**33.0 ± 18**	4.0 ± 21
19	1.65	77.0 ± 5	73.9 ± 4	69.7 ± 4	75.8 ± 5	-3.1 ± 9	-4.2 ± 8	6.1 ± 9
JLD to Moose	43.5	121 ± 7	102 ± 6	119 ± 7	133 ± 8	-19.0 ± 13	17.0 ± 13	14 ± 15

Table 2-13: Braid index (BI) by reach calculated as the ratio of total channel length to main channel length, MCL. Total channel length is the sum of the MCL and side channel length, SCL. Δ BI = change in braid index between photograph series. Ranges in error are the combination of 1% error from the two photograph series being compared. Reaches with asterisks are unstable, multi-thread reaches; all other reaches are stable and single-thread.

	1945			1969			1990/1991			2002			Δ BI		
Reach #	MCL (km)	SCL (km)	BI	MCL (km)	SCL (km)	BI	MCL (km)	SCL (km)	BI	MCL (km)	SCL (km)	BI	1945-1969	1969-1990/1991	1990/1991-2002
1	1.99	0.000	1.00	1.99	0.000	1.00	2.00	0.000	1.00	1.99	0.000	1.00	0.00	0.00	0.00
2	1.66	1.42	1.86	1.67	1.71	2.02	1.66	1.61	1.97	1.65	1.47	1.89	0.16 ± 0.04	-0.05 ± 0.04	-0.08 ± 0.04
3	2.40	0.981	1.41	2.40	0.828	1.35	2.38	0.742	1.31	2.39	0.939	1.39	-0.06 ± 0.02	-0.04 ± 0.02	0.08 ± 0.02
4	2.59	0.000	1.00	2.58	0.000	1.00	2.59	0.000	1.00	2.59	0.000	1.00	0.00	0.00	0.00
5	0.305	0.000	1.00	0.295	0.000	1.00	0.306	0.000	1.00	0.303	0.000	1.00	0.00	0.00	0.00
6*	0.765	0.000	1.00	0.753	0.535	1.71	0.760	0.415	1.55	0.764	0.436	1.57	0.71 ± 0.01	-0.16 ± 0.02	0.02 ± 0.02
7*	0.253	0.199	1.79	0.234	0.203	1.87	0.177	0.107	1.60	0.193	0.101	1.52	0.08 ± 0.04	-0.27 ± 0.03	-0.08 ± 0.02
8*	2.00	2.39	2.20	2.06	4.64	3.25	1.82	4.79	3.63	2.00	4.93	3.47	1.05 ± 0.07	0.38 ± 0.11	-0.16 ± 0.11
9	0.292	0.000	1.00	0.293	0.000	1.00	0.294	0.000	1.00	0.294	0.000	1.00	0.00	0.00	0.00
10*	2.45	1.28	1.52	2.58	1.74	1.67	2.62	1.54	1.59	2.72	1.47	1.54	0.15 ± 0.03	-0.08 ± 0.03	-0.05 ± 0.02
11	0.827	0.000	1.00	0.824	0.099	1.12	0.826	0.000	1.00	0.825	0.000	1.00	0.12 ± 0.00	-0.12 ± 0.00	0.00
12	0.213	0.000	1.00	0.213	0.000	1.00	0.213	0.000	1.00	0.212	0.000	1.00	0.00	0.00	0.00
13*	1.62	0.58	1.36	1.78	0.903	1.51	1.87	0.902	1.48	1.95	1.20	1.62	0.15 ± 0.02	-0.03 ± 0.02	0.14 ± 0.02
14	2.12	0.000	1.00	2.14	0.000	1.00	2.15	0.000	1.00	2.17	0.000	1.00	0.00	0.00	0.00
15*	6.23	7.00	2.12	5.83	8.86	2.52	5.69	5.14	1.90	5.99	7.04	2.18	0.40 ± 0.05	-0.62 ± 0.05	0.28 ± 0.04
16	4.30	0.31	1.07	4.35	0.732	1.17	4.34	0.724	1.17	4.36	0.528	1.12	0.10 ± 0.00	0.00	-0.05 ± 0.00
17*	10.4	13.0	2.25	10.7	16.3	2.52	10.1	22.0	3.18	10.5	24.6	3.34	0.27 ± 0.05	0.66 ± 0.07	0.16 ± 0.08
18*	1.32	3.24	3.45	1.25	3.75	4.00	1.38	1.60	2.16	1.48	2.65	2.79	0.55 ± 0.10	-1.84 ± 0.08	0.63 ± 0.05
19	1.66	0.197	1.12	1.65	0.306	1.19	1.65	0.302	1.18	1.65	0.297	1.18	0.07 ± 0.00	-0.01 ± 0.00	0.00
JLD to Moose	43.4	30.6	1.71	43.6	40.6	1.93	42.8	39.9	1.93	44.0	45.7	2.04	0.22 ± 0.03	0.00 ± 0.04	0.11 ± 0.04

Table 2-14: Area, main channel length (MCL), width, and braid index values for the Snake River from JLD to Moose. Area data from 1975 and 1989 were modified from the maps of Mills (1991). Area calculations in this table include all side channels because we cannot determine side channels on 1975 and 1989, thus the discrepancy between these values and those in earlier tables. MCL, width, and braid index were calculated based on bankfull length measurements; without the aerial photographs from 1975 and 1989, we could not determine bankfull lengths for these maps. Ranges in error are 5% of the area, 1% of the MCL, 6% of the width, and 1% of the braid index.

Year of Map Series	Area (km2)	MCL (km)	Width (m)	Braid Index
1945	5.93 ± 0.297	43.4 ± 0.4	121 ± 7	1.71 ± 0.01
1969	5.18 ± 0.259	43.6 ± 0.4	102 ± 6	1.93 ± 0.02
1975	5.61 ± 0.281	--	--	--
1989	5.72 ± 0.286	--	--	--
1990/1991	5.65 ± 0.283	42.8 ± 0.4	119 ± 7	1.93 ± 0.02
2002	6.29 ± 0.315	44.0 ± 0.4	133 ± 8	2.04 ± 0.02

Table 2-15: Median grain size (D_{50}) of clasts in the vicinity of tracer rocks in each segment of the Snake River. Q = discharge during 2005 released flood; S = local slope based on surveys during 2005 released flood. Moose EP2 = study site above the bridge at Moose; Moose EP1 = study site below the bridge at Moose.

Segment	# of Clasts Measured	D_{50} (mm)	Q (m^3s)	S
1	225	45	125	0.0005
2	110	31	144	0.0021
3 (Deadmans Bar)	144	63	171	0.0021
3 (Schwabachers Landing)	226	98	170	0.0039
4 (Moose EP2)	113	65	175	0.0013
4 (Moose EP1)	110	62	175	0.0013

Table 2-16: Percent of clasts inundated by water that moved during peak flows.

	Tracers placed within active channel					Tracers marked in situ				
		All tracers that moved		Tracers that moved ≥1m			All tracers that moved		Tracers that moved ≥1m	
Segment	Total #	#	%	#	%	Total #	#	%	#	%
1	90	16	18	0	0	523	75	14	1	0.2
2	105	35	33	5	5	309	9	3	1	0.3
3	16	15	94	13	81	1232	90	7	25	2
4	53	43	81	26	49	1782	268	15	71	4

Table 2-17: Minimum (Min), maximum (Max), and median (Med) grain size (in mm) of tracers that moved in each segment of the Snake River based on the b-axis diameter.

	Tracers placed within active channel						Tracers marked in situ					
	All tracers that moved			Tracers that moved ≥ 1m			All tracers that moved			Tracers that moved ≥ 1m		
Segment	Min	Max	Med	Min	Max	Med	Min	Max	Med	Min	Max	Med
1	40	107	52	--	--	--	25	87	46	55	55	55
2	23	89	32	30	89	30	23	49	33	33	33	33
3	30	100	60	30	100	60	23	120	40	23	78	37
4	28	108	60	30	100	60	23	120	46	23	105	43

Table 2-18: Number of tracer clusters in each mobility category in each flood.

	In Situ Tracers			Placed Tracers		
Segment	Immobile	Partially Mobile	Fully Mobile	Immobile	Partially Mobile	Fully Mobile
Natural Flood – May 21						
1	--	--	--	--	--	--
2	1	0	0	7	0	1
3	16	3	0	4	0	0
4	18	0	0	18	0	0
Dam-Released Flood – June 15-18						
1	2	4	0	17	13	0
2	2	0	0	7	20	2
3	15	3	1	0	1	3
4	10	6	2	0	7	11

FIGURES

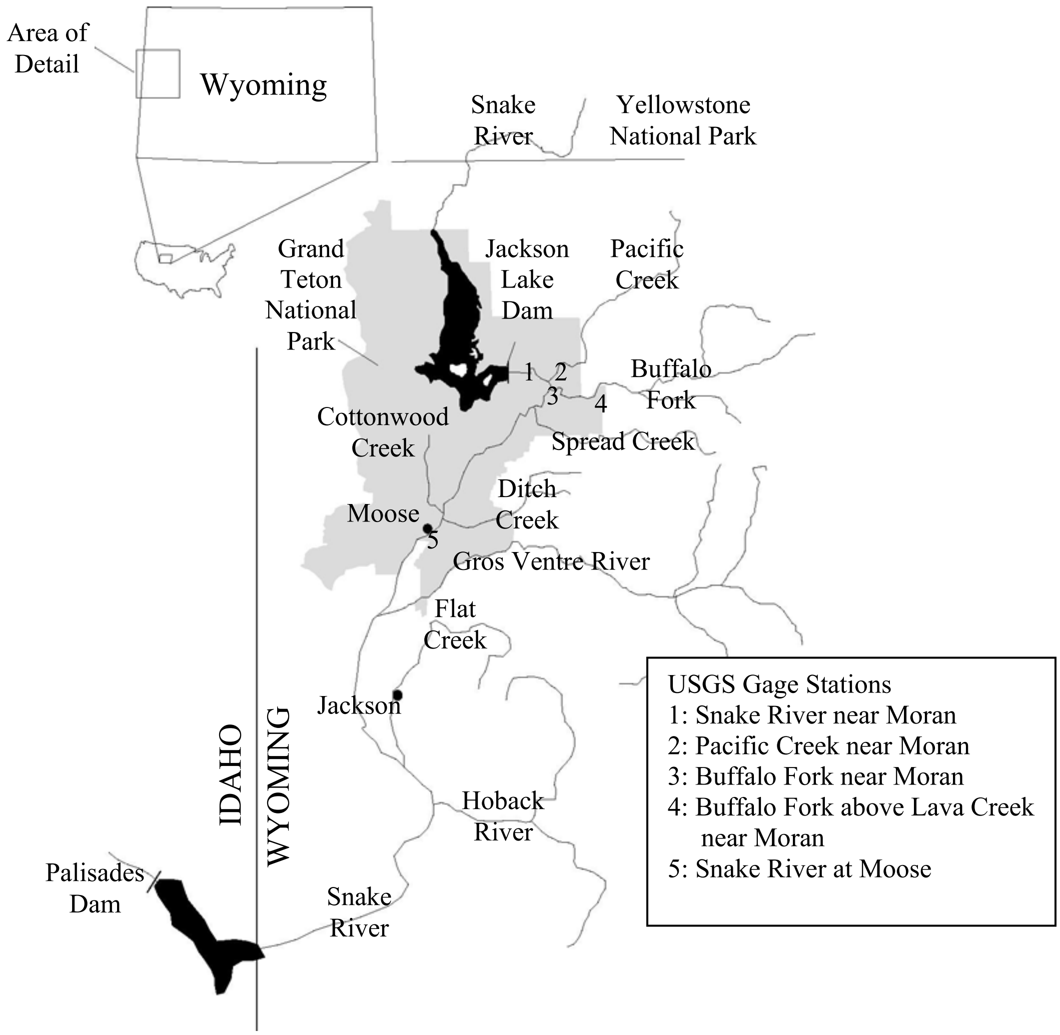

Figure 2-1: The Snake River as it flows from Yellowstone National Park to Palisades Reservoir. The study reach is from Jackson Lake Dam to Moose.

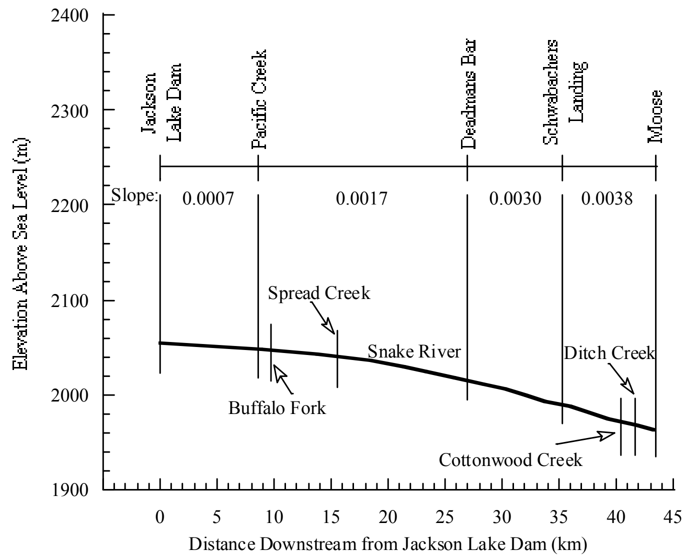

Figure 2-2: Longitudinal profile of the Snake River from JLD to Moose with tributaries and changes in slope indicated, based on 1:24,000 maps.

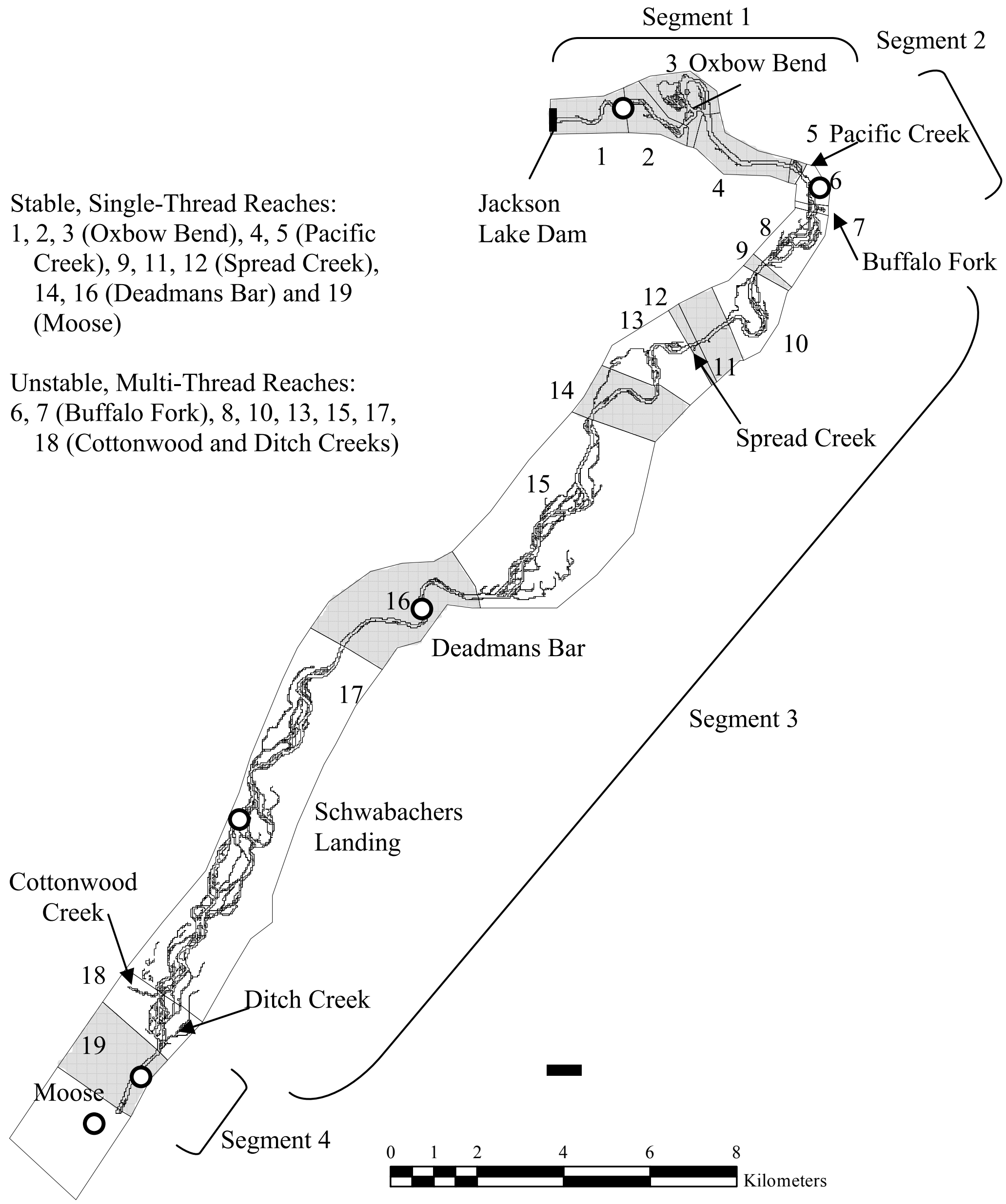

Figure 2-3: Map of the Snake River from JLD to Moose. Shaded reaches have stable, single-thread channels; the four segments are the portions of the river analyzed for hydrologic change; numbers refer to reaches analyzed for channel change, outlined with thin black lines; hollow circles are locations of painted rocks; the river channel is that of 2002.

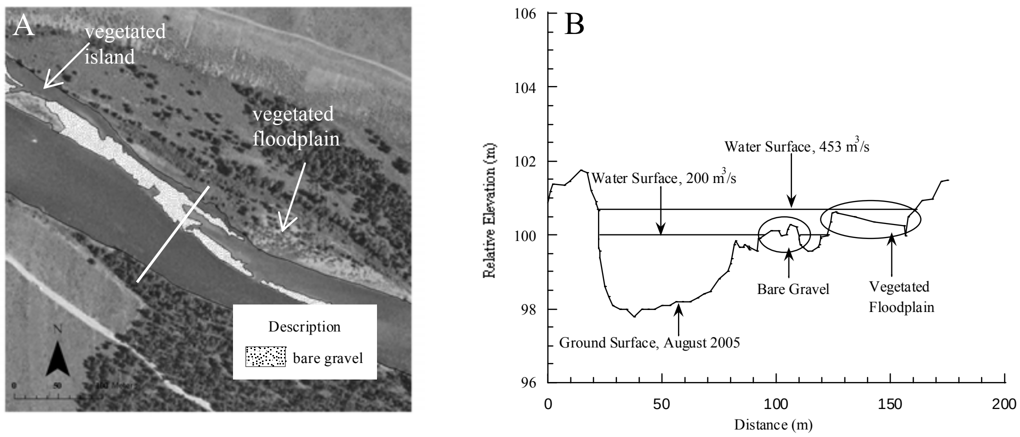

Figure 2-4: We identified bare gravel bars in aerial photographs and considered them part of the bankfull channel (A). The white line corresponds to the cross section in Figure 2-4B, in which these bare gravel bars are shown to be below the elevation of the vegetated floodplain.

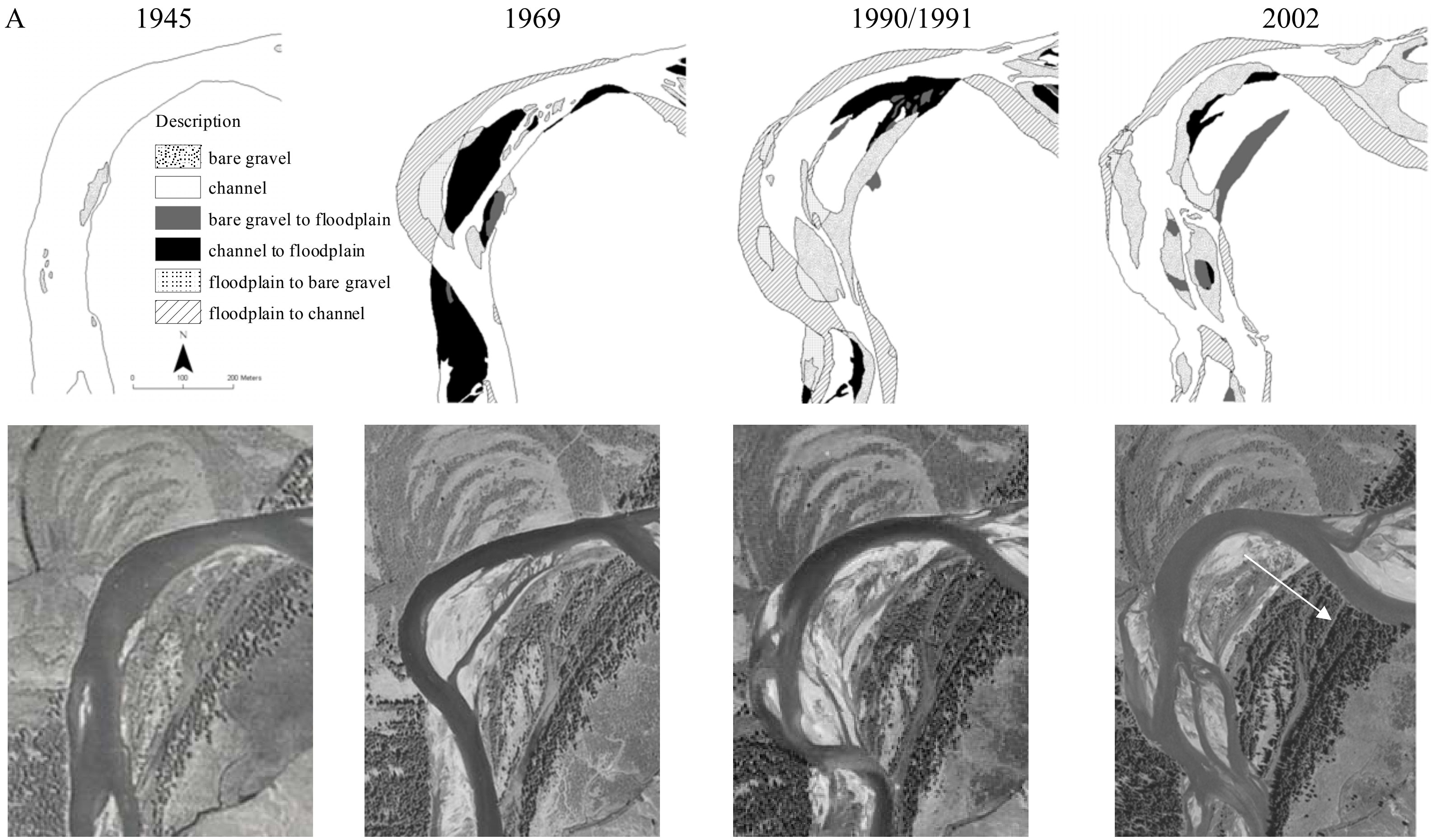

Figure 2-5A: Example of channel change from 1945 to 2002 about 0.5 km downstream from Spread Creek. Deposition occurred in areas identified as having changed from 'bare gravel to floodplain' and from 'channel to floodplain.' Erosion occurred in areas identified as having changed from 'floodplain to bare gravel' and from 'floodplain to channel.' White arrow corresponds to the view in Figure 2-5B.

Figure 2-5B: Ground photograph of the gravel bar in Figure 5A with varying stages of vegetation growth. Though the entire bar is at a similar elevation, the sparsely vegetated portion of the bar in the foreground was built after 1969, whereas the mature cottonwood/blue spruce floodplain furthest away was build prior to 1945.

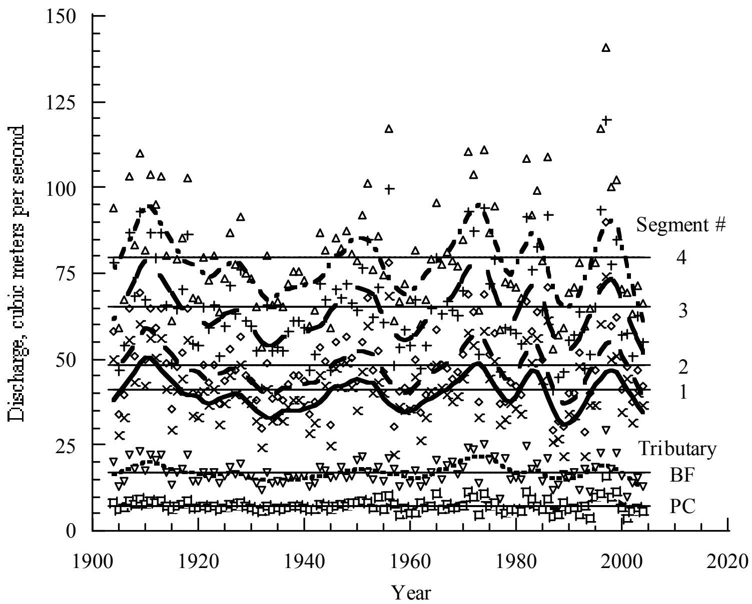

Figure 2-6: Mean annual flows for Segments 1 (x), 2 (◊), 3 (+), and 4 (Δ) of the Snake River and for the tributaries Pacific Creek (PC: □) and Buffalo Fork (BF: Q). Curve fit lines are locally weighted using the closest 10% of the data; solid horizontal lines are the average mean annual discharge over the entire period for each segment or tributary.

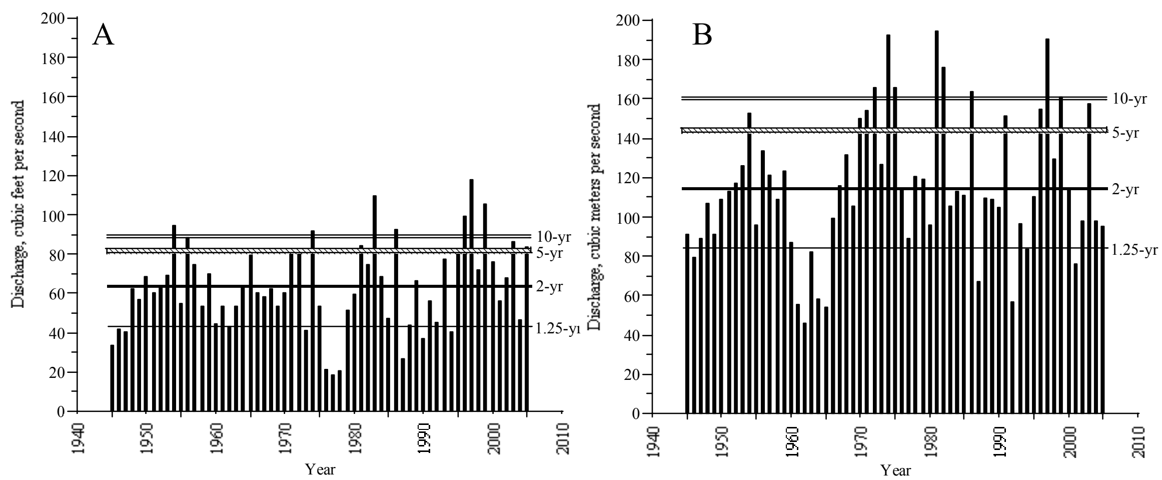

Figure 2-7: Peak flows for the two largest tributaries of the Snake River, A) Pacific Creek and B) Buffalo Fork. Data based on highest mean daily flow of each year for the period of record, 1945-2005. Horizontal lines represent magnitudes of floods of four recurrence intervals.

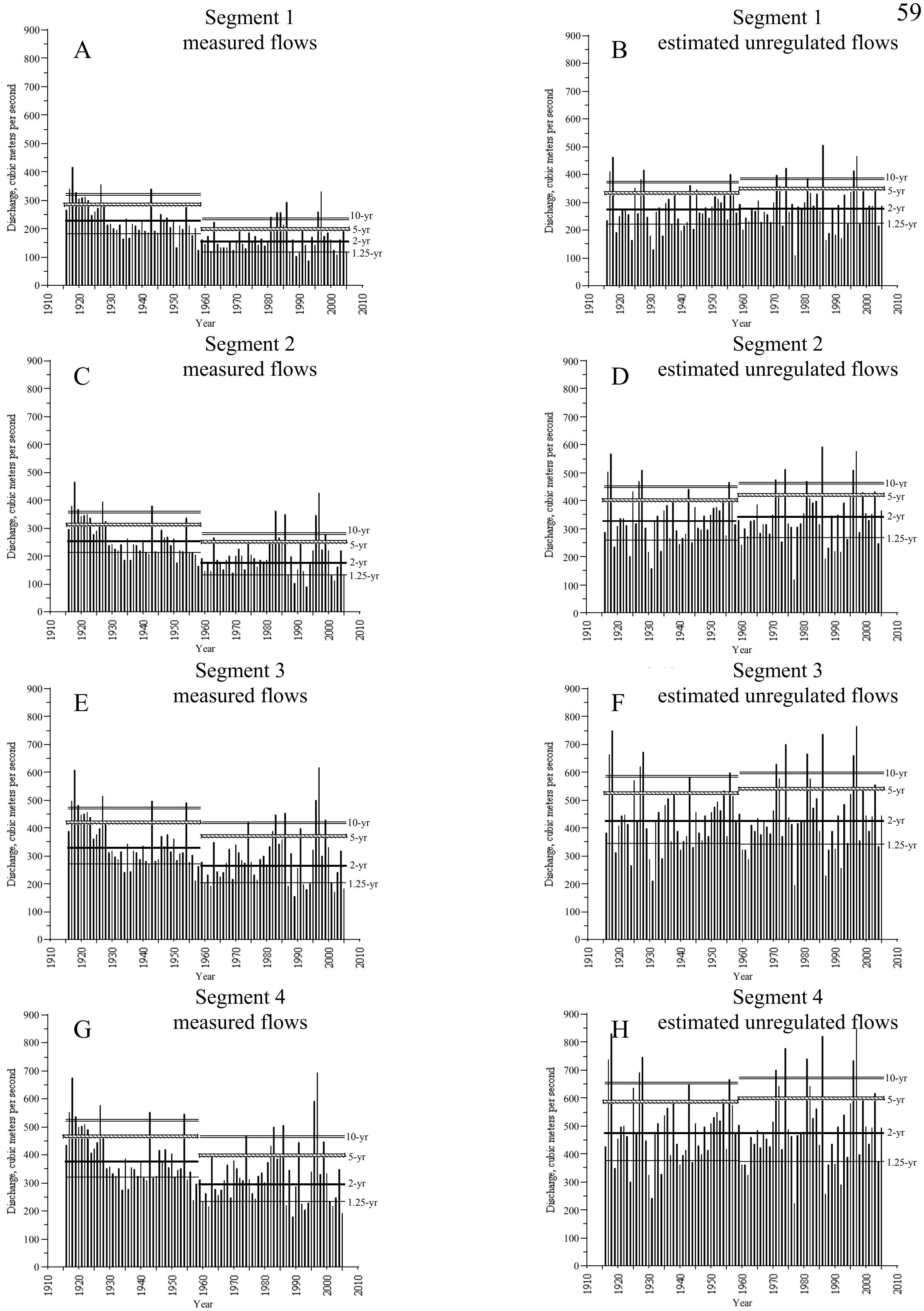

Figure 2-8: Peak flows based on highest mean daily flow of each year, 1916-2005. Horizontal lines indicate magnitudes of four recurrence floods before and after 1958.

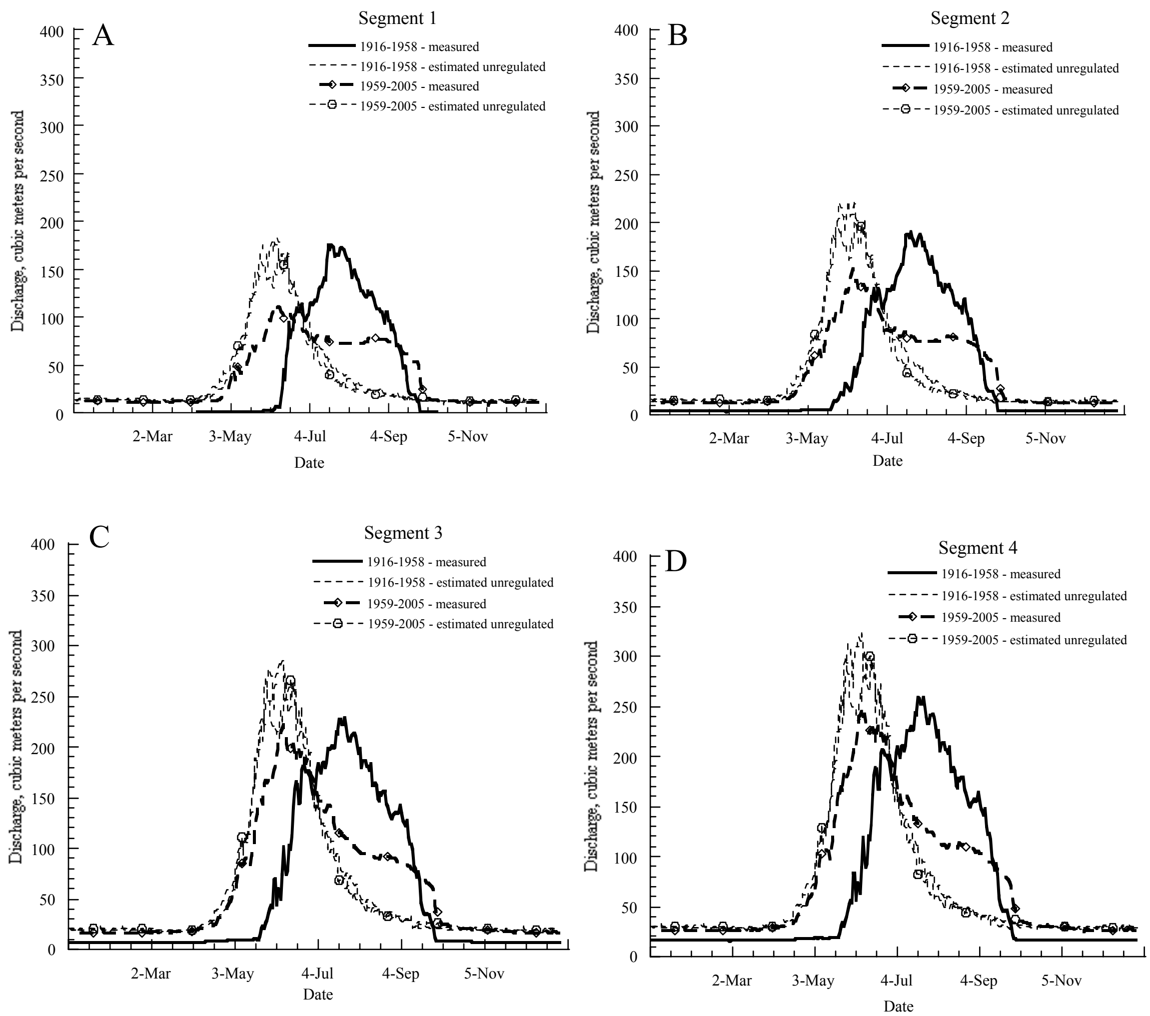

Figure 2-9: Average hydrographs for measured and estimated unregulated flows before and after 1958 for (A) Segment 1, (B) Segment 2, (C) Segment 3, and (D) Segment 4 of the Snake River. Each annual hydrograph is composed of the median mean daily discharge for each day for the indicated period.

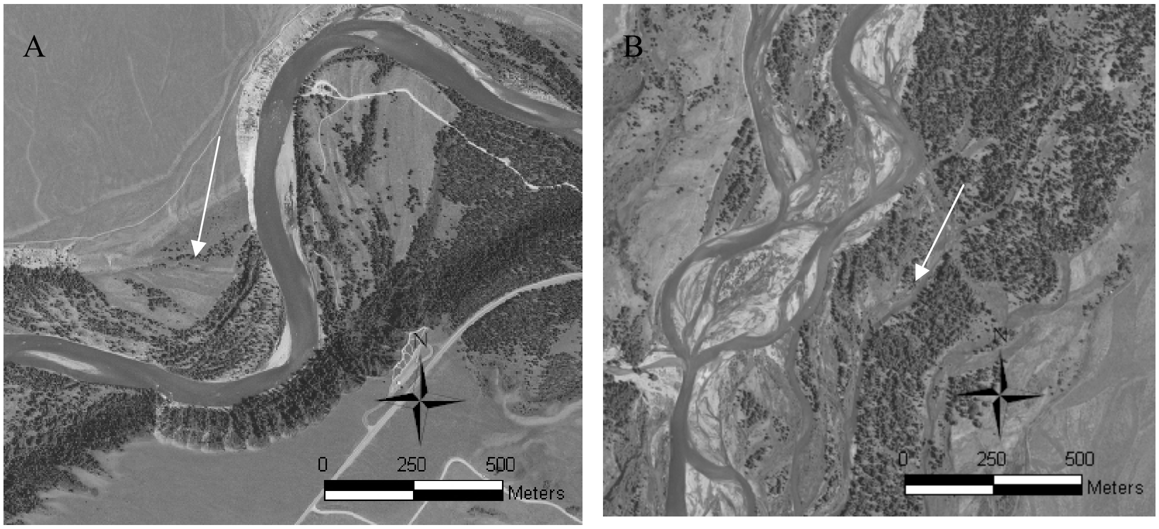

Figure 2-10: Examples of (A) a single-thread channel at Deadman's Bar and (B) a multi-thread channel near the confluence with Cottonwood Creek. Arrows indicate flow direction.

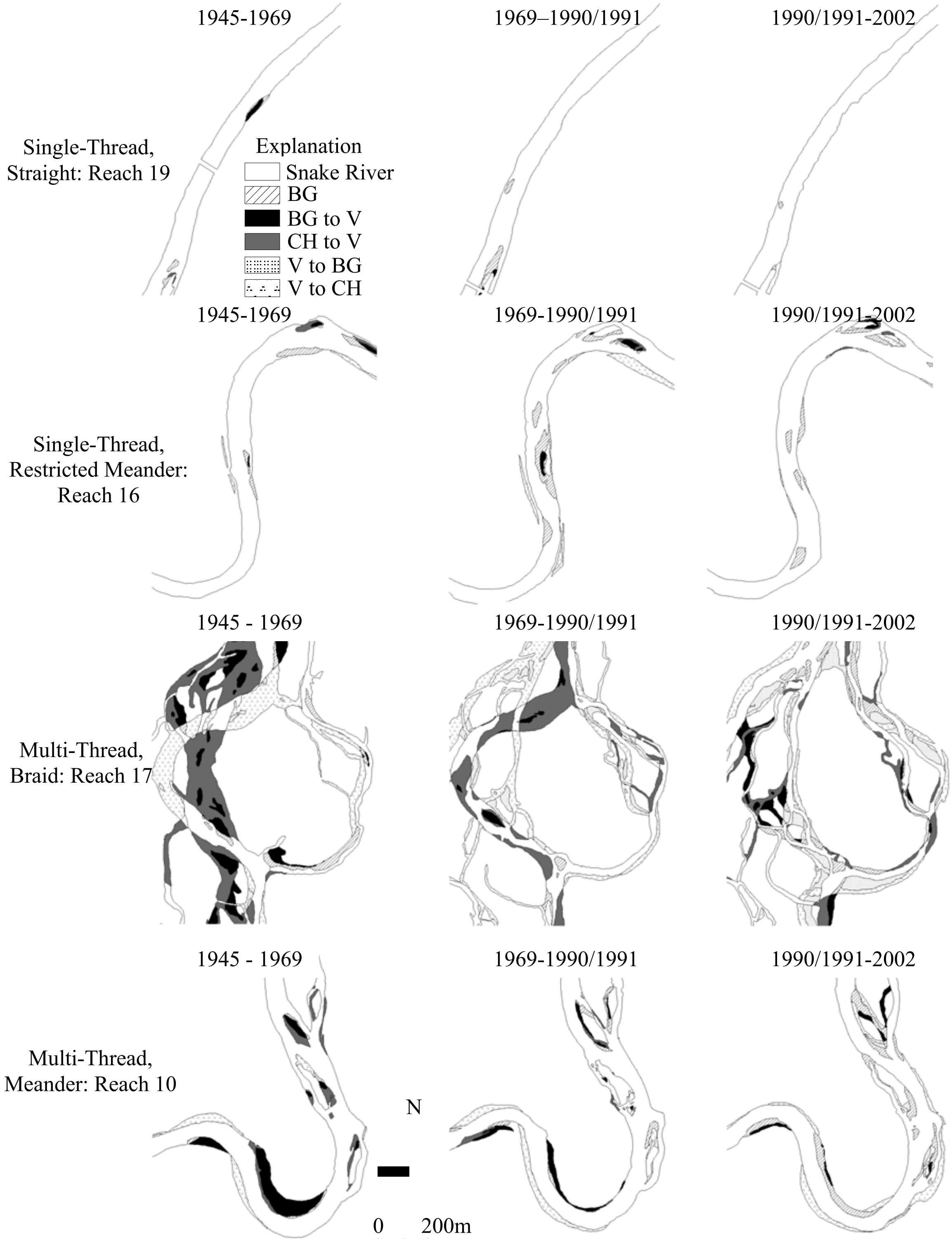

Figure 2-11: Examples of four types of channel along the Snake River and the erosion and deposition that occurred between photograph series. BG = bare gravel; V = vegetation; CH = channel; 'BG to V' = changed from bare gravel to vegetation in time period indicated. Flow direction is from the top to the bottom of the figures.

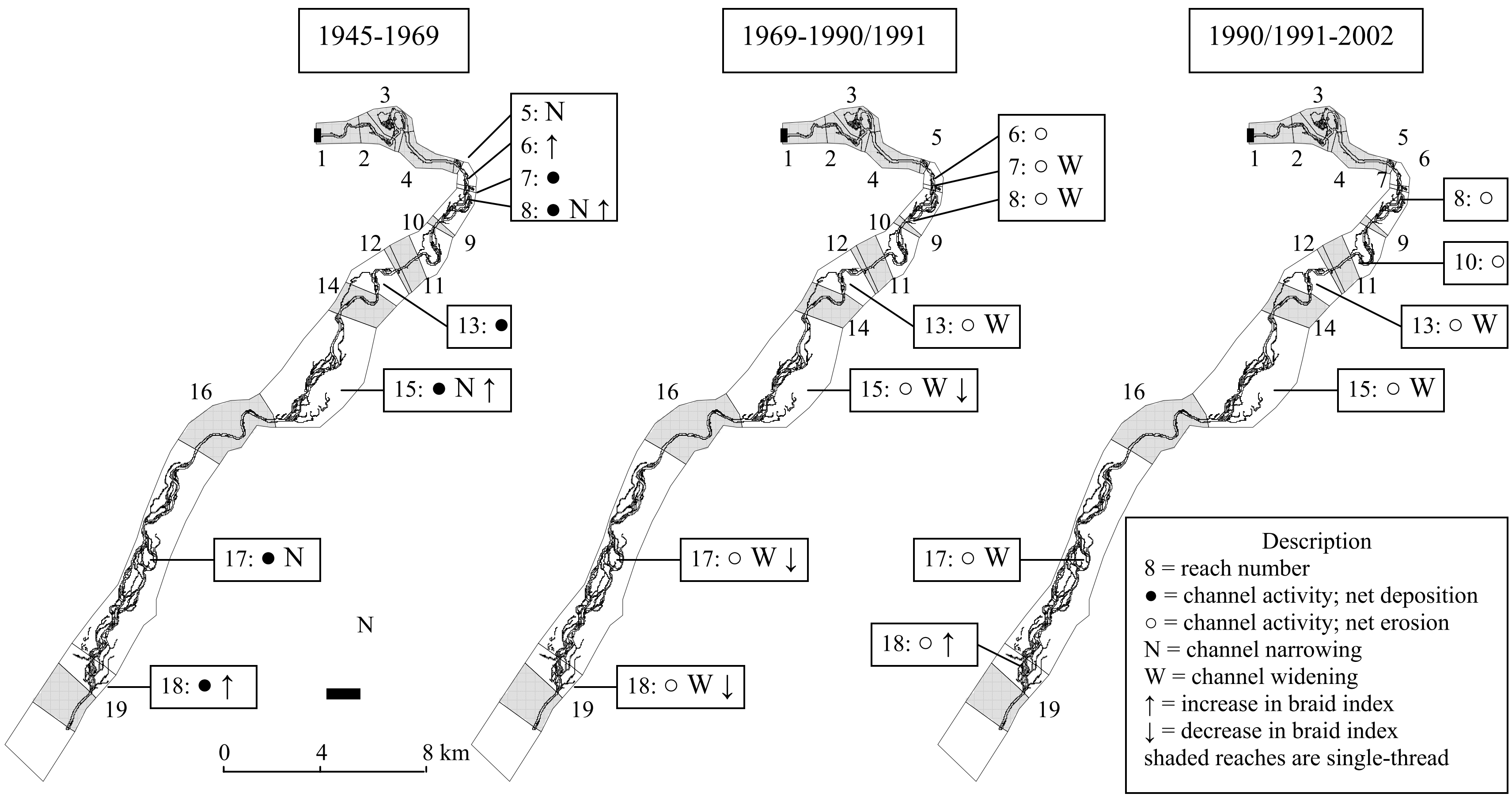

Figure 2-12: Substantial changes in channel activity (>1000 m^2/km-yr), bankfull channel width (> than total error inherent in methods), and braid index (> a change of 0.5) for the periods between years of aerial photography.

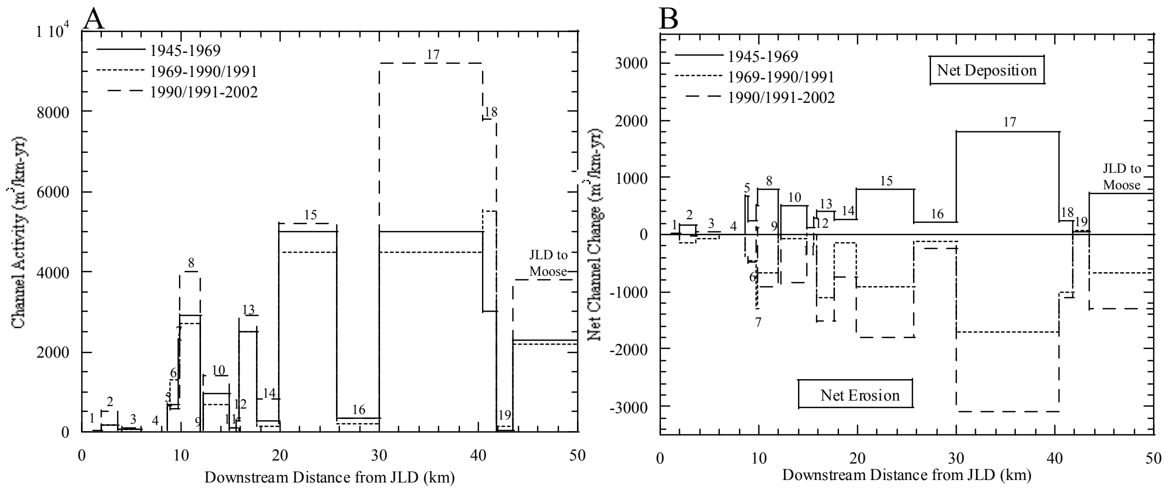

Figure 2-13: Annual length-weighted (A) total channel activity and (B) net channel change on the Snake River for each time period. Numbers within figures refer to the reach number. The stable, single-thread reaches are 1-4, 5 (Pacific Creek), 9, 11, 12 (Spread Creek), 14, 16, and 19; unstable, multi-thread reaches are 6, 7 (Buffalo Fork), 8, 10, 13, 15, 17, and 18 (Cottonwood and Ditch Creeks).

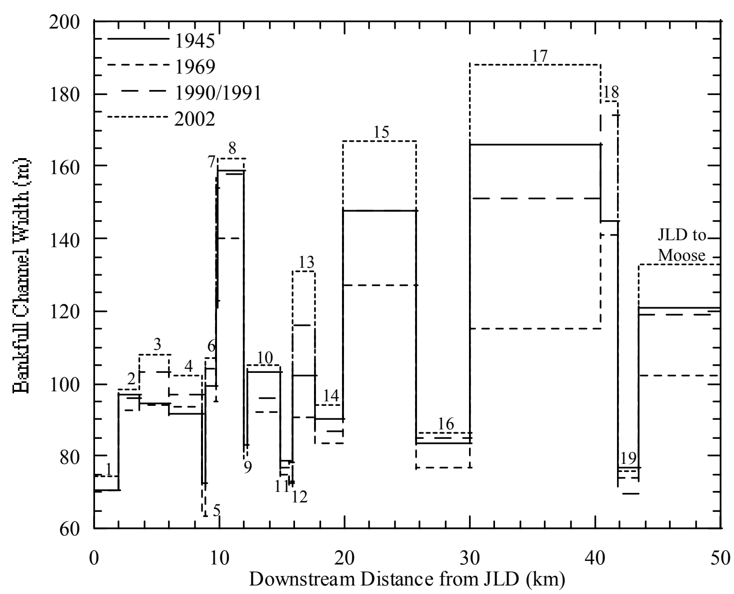

Figure 2-14: Bankfull channel width by reach for each photograph series. Numbers within figure refer to the reach number. The stable, single-thread reaches are 1-4, 5 (Pacific Creek), 9, 11, 12 (Spread Creek), 14, 16, and 19; unstable, multi-thread reaches are 6, 7 (Buffalo Fork), 8, 10, 13, 15, 17, and 18 (Cottonwood and Ditch Creeks).

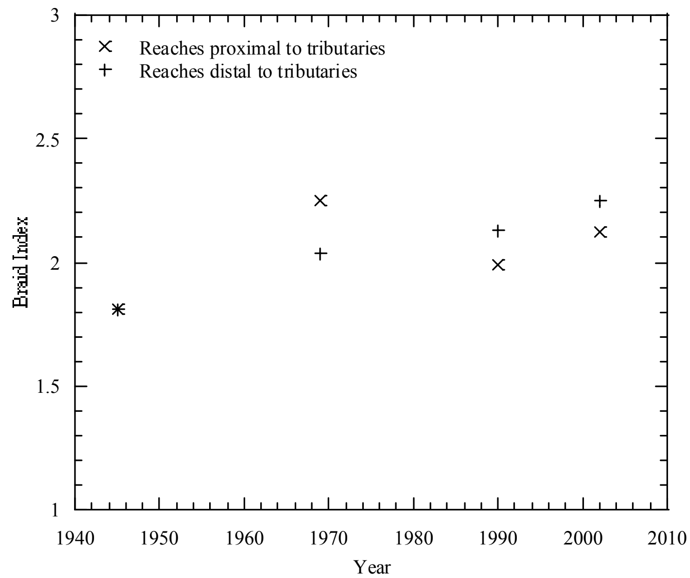

Figure 2-15: Changes in braid index between each series of aerial photographs for reaches proximal (Reaches 5-8, 12, 13, 18, and 19) and distal (9-11, 14-17) to tributaries.

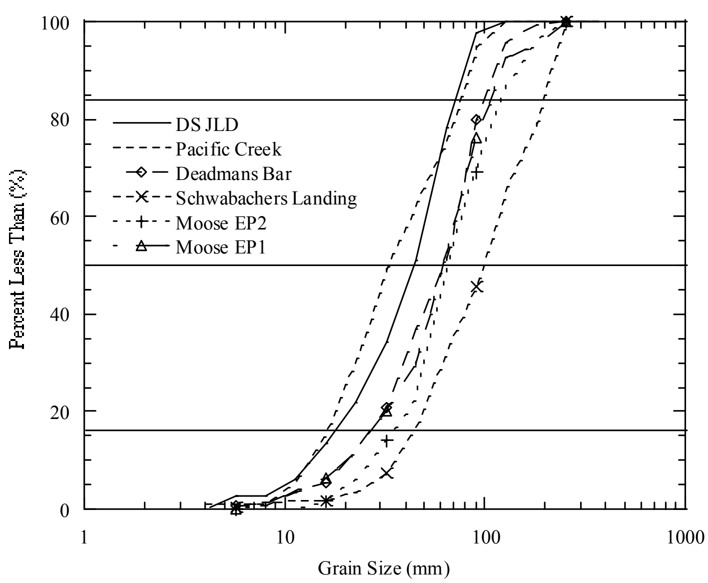

Figure 2-16: Grain size distribution for gravel bars on the Snake River. Each distribution represents the gravel bar at the location of tracer rocks. The horizontal lines are the 16th, 50th, and 84th percentiles. Moose EP2 refers to the endpoint and corresponding lines of rocks north of the bridge at Moose, and Moose EP1 refers to the endpoint and line of rocks south of the bridge. DS = downstream.

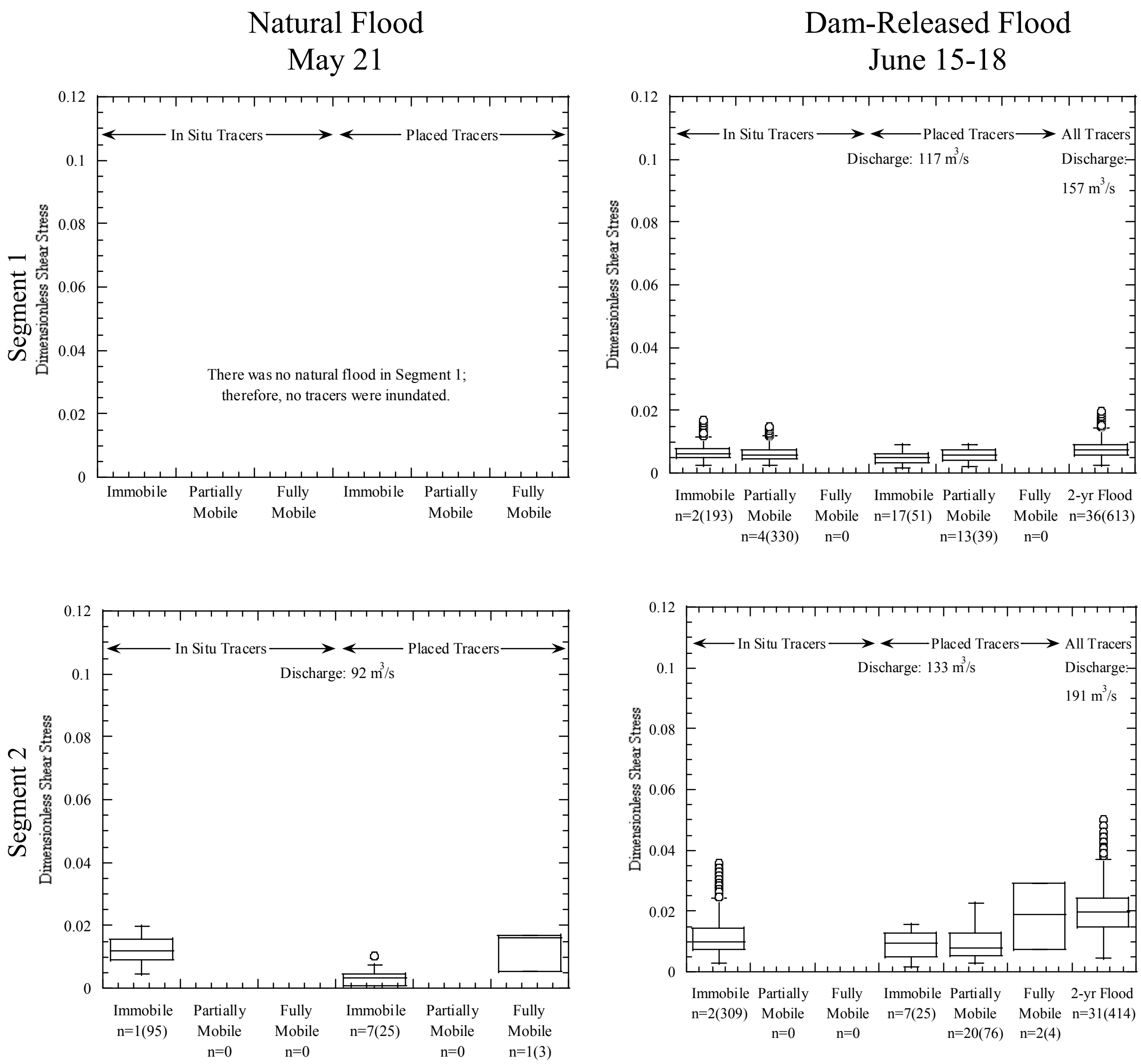
Natural Flood
May 21
Dam-Released Flood
June 15-18
Segment 1
Segment 2
Dimensionless Shear Stress
0.12
0.1
0.08
0.06
0.04
0.02
0
In Situ Tracers
Placed Tracers
All Tracers
There was no natural flood in Segment 1; therefore, no tracers were inundated.
Discharge: 117 m3/s
Discharge: 157 m3/s
Discharge: 92 m3/s
Discharge: 133 m3/s
Discharge: 191 m3/s
Immobile
Partially Mobile
Fully Mobile
Immobile n=2(193)
Partially Mobile n=4(330)
Fully Mobile n=0
Immobile n=17(51)
Partially Mobile n=13(39)
Fully Mobile n=0
2-yr Flood n=36(613)
Immobile n=1(95)
Partially Mobile n=0
Fully Mobile n=0
Immobile n=7(25)
Partially Mobile n=0
Fully Mobile n=1(3)
Immobile n=2(309)
Partially Mobile n=0
Fully Mobile n=0
Immobile n=7(25)
Partially Mobile n=20(76)
Fully Mobile n=2(4)
2-yr Flood n=31(414)

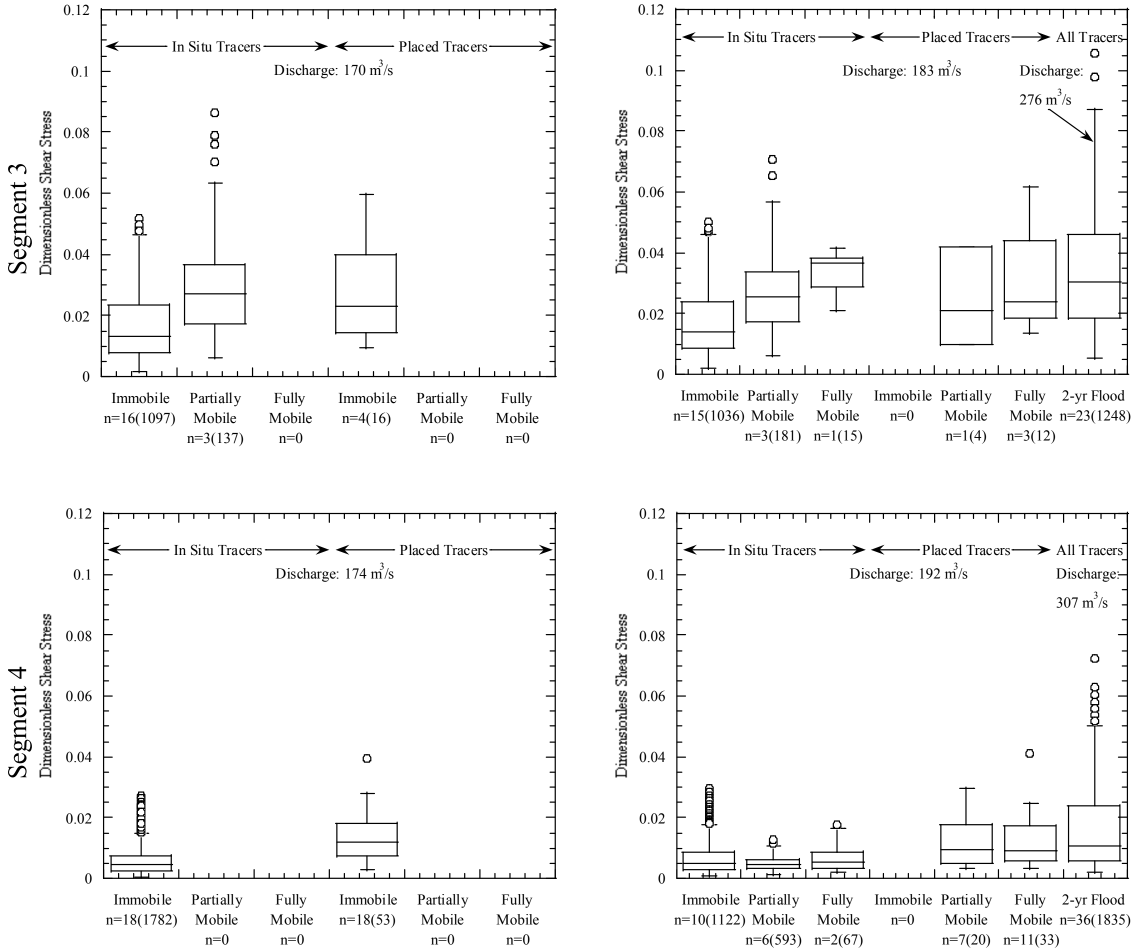

Figure 2-17: Dimensionless shear stress values calculated for tracers in each segment of the Snake River during the 2005 floods. Plots on the left represent the values in each mobility category during the first, natural flood, and those on the right during the second, dam-released flood. ‘In situ Tracers’ were those tracers marked in situ; ‘Placed Tracers’ were those tracers placed on gravel bars or in the low flow channel; ‘All Tracers’ included both in situ and placed tracers; locations of tracers that were ‘Immobile,’ ‘Partially Mobile,’ and ‘Fully Mobile’ were those with active proportions less than 10%, between 10 and 90%, and greater than 90% respectively; ‘2-yr Flood’ represents the dimensionless shear stress values for all tracers during a 2-yr recurrence flood; ‘n’ equals the number of tracer locations, with the number of individual tracers in parentheses. The horizontal line in the middle of each box represents the median value while the upper and lower limits of the box represent the upper and lower quartiles enclosing 25% of the values greater and less than the median value respectively. Hollow circles represent outliers, which are defined as either greater than the sum of the upper quartile and 1.5 times the interquartile distance (difference between the upper and lower quartiles), or less than the difference of the lower quartile and 1.5 times the interquartile distance. The vertical bars above and below the boxes represent the values between the outliers and the upper and lower quartiles.

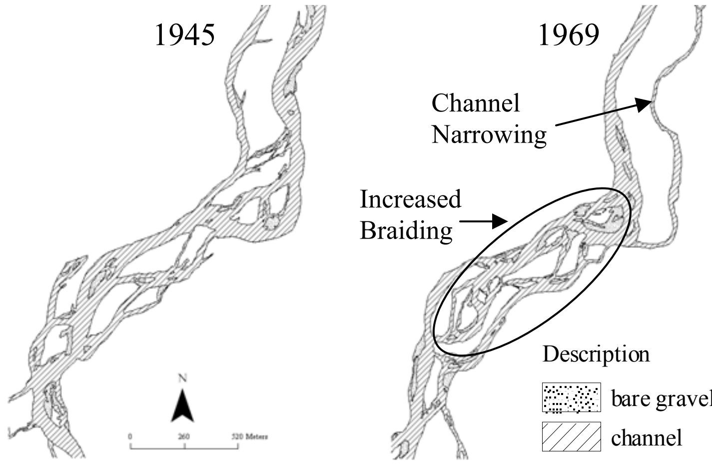

Figure 2-18: Example of a reach (Reach 15) experiencing both channel narrowing and an increase in braid index between 1945 and 1969.

CHAPTER 3

FLOODPLAIN CONSTRUCTION ON THE BRAIDED, GRAVEL-BED SNAKE RIVER, GRAND TETON NATIONAL PARK, WYOMING

Abstract

We identified four distinct alluvial deposits within the Snake River Holocene valley. The deposits were distinguished based on five characteristics: 1) elevation above the water surface at the time of the mapping, 2) stratigraphy, 3) surface textures, 4) associated facies, and 5) differences in vegetation. Bare gravel bars are less than 2 m above the water surface with less than 10% areal coverage of vegetation. These are clast-supported deposits containing sub-angular to rounded clasts, fine-grained gravel to cobble in size. The lower floodplain is 0.2 to 0.7 m above the water surface and is composed of up to two fine-grained layers of sediment overlying a basal layer of gravel and cobbles. The abandoned channel and channel-margin facies of the lower floodplain support grasses, scouring rush (*Equisetum* spp.), and small shrubs. The upper floodplain is up to 1.3 m higher in elevation than the lower floodplain and is made up of abandoned bars and channels that support grasses, saplings, and mature blue spruce (*Picea pungens*) and narrow-leaved cottonwood (*Populus angustifolia*). Up to 1.5 m of fine sediment overlies the basal layer of gravel and cobbles, similar in composition to the bare gravel bars and the coarse-grained layer of the lower floodplain. The lowest terrace is a relic floodplain, built by a previous flow regime and bed elevation, which is more than 2.0 m above the water surface and primarily supports sagebrush (*Artemisia* spp).

We estimated the inundating flows for the two floodplains and terrace by surveying the topography of the Holocene alluvial valley and conducting one-dimensional backwater flow modeling. The recurrence of inundating flows is 1.2 years for the lower floodplain and more than 10 years for the upper floodplain under the current, dam-regulated flow regime; under estimated unregulated conditions, the inundation recurrence for the upper floodplain is 1.9 years. The lowest terrace was likely never inundated during the period of record. We overlaid the maps of the alluvial deposits onto channel change maps drawn from aerial photographs taken in 1945, 1969, 1990/1991, and 2002 to estimate periods of floodplain deposition. Both floodplains have been built in all time periods, including before 1945, which was prior to the dam-induced flow regime change in 1958.

1. Introduction

Floodplains have received increased attention in recent decades from the scientific community due to their physical and biological importance to riparian corridors and local ecosystems (Martin and Johnson, 1987; Scott et al., 1997; Bendix and Hupp, 2000; Cooper et al., 2003). Floodplains are complex landforms that may be composed of multiple deposits at different elevations and often support swamps, lakes, and vegetation at various stages of maturity. This complexity has led to challenges in precisely defining floodplains. Hydrologists and engineers define the hydraulic floodplain as the surface adjacent to the channel that is inundated by a specified recurrence (Ward, 1978; Graf, 1981). Geomorphologists define floodplains genetically as alluvial landforms, adjacent to a channel, that are built by sediment carried by the modern flow regime (Leopold and Wolman, 1957; Wolman and Leopold, 1957; Wolman and Miller, 1960; Andrews, 1980; Nanson and Croke, 1992; Leopold, 1994; Bridge, 2003). The modern flow regime determines the timing and frequency of floodplain inundation; coupled with the sediment supply available in the system, the modern flow regime is largely responsible for the channel geometry and the size and shape of the adjacent floodplains (Wolman and Miller, 1960; Andrews, 1980; Leopold, 1994; Nash, 1994).

Our understanding of floodplain formation has improved significantly since the relatively simplistic distinction between laterally accreting point bar deposition and vertically accreting overbank deposition in meandering rivers (Wolman and Leopold, 1957). Meandering rivers may also build within-channel benches or point benches (Woodyer et al., 1979; Ferguson and Brierley, 1999a, b), concave-bank benches formed within separation zones of sharp meanders (Taylor and Woodyer, 1978; Woodyer et al., 1979; Hickin, 1979, 1986; Page and Nanson, 1982), channel-expansion floodplains that result following some large floods (Moody et al., 1999), or active channel shelves (Hupp and Osterkamp, 1985; Hupp, 1986). There are relatively few studies regarding braided river floodplain development and this is likely due to the complex nature of braided rivers themselves. Some researchers have argued that braiding is a temporary river form caused by decreased bank resistance (Mackin, 1956) or the inability of a river to mobilize its bed (Fahnestock, 1963). Others, however, have demonstrated that braiding is the equilibrium state of many river systems and occurs in a variety of climates and ecosystems (Leopold et al., 1964, in Knighton, 1972). Our understanding of braided channel and braid bar formation has improved through both field (Knighton, 1972; Cheetham, 1979; Graf, 1988; Ashworth et al., 1992; Bridge and Gabel, 1992; Ferguson et al., 1992) and flume (Hong and Davies, 1979; Ashmore, 1991; Ashworth et al., 2004) studies. Few researchers, however, have focused on floodplain formation in braided river systems; our descriptions of floodplains in this study will contribute to this growing body of knowledge.

Reinfelds and Nanson (1993) define a braided river floodplain as an "extensive, vegetated and horizontally bedded alluvial landform, sometimes composed of a mosaic of units at various stages of development, formed by the present regime of the river, occurring within or adjacent to the unvegetated active river bed" (p. 1114) that is regularly inundated. This is the definition we will use when referring to braided river floodplains in this paper. As with meandering rivers, there may be multiple topographic levels of the floodplain along braided rivers (Williams and Rust, 1969). Some braided floodplains are formed by point bar lateral accretion and overbank deposition, similar to the dominant formative processes common on meandering rivers. Floodplains in braided systems may also be formed by vertical accretion of abandoned channels and bars following channel migration or avulsion, stabilization and vertical accretion of within-channel gravel bars to the level of the floodplain, and channel incision resulting in new surfaces that may develop into narrow floodplains (Miall, 1977; Reinfelds and Nanson, 1993; Brierley and Fryirs, 2005).

The Snake River in Grand Teton National Park (GTNP), Wyoming, is a steep, predominantly braided, gravel-bed river. Jackson Lake Dam (JLD) has regulated the Snake River in the study area since 1908 (Marston et al., 2005; Chapter 2 in Nelson, 2007). The purpose of this paper is to demonstrate how floodplains are formed and maintained along this gravel-bed braided river. We identified alluvial deposits through field mapping and channel change maps and supplemented this mapping with estimates of the magnitude, frequency, and duration of inundating flows. We overlaid the maps of the alluvial deposits onto channel maps drawn from four series of aerial photography in a geographic information system (GIS) to analyze the mechanisms by which alluvial deposits form and to constrain the dates of formation of these deposits.

2. Study Area

This study focuses on over 43 km of the Snake River from JLD to Moose, WY (Figure 3-1). Five tributaries contribute substantial volumes of water and sediment to the study area and increase the drainage area of the Snake River from 2090 km^2 at the dam to 4343 km^2 at Moose. The two largest tributaries, Pacific Creek and Buffalo Fork, join the Snake River within 10 km of JLD, contributing a combined 1417 km^2 to the drainage area and partially mitigating the effects of the regulated hydrology of the Snake River (Chapter 2 in Nelson, 2007). Three smaller tributaries, Spread Creek, Cottonwood Creek, and Ditch Creek, join the Snake River 15.8, 40.4, and 41.8 km downstream from JLD respectively.

JLD was built at the outlet of Jackson Lake, a pre-existing lake scoured by Pleistocene glaciation and impounded by glacial moraines (Love et al., 2003). Originally built in 1908 and rebuilt in 1916, JLD did not substantially alter the downstream flux of sediment, as Jackson Lake was historically a sediment trap. Thus, the decreased magnitude of annual floods following impoundment would necessarily have resulted in conditions of sediment surplus downstream from significant sediment sources, though the magnitude of that surplus is unknown.

2.1. Hydrology

The primary effect of nearly 100 years of flow regulation has been decreased flood magnitudes (Marston et al., 2005; Chapter 2 in Nelson, 2007), the severity of which has been somewhat mitigated by tributary inflows (Chapter 2 in Nelson, 2007). The U.S. Geological Survey (USGS) has collected mean daily and annual peak discharge measurements for the Snake River below JLD since 1903; flow records for Pacific Creek, Buffalo Fork, and the Snake River at Moose began later in the 20th century. The U.S. Bureau of Reclamation estimated mean daily flows without JLD for the Snake River since 1909 (<http://www.usbr.gov/pn/hydromet/arcread.html>). Marston et al. (2005) analyzed flow data for the Snake River below JLD, but did not account for tributary inflows. Nelson (Chapter 2 in Nelson, 2007) analyzed all available main stem, tributary, and estimated unregulated flow data to describe the hydrology of four segments of the Snake River, the same segments discussed in this paper (Figure 3-2).

Palisades Dam was built approximately 160 km downstream from JLD on the Snake River in Idaho in 1958 to fulfill irrigation needs. After 1958, there was a change in flow regime below JLD as managers were allowed greater flexibility in the magnitude and timing of releases. The magnitude of the 2-yr recurrence flood from 1916 to 1958 was 17% and 24% lower in Segments 1 and 4, respectively, than estimated unregulated 2-yr floods; the 2-yr recurrence flood was further reduced from 1959 to 2005, with flood magnitudes 45% and 36% lower in Segments 1 and 4, respectively, than estimated unregulated floods (Chapter 2 in Nelson, 2007).

2.2. Geomorphology

The Snake River is a braided gravel-bed river increasing in gradient from 0.0007 between JLD and Pacific Creek to 0.0038 between Schwabachers Landing and Moose (Figure 2-2, Chapter 2 in Nelson, 2007). Mills (1991) and Marston et al. (2005) investigated geomorphic change in the same study area and determined that total sinuosity, their surrogate metric for channel stability, increased over time and was greatest below tributaries and in wide alluvial valleys. They attributed greater channel activity below tributaries to the inability of lower-magnitude floods to mobilize the delivered sediment load (Marston et al., 2005).

Nelson (2007) analyzed four series of aerial photographs from 1945, 1969, 1990/1991, and 2002 in an improved GIS, arguing that the Snake River channel has remained active throughout the study area since 1945, though the majority of channel activity was concentrated in the unstable reaches with multi-thread channels (Chapter 2 in Nelson, 2007). Increased deposition and channel narrowing occurred during periods of relatively low-magnitude annual floods, from 1945 to 1969, while erosion and channel widening occurred during periods of higher-magnitude annual floods, from 1969 to 1990/1991 and from 1990/1991 to 2002 (Chapter 2 in Nelson, 2007). Channel activity and changes in channel width occurred in reaches both proximal and distal to tributaries. Nelson (2007) argued that, although the channel and floodplain form may have been affected following the flow regime change in 1958, the Snake River has recovered, remains active through most of GTNP, and is capable of mobilizing portions of the bed downstream from tributaries (Chapter 2 in Nelson, 2007).

3. Methods

3.1. Mapping of Alluvial Deposits

Alluvial deposits were mapped in the field from JLD to Deadmans Bar and at Moose. The mapping was completed on aerial photographs (1:12,000 scale) taken in July 2002 (mean daily discharge in Segment 1 was 70 m^3/s). We walked approximately 95% of the contacts while referring to aerial photographs taken in 1945, 1969, and 1990/1991. The mapping was completed in 2005 from mid-July to early October when flows in Segment 1 averaged 47 m^3/s and varied less than 16 m^3/s. Five characteristics were established for each mapped deposit: 1) elevation above the water surface at the time of mapping, 2) stratigraphy, 3) surface textures, 4) associated facies, and 5) differences in vegetation growing on the deposit (no vegetation surveys were conducted, so these differences were based on observations made while mapping alluvial deposits). We digitized the completed maps into a GIS using the 2002 orthophotographs as a base-map. We assumed a maximum linear error of 3 m, calculated as the half-width of a 0.5 mm pencil line on 1:12,000 scale photographs.

3.2. Inundation Frequency

We estimated the magnitude of flows that inundated the alluvial deposits by surveying the topography of the Holocene alluvial valley along 78 cross sections in four locations (Table 3-1, Figure 3-2) during July and August 2005. The topography in the main channel of the Snake River was estimated with a digital depth sounder. Depth measurements were recorded at regular intervals across the channel and overlapped with at least two land-based survey measurements.

We used the cross section data to develop one-dimensional flow models in HEC-RAS, a modeling program developed by the U.S. Army Corps of Engineers. We estimated the overbank roughness coefficient for all cross sections to be 0.08, a typical value for floodplains covered by grasses, bushes, and fallen and standing trees (Chow, 1959), such as is found along much of the Snake River alluvial valley. The stages of the modeled flows often did not precisely match those measured in the field during the specified flow; thus, we calibrated the flows at each cross section by changing the roughness coefficient of the channel until the stages of the modeled flows best matched those of the measured flows. We calibrated the flow models using water surface elevation data surveyed at each cross section during the 2005 dam-released flood, as this flood was closer in magnitude to the floods necessary to inundate the alluvial deposits than the late summer flows: the magnitude of the 2005 flows we surveyed ranged from

59 m^3/s to 171 m^3/s in Segment 3 (Table 3-2); the magnitudes of flows we modeled ranged from 213 m^3/s to 889 m^3/s in Segment 3.

With the models calibrated to the 2005 peak flows, roughness coefficient values ranged from 0.015 to 0.05 in Segment 1, 0.02 to 0.048 in Segment 2, 0.022 to 0.05 in Segment 3, and 0.017 to 0.068 in Segment 4 (Table 3-3). Despite these adjustments to the roughness coefficient values, slight differences between modeled and measured water surface elevations for the 2005 peak flows remained. The greatest difference between measured and modeled water surface elevation was 0.11 m though the mean difference was less than 0.05 m for each reach (Table 3-4). All differences in stage were less than 7% of the maximum water depth along the cross section.

After calibrating the models, we estimated the water surface elevation for up to 16 discharges at the upstream and downstream cross sections based on survey data and stage-discharge rating relationships, developed within HEC-RAS or from USGS gage data. We applied these reach boundary conditions in HEC-RAS and computed steady flow analyses under sub-critical flow conditions. We then identified the alluvial deposits on the cross section profiles and calculated the average value of inundating flows for each deposit at each study site.

3.3. Initiation of Floodplain Formation

We overlaid the maps of the alluvial deposits onto the bankfull channel maps that have been developed for the years 1945, 1969, 1990/1991, and 2002 (Chapter 2 in Nelson, 2007) to determine the approximate age of each alluvial deposit: up to 14 years if built since 1990/1991, 14 to 36 years if built between 1969 and 1990/1991, 36 to 60 years if built between 1945 and 1969, and older than 60 years if built prior to 1945. We then calculated the total area of alluvial deposits formed in each time period in each reach to analyze the spatial and temporal variation in depositional activity and look for trends related to dam operations. The error involved in these analyses was calculated in the same manner as that described in Chapter 2 of Nelson (2007).

4. Results/Analysis

4.1. Characteristics of Alluvial Deposits

We identified four distinct alluvial deposits in the study area: 1) bare gravel bars, 2) lower floodplain, 3) upper floodplain, and 4) lowest terrace. These deposits were distinguished based on their elevation above the water surface, stratigraphy, surface texture, associated facies, and vegetation characterization.

4.1.1. Bare Gravel Bars

Bare gravel bars occur within the bankfull channel and are less than 2 m above the water surface during the late-summer flows. These clast-supported deposits consist of subangular to rounded clasts ranging in size from fine gravel to cobble and contain a matrix of silt to coarse sand (Figure 3-3). Portions of some bars contain thin layers of silt to coarse sand. Less than 10% of the areal extent of these deposits is vegetated with grasses and shrubs less than 0.5 m in height. There are three types of bare gravel bars: mid-channel bars are elongate and up to 500 m in length and are separated from both banks by active channels; bank-attached bars are typically only attached on the upstream end of the bar, but they typically contain isolated pools of water between the bar and channel banks when the bar is attached at both the upstream and downstream extents; point bars develop on the inside of bends, similar to those on meandering rivers (Figure 3-3).

4.1.2. Lower floodplain

Lower floodplain deposits are between 0.2 and 0.7 m above the water surface during the late-summer flows. These deposits consist of up to 0.5 m of fine-grained sediments overlying clast-supported fine to cobble-sized gravel with a matrix of coarse sands to silt, similar to the bare gravel bar deposits; the contact between the fine-grained sediments and the gravels is sharp. There are no bedforms in the overlying fine-grained deposits, which consist of one or two layers of fine sands and silts (Table 3-5, Figure 3-4).

The lower floodplain is distinguished from other alluvial deposits by its low elevation and the vegetation it supports. This deposit is fully covered with scouring rush (*Equisetum* spp.), which is rarely found on other alluvial deposits, grasses, and occasional small shrubs. Bioturbation and root growth associated with this vegetation may be partially responsible for the lack of bedforms in the fine-grained layers (Reinfelds and Nanson, 1993).

The lower floodplain is made up of two facies, channel margins and abandoned channels (Figure 3-4). Channel margins are inset within the upper floodplain or terraces, are often less than 2 m in width, less than 200 m in length, and are located discontinuously and infrequently between JLD and Moose. Abandoned channels are wider and longer, depending on the size of the abandoned channel, and are more common throughout the study area.

4.1.3. Upper floodplain

Upper floodplain deposits are approximately 0.7 to 2.0 m above the water surface during the late-summer flows. Similar to the lower floodplain, these deposits consist of fine-grained layers overlying clast-supported gravel and cobbles. The fine-grained layers of the upper floodplain, however, range in depth from 1.5 m to a thin veneer with exposed gravel and cobbles. The clast-supported, coarse-grained layer is similar in composition to the bare gravel bars and the basal layer of the lower floodplain, but is up to 1.5 m thick. The subangular to rounded clasts range in size from fine gravel to cobble and contain a matrix of silt to coarse sand.

The upper floodplain is composed of two facies, abandoned bars and abandoned channels (Figure 3-5). The fine-grained deposits are thinner on the abandoned bars than the abandoned channels. There are many fine-grained layers in the abandoned channel deposits that alternate between fine sand and silt (Figure 3-5). Though the grain size distribution of the fine sand and silt layers in the upper and lower floodplains are similar (Table 3-5), the two deposits are distinguishable by the higher elevation of the upper floodplain, the greater depth of its fine-grained layers, and the differences in vegetation.

The vegetation along the upper floodplain includes grasses, shrubs, and saplings on recently abandoned channels and bars to mature narrow-leaved cottonwood (*Populus angustifolia*) and blue spruce (*Picea pungens*) trees on abandoned bars and channels that have not been part of the bankfull channel since before 1945. Though the abandoned bars are generally higher in elevation than the abandoned channels, distinguishing between these two facies within the upper floodplain is sometimes difficult where both have accreted to a similar elevation and support the same vegetation at a similar stage of maturity.

4.1.4. Lowest Terrace

Lowest terrace deposits are approximately 2.0 to 3.5 m above the water surface during the late-summer flows. The lowest terrace is similar to the upper floodplain in both composition and associated facies, but occurs at higher elevations above the water surface. The lowest terrace predominantly supports sagebrush (*Artemisia* spp.), a more xerophytic species, as well as smaller populations of *P. pungens*, *P. angustifolia*, quaking aspen (*Populus tremuloides*), and lodgepole pine (*Pinus contorta*). Similar to the upper floodplain, up to 1.5 m of fine sediment overlies a basal layer of gravels and cobbles (Figure 3-6). The grain size distribution of the fine- and coarse-grained layers and the roundness of the gravels and cobbles in the lowest terrace is similar to that of the respective layers and clasts in the upper floodplain.

Exposed deposits in cutbanks reveal that the lowest terrace is composed of abandoned bar and channel facies, with a far thicker layer of fine-grained sediment overlying the gravel and cobble layer of the abandoned channels than that of the abandoned bars (Figure 3-6). These two facies within the lowest terrace are not mapped separately because they support similar vegetation and have accreted to similar elevations, making it difficult to accurately identify their boundaries. The boundary between the lowest terrace and the upper floodplain is sometimes difficult to determine as the two deposits occasionally grade into each other, likely a result of the varying elevations of the channel bed from avulsions. We used anecdotal differences in vegetation to distinguish the two deposits in these cases as the sediment composition and surficial textures are often similar.

4.2. Spatial Patterns of Alluvial Deposits

The bare gravel bar deposits make up 4% of the mapped Holocene alluvial valley; the bankfull channel, which consists of the wetted channel and bare gravel bars, accounts for 22% of the mapped area (Table 3-6). Mid-channel bare gravel bars are more prevalent in the multi-thread reaches than the single-thread reaches, whereas point bars are primarily located in the single-thread reaches with constrained and meandering channels. Bank-attached bars are built with similar frequency in both channel types.

Lower floodplain deposits make up only 3.5% of the mapped alluvial valley. They are located in most reaches, but are discontinuous, narrow, and typically only a few channel widths in length. Of the two facies of the lower floodplain, the abandoned channels are more prevalent and are located primarily in the unstable, multi-thread reaches where channels are frequently abandoned due to channel migration and avulsions. The channel margin facies are located along the edges of the primary channels in both multi-thread and single-thread reaches.

Upper floodplain deposits make up 36% of the mapped alluvial valley. These are the most widespread deposits and are nearly continuous from Pacific Creek to Moose. The upper floodplain is located in all reaches but generally accounts for a larger proportion of the alluvial valley in the wide, multi-thread reaches.

Lowest terrace deposits are only slightly less prevalent than the upper floodplain deposits, making up 35% of the mapped alluvial valley. The lowest terrace is located throughout the study area but is not as continuous as the upper floodplain. There is little difference in the relative proportion of the lowest terrace between single- and multi-thread reaches.

4.3. Depositional Processes

Bare gravel bars developed in low-energy portions of the channel and grew laterally and/or downstream. Mid-channel bars often developed in the scour pools created by obstructions such as boulders or fallen trees, whereas marginal bars were often located in the relatively calm waters protected by sharp channel bends or point bars (Figure 3-7) (Leopold and Wolman, 1957; Miall, 1977). As on meandering rivers, point bars aggraded laterally in the low energy part of the channel along the inside of meander bends (Leopold and Wolman, 1957; Miall, 1977).

Portions of the upper and lower floodplains formed by different processes. The abandoned bars of the upper floodplain were often the result of channel migration and avulsion that isolated the bars from most flows (Figure 3-8) (Miall, 1977; Ashmore, 1991; Reinfelds and Nanson, 1993; Brierley and Fryirs, 2005). They also developed by gradual vertical and downstream accretion of active bars into relatively stable islands, reaching elevations higher than most floods and becoming more stable with vegetative growth (Bridge and Gabel, 1992; Reinfelds and Nanson, 1993). The lower magnitude floods often continued to inundate the abandoned channels and deposit fine-grained sediment until they had vertically accreted to a similar, though usually still lower, elevation as the abandoned bars (Figure 3-8) (Miall, 1977).

Vertical accretion of abandoned channels within the lower floodplain occurred in a similar manner as the same features in the upper floodplain: abandonment via channel migration or avulsion and the gradual accretion of fine sediments carried by flood flows that inundated the old channel (Figure 3-9). Channel margin deposits developed by vertical accretion of fine sediments on top of gravels exposed near the banks of the channel. The grasses and *Equisetum* spp. that colonized the channel margin deposits likely aided in their development through increased bank resistance and fine-grained sediment trapping during flood flows.

We found no distinct contacts between the gravel and cobble layers of the lower and upper floodplain, lower floodplain and lowest terrace, or upper floodplain and lowest terrace, though these are three distinct landforms (Figure 3-10). There are two possible explanations for this lack of a distinct contact: first, the lower floodplain, upper floodplain, and lowest terrace may be three facies within one alluvial deposit that has undergone incision rather than cut and fill; second, cut and fill may be occurring, but the contact may not be apparent because the sediment composition of these layers is similar in all three deposits. In either case, the lower and upper floodplains and lowest terrace are distinct landforms composed of varying depths of a gravel and cobble layer overlaid by varying depths of a sand/silt layer.

4.4. Flood Frequency, Flow Duration of Inundating Flows

The recurrence of floods inundating the alluvial deposits decreased and inundation periods of these surfaces increased downstream from Buffalo Fork under the current flow regime. At the time and place of each survey, the flows were 125 m^3/s in Segment 1, 144 m^3/s in Segment 2, 170 m^3/s in Segment 3, and 175 m^3/s in Segment 4. These floods had recurrence intervals of 1.2, 1.2, 1.1, and 1.0 years for each segment respectively.

4.4.1. Lower Floodplain

The inundation discharges for the lower floodplain increased downstream from 142 m^3/s in Segment 1 to 222 m^3/s in Segment 4 (Table 3-7). The recurrence for these inundating flows since 1958, were 1.6 years and 1.7 years for Segments 1 and 2, respectively, whereas those for Segments 3 and 4 were 1.2 years. Thus, floods inundated the lower floodplain 25% to 29% more frequently downstream from Buffalo Fork than downstream from JLD and Pacific Creek respectively. Prior to 1958, floods inundated the lower floodplain approximately every year. Since 1958, the magnitude of inundating flows was equaled or exceeded in 32, 30, 37, and 41 of the 47 years in Segments 1 through 4 respectively (Table 3-8).

The lower floodplain was inundated 3.5% of the time, or an average of 12.9 days per year in Segment 1 since 1958, and the period of inundation increased downstream to 24.2 days per year, or 6.6% of the period, in Segment 4. Prior to 1958, the lower floodplain was inundated more than twice as long as during the current flow regime in most segments. Inundation durations in this time period increased downstream from 29.9 days per year in Segment 2 to 43.1 days per year in Segment 4.

4.4.2. Upper Floodplain

The inundation discharge of the upper floodplain in Segment 1 was 252 m^3/s and increased downstream to 467 m^3/s in Segment 4 (Table 3-7). The recurrences decreased downstream from JLD since 1958 from 16.5 years in Segment 1 to 12.3 years in Segment 2, 10.8 years in Segment 3, and 10.0 years in Segment 4. The magnitude of inundating flows for the upper floodplain was equaled or exceeded by the maximum mean daily discharge in fewer than 15 years between 1916 and 1958 and in no more than five years between 1959 and 2005 (Table 3-8). Most of the occurrences of inundation since 1958 were between 1983 and 1986 and between 1996 and 1999.

The length of time that the upper floodplain was inundated during these floods decreased substantially following the flow regime change in 1958: 82% in Segment 1, from almost four days to less than one day, and 58% in Segment 4, from less than two days to less than one day. Recurrence intervals increased and inundation periods decreased downstream from tributaries from 1916 to 1958 due to the offset in timing of released floods and natural tributary floods.

4.4.3. Lowest Terrace

Though the lowest terrace is located in many places in Segment 1, it was surveyed in only one cross section and therefore inundating flows could not be estimated in this segment with acceptable precision. Inundating flows in Segments 2 through 4 were 431, 889, and 795 m^3/s respectively. Prior to 1958, these flows were exceeded only in Segment 2, from June 11-16, 1918. Since 1958, the flows had recurrence intervals of approximately 121, 340, and 171 years in Segments 2 through 4 respectively and have never been exceeded. The high variability in the magnitude of inundating flows was a result of the variability in elevation of the terrace above the surrounding floodplains and water surface: the lowest terrace ranged from 2 to 3.5 m above the water surface in late summer of 2005 and from 0 to nearly 3 m above the level of the upper floodplain. Representative terrace surfaces were not always captured in the surveys because the surveyed reaches were short (1.5 km) and only the topography along the cross-sections was surveyed.

Our calculations of inundating flows for the lowest terrace are based on the present flow regime and channel bed elevation. However, the lowest terrace was built during a period when the bed elevation was higher than it is today. Therefore, our calculations of the magnitude of flows that inundate the lowest terrace likely overestimate the magnitude of flows that built this deposit.

4.5. Initiation of Floodplain Formation

The lower and upper floodplain surfaces have developed in every time period as defined by the aerial photograph series analyzed: before 1945, between 1945 and 1969, between 1969 and 1990/1991, and between 1990/1991 and 2002 (Table 3-9, Figure 3-11). There has been no growth of the lowest terrace since 1945. Most of the annual floodplain growth occurred in the braided reaches (Table 3-10), as was expected from the substantially greater amounts of channel activity in these reaches than the single-thread reaches (Chapter 2 in Nelson, 2007). There was little growth in any time period in the single-thread reaches of Segment 1 (Reaches 1 through 5) and no growth between 1945 and 2002 in Reaches 1, 4, and 9. The floodplain formation in Reaches 14 and 16 was greater than might be expected in single-thread reaches because these were restricted meandering reaches that contained active point bars and cut banks.

Annual development of the lower floodplain was greatest in the multi-thread Reach 8 from 1990/1991 to 2002 (470 m^2/km-yr), followed by Reach 15, another multi-thread reach, from 1945 to 1969 (350 m^2/km-yr). The period of greatest lower floodplain growth for three of the six multi-thread reaches was from 1990/1991 to 2002.

Annual upper floodplain development was far greater in Reach 15 in all time periods than in any other reach, peaking at 1700 m^2/km-yr from 1945 to 1969. Reach 8 followed in upper floodplain productivity with 1100 m^2/km-yr built between 1945 and 1969 and 1000 m^2/km-yr built from 1990/1991 to 2002. There was no upper floodplain development in any time period in Segment 1 except for slight growth in Reach 2 from 1990/1991 to 2002. Downstream from Pacific Creek, greater upper floodplain growth occurred between 1945 and 1969 in eight of the 12 reaches, and five of the six multi-thread reaches, analyzed. Only seven reaches experienced any upper floodplain growth from 1990/1991 to 2002, and only four of these, all multi-thread, were greater than 100 m^2/km-yr.

5. Discussion

5.1. Floodplain Formation

A significant difference between the upper floodplain on the Snake River and the floodplains described in many studies is that the recurrence of inundation of the upper floodplain is now approximately 10 years for most of the study area. Our estimates of inundating discharges were calculated from flow models, which have limitations. Flow models do not account for sediment transport or changes in bed elevation; thus, the lowest terrace may have been formed under a similar flow regime but a higher-in-elevation channel bed. In addition, our flow models were based on cross section topography of three single-thread channels and one relatively stable multi-thread channel. Because the topography was only measured along cross sections within these four reaches, the topography between cross sections was not accounted for within the modeled reaches, much less the remainder of the study area. Much of the Snake River is complex with multiple channels and variable floodplain topography; the models provide estimates, but they do not precisely explain the nature of inundating flows everywhere.

Although the bankfull recurrence intervals on many rivers are between one and two years, some have been shown to exceed two years and even reach the decadal scale with recurrence intervals greater than 20 or 30 years (Pickup and Warner, 1976; Williams, 1978; Nash, 1994). The frequency of inundating flows varies widely among river systems, and recurrences of 10 to 16 years for a floodplain, as for the upper floodplain in this study, are unusual, but not unique.

The nature of braided river systems may be the cause of the upper floodplain continuing to be built even during a reduced flow regime. Braided rivers move bed material, build gravel bars and floodplains, and erode floodplains, often undercutting channels banks and causing mature trees to fall into the river. This occurrence is common along the Snake River, and these trees often block channel entrances, or otherwise change the direction of flow, causing the river to avulse. Avulsions result in active channels that are at different elevations in the same reach, causing floodplains to be built at different elevations as well. Therefore, even in a reduced flow regime, floodplains at higher elevations may still be built because of avulsions and the occurrence of active channels at varying elevations.

Researchers have described inset deposits below the elevation of the primary floodplain similar to the lower floodplain channel-margin facies analyzed in this study. ‘Channel expansion deposits’ are built along the channel margins after large floods widen the channel, are generally wider than the channel-margin deposits described here, and are an intermediate stage of the mature floodplain (Moody et al., 1999). Trees growing at the edge of water may create low benches by trapping fine-grained sediments (Woodyer et al., 1979). There are no trees growing on the lower floodplain deposit, though once the grasses and *Equisetum* spp. become established they likely trap fine-grained sediments. Ferguson and Brierley (1999a) mentioned low benches that formed along straight reaches and Williams and Rust (1969) described ‘Level 2’ channels, both similar to the lower floodplain here, but neither study described how the surfaces were formed.

We will consider three possible explanations for the development of lower floodplain channel-margin facies. First, they may be similar to, though much narrower than, the ‘channel-expansion deposits’ of Moody et al. (1999). There have been large floods in every time period in which aerial photographs were analyzed that may have resulted in channel widening; these floods may have subsequently deposited the basal gravels and overlying fine-grained sediments necessary for the development of the lower floodplain. It is possible that these channel-margin facies did not develop to the level of the upper floodplain, and that more mature vegetation was not able to survive, because of subsequent floods periodically eroding these deposits. Moody et al. (1999) observed and measured the development of the 'channel-expansion deposits' over an 18 yr period; a similar length of observation on the Snake River would be necessary to provide sufficient evidence to support or repudiate this explanation.

Second, the lower floodplain deposit may be the result of decreased flood magnitudes building a new floodplain to a new bankfull level. However, if this were the cause of deposition, we would expect the lower floodplain to be relatively continuous and on both banks of the main channel in at least the single-thread reaches, if not throughout the study area. Also, if this were the new bankfull deposit, we would expect little continued development of the upper floodplain (Everitt, 1993; Johnson, 1994 and 1998; Grams and Schmidt, 2002). The sporadic and discontinuous nature of the lower floodplain and the continued development of the upper floodplain in all time periods analyzed suggest that this process does not adequately explain the development of the lower floodplain.

Third, the lower floodplain channel-margin facies may have historically been part of the active morphology, distinct from the upper floodplain, and similar to the 'benches' (Taylor and Woodyer, 1978; Woodyer et al., 1979; Ferguson and Brierley, 1999a), 'second level channels' (Williams and Rust, 1969; Miall, 1977), or 'active-channel shelves' (Hupp and Osterkamp, 1985; Hupp, 1986) that have naturally developed on other river systems. This explanation is supported by the occurrence of similar deposits along the Snake River near Flagg Ranch, upstream from Jackson Lake (Figure 3-12). Between its headwaters and Jackson Lake, the Snake River is virtually pristine, with no impoundment structures or development impeding or redirecting its flow. The 'lower floodplain' deposits documented upstream from the USGS gage station near Flagg Ranch (station number 13010065) were narrow, discontinuous, inset into a higher-elevation floodplain, less than 1 m above the flows on September 17, 2005 (8.1 m^3/s), and were host to mainly grasses and *Equisetum* spp., the same characteristics as the lower floodplain channel-margin deposits downstream from JLD. Thus, the lower floodplain is likely a naturally developing, vertically accreting surface built by floods with recurrence intervals of approximately 1 to 1.5 years, as is common on many rivers (Leopold and Wolman, 1957; Wolman and Leopold, 1957; Wolman and Miller, 1960; Andrews, 1980).

5.2. Impacts of Regulation

Flow regulation in the study area has substantially increased the recurrence interval of inundating flows and decreased the duration of time that both floodplains are inundated (Table 3-7). Except for one day in 1974 in Segment 4, the average inundation discharge for the upper floodplain was not exceeded for 25 years between the flow regime change in 1958 and 1983 in any of the four segments. During this period, the lower levels of the variable topography of the upper floodplain were likely inundated, but the higher surfaces were not inundated. The floodplain vegetation likely matured during this period and may have led to the establishment of later successional species in some areas of the upper floodplain.

The two levels of floodplain along the Snake River continued to develop in every time period analyzed, but the changes in inundating recurrence intervals and flow durations may have resulted in changes to the relative proportion of floodplain development. The ratio of upper floodplain to lower floodplain development decreased over time in six of the eight reaches, and over about half the channel length, in which large amounts of each floodplain developed (Table 3-11). The upper floodplain may form during large floods and the lower floodplain may form during more common floods.

6. Conclusions

The modern Snake River alluvial valley contains two distinct floodplain deposits at different elevations above the water surface that have both been developing since before 1945. The lower floodplain is a fine-grained alluvial deposit that is inundated by relatively frequent, low-magnitude floods. These floods build narrow channel-margin facies inset into the upper floodplain or terrace or gradually fill in abandoned channels with sediment. Less frequent, higher-magnitude floods continue to alter the landscape of the upper floodplain, which is composed of abandoned alluvial bars and channels and is covered with vegetation at various stages of development. The lowest terrace is a relic floodplain that has likely not been inundated in the last 100 years of discharge records. Regulation on the Snake River has caused floods that inundate the floodplain deposits to occur less frequently.

REFERENCES

Andrews, E.D., 1980. Effective and Bankfull Discharges in the Yampa River Basin, Colorado and Wyoming. Journal of Hydrology 46: 311-330.

Ashmore, P.E., 1991. How do Gravel-Bed Rivers Braid? Canadian Journal of Earth Sciences 28, 326-341.

Ashworth, P.J., Best, J.L., and Jones, M., 2004. Relationship Between Sediment Supply and Avulsion Frequency in Braided Rivers. Geology 32 (1), 21-24.

Ashworth, P.J., Ferguson, R.I., Ashmore, P.E., Paola, C., Powell, D.M., and Prestegaard, K.L., 1992. Measurements in a Braided River Chute and Lobe; 2, Sorting of Bed Load During Entrainment, Transport and Deposition. Water Resources Research 28 (7), 1887-1896.

Bendix, J. and Hupp, C.R., 2000. Hydrological and Geomorphological Impacts on Riparian Plant Communities. Hydrological Processes 14, 2977-2990.

Bridge, J.S., 2003. Rivers and Floodplains. Blackwell Publishing, Malden, MA. 491 pp.

Bridge, J.S. and Gabel, S.L., 1992. Flow and Sediment Dynamics in a Low Sinuosity, Braided River: Calamus River, Nebraska Sandhills. Sedimentology 39, 125-142.

Brierley, G.J. and Fryiers, K.A., 2005. Geomorphology and River Management: Applications of the River Styles Framework. Blackwell Publishing, Malden, MA. 398pp.

Cheetham, G.H., 1979. Flow Competence in Relation to Stream Channel Form and Braiding. Geological Society of America Bulletin 90, 877-886.

Chow, V.T., 1959. Open Channel Hydraulics. McGraw-Hill, New York. 680 pp.

Cooper, D.J., Anderson, D.C., and Chimner, R.A., 2003. Multiple Pathways for Woody Plant Establishment on Floodplains at Local to Regional Scales. Journal of Ecology 91, 182-196.

Everitt, B., 1993. Channel Responses to Declining Flow on the Rio Grande between Ft. Quitman and Presidio, Texas. Geomorphology 6, 225-242.

Fahnestock, R.K., 1963. Morphology and Hydrology of a Glacial Stream – White River, Mount Rainier Washington. U.S. Geological Survey Professional Paper, 422-A.

Ferguson, R.I., Ashmore, P.E., Ashworth, P.J., Paola, C., and Prestegaard, K.L., 1992. Measurements in a Braided River Chute and Lobe; 1, Flow Pattern, Sediment Transport, and Channel Change. Water Resources Research 28 (7), 1877-1886.

Ferguson, R.J. and Brierley, G.J., 1999a. Downstream Changes in Valley Confinement as a Control on Floodplain Morphology, Lower Tuross River, New South Wales, Australia. In: Miller, A.J., Gupta, A. (Eds.), Varieties of Fluvial Form, John Wiley and Sons, New York, NY, pp. 377-407.

Ferguson, R.J. and Brierley, G.J., 1999b. Levee Morphology and Sedimentology Along the Lower Tuross River, South-Eastern Australia. Sedimentology 46, 627-648.

Graf, W.L., 1981. Channel Instability in a Braided, Sand Bed River. Water Resources Research 17 (4), 1087-1094.

Grams, P.E. and Schmidt, J.C., 2002. Streamflow Regulation and Multi-Level Flood Plain Formation: Channel Narrowing on the Aggrading Green River in the Eastern Uinta Mountains, Colorado and Utah. Geomorphology 44, 337-360.

Hickin, E.J., 1979. Concave-Bank Benches on the Squamish River, British Columbia, Canada. Canadian Journal of Earth Sciences 16, 200-203.

Hickin, E.J., 1986. Concave-Bank Benches in the Floodplains of Muskwa and Fort Nelson Rivers, British Columbia. The Canadian Geographer 30 (2), 111-122.

Hong, L.B. and Davies, T.R.H., 1979. A Study of Stream Braiding: Summary. Geological Society of America Bulletin 90, 1094-1095.

Hupp, C. R., 1986. Upstream Variation in Bottomland Vegetation Patterns, Northwestern Virginia. Bulletin of the Torrey Botanical Club 113 (4), 421-430.

Hupp, C. R. and Osterkamp, W.R., 1985. Bottomland Vegetation Distribution along Passage Creek, Virginia, in Relation to Fluvial Landforms. Ecology 66 (3), 670-681.

Johnson, W.C., 1994. Woodland Expansion in the Platte River, Nebraska: Patterns and Causes. Ecological Monographs 64 (1), 45-84.

Johnson, W.C., 1998. Adjustment of Riparian Vegetation to River Regulation in the Great Plains, USA. Wetlands 18 (4) 608-618.

Knighton, A.D., 1972. Changes in a Braided Reach. Geological Society of America Bulletin 83, 3813-3822.

Leopold, L.B., 1994. A View of the River. Harvard University Press, Cambridge, MA. 298 pp.

Leopold, L.B. and Wolman, M.G., 1957. River Channel Patterns-Braided, Meandering, and Straight. U.S. Geological Survey Professional Paper, 282-B.

Leopold, L.B., Wolman, M.G., and Miller, J.P., 1964. Fluvial Processes in Geomorphology. Freeman and Co., San Francisco. 522 pp.

Love, D.L., Reed, J.C., and Pierce, K.L., 2003. Creation of the Teton Landscape: A Geological Chronicle of Jackson Hole and The Teton Range. Grand Teton Natural History Association. Moose, WY. 132 pp.

Mackin, J.H., 1956. Cause of Braiding by a Graded River. Geological Society of America Bulletin 67 (12), 1717-1718.

Marston, R.A., Mills, J.D., Wrazien, D.R., Bassett, B., and Splinter, D.K., 2005. Effects of Jackson Lake Dam on the Snake River and its floodplain, Grand Teton National Park, Wyoming, USA. Geomorphology 71, 79-98.

Martin, C.W. and Johnson, W.C., 1987. Historical Channel Narrowing and Riparian Vegetation Expansion in the Medicine Lodge River Basin, Kansas, 1871-1983. Annals of the Association of American Geographers 77 (3), 436-449.

Miall, A.D., 1977. A Review of the Braided-River Depositional Environment. Earth-Science Reviews 13, 1-62.

Mills, J.D., 1991. Wyoming's Jackson Lake Dam, Horizontal Channel Stability, and Floodplain Vegetation Dynamics. Masters Thesis from the University of Wyoming. Laramie, WY. 54 pp.

Moody, J.A., Pizzuto, J.E., and Meade, R.H., 1999. Ontogeny of a Floodplain. Geological Society of America Bulletin, 111 (2), 291-303.

Nanson, G.C. and Croke, J.C., 1992. A Genetic Classification of Floodplains. Geomorphology 4, 459-486.

Nash, D.B., 1994. Effective Sediment-Transporting Discharge from Magnitude-Frequency Analysis. The Journal of Geology 102, 79-95.

Nelson, N.C., 2007. Hydrology and Geomorphology of the Snake River in Grand Teton National Park, WY. Master's thesis, Utah State University, Logan, UT. 126 pp.

Page, K. and Nanson, G., 1982. Concave-Bank Benches and Associated Floodplain Formation. Earth Surface Processes and Landforms 7, 529-543.

Pickup, G. and Warner, R.F., 1976. Effects of Hydrologic Regime on Magnitude and Frequency of Dominant Discharge. Journal of Hydrology 29, 51-75.

Reinfelds, I. and Nanson, G., 1993. Formation of Braided River Floodplains, Waimakariri River, New Zealand. Sedimentology 40, 1113-1127.

Scott, M.L., Auble, G.T., and Friedman, J.M., 1997. Flood Dependency of Cottonwood Establishment Along the Missouri River, Montana, USA. Ecological Applications 7 (2), 677-690.

Taylor, G. and Woodyer, K.D., 1978. Bank Deposition in Suspended-Load Streams. In: Miall, A.D. (Ed.), Fluvial Sedimentology. Canadian Society of Petroleum Geologists, Calgary, Alberta, pp. 257-275.

Ward, R., 1978. Floods: A Geographical Perspective. John Wiley and Sons, New York, NY. 244 pp.

Williams, G.P., 1978. Bank-Full Discharge of Rivers. Water Resources Research 14 (6), 1141-1154.

Williams, P.F. and Rust, B.R., 1969. The Sedimentology of a Braided River. Journal of Sedimentary Petrology 39 (2), 649-679.

Wolman, M.G. and Leopold, L.B., 1957. River Flood Plains: Some Observations on their Formation. U.S. Geological Survey Professional Paper, 282-C.

Wolman, M.G. and Miller, J.P., 1960. Magnitude and Frequency of Forces in Geomorphic Processes. Journal of Geology 68 (1), 54-74.

Woodyer, K.D., Taylor, G., and Crook, K.A.W., 1979. Depositional Processes Along a Very Low-Gradient, Suspended-Load Stream: The Barwon River, New South Wales. Sedimentary Geology 22, 97-120.

http://www.usbr.gov/pn/hydromet/arcread.html

TABLES

Table 3-1: Cross sections surveyed during 2005.

Segment #	# of Cross Sections	Reach Length (km)	Average Distance between Cross Sections (m)	Average Channel Width of Cross Sections (m)*
1	20	1.2	63	94
2	21	1.5	73	104
3	19	1.5	81	87
4	18	1.5	88	88

*Based on measurements during dam-released flood.

Table 3-2: Water surface elevation and detailed cross section surveys conducted in 2005.

Date of Survey	Segment #	Cross Section Survey	Water Surface Survey	Discharge (m^3/s)
June 7, 2004*	2-4		X	217, 285, 306
June 10, 2004*	2-4		X	237, 354, 374
June 22, 2004*	2-4		X	139, 179, 208
June 2, 2005	1, 2		X	8, 33
June 3, 2005	3		X	60
June 4, 2005	4		X	70
June 15, 2005	2		X	144
June 16, 2005	1, 3, 4		X	125, 171, 175
July 15-17, 2005	4	X		82
July 18-20, 2005	1	X		47
July 31-August 3, 2005	2	X		51
August 3-5, 2005	3	X		59

*Surveys based on flags placed at the edge of water on these dates by a U.S. Forest Service hydrologist.

Table 3-3: Differences between calculated Manning's roughness coefficients (*n*) and those used in the HEC-RAS flow models.

Segment	Discharge at time of survey (m^3/s)	Calculated reach-averaged *n*	Range of *n* values used in models (min:max)	Median *n* values used in models	Mean *n* values used in models
1	125	0.034	0.015: 0.050	0.034	0.034
2	144	0.028	0.020: 0.048	0.027	0.028
3	171	0.031	0.022: 0.050	0.031	0.031
4	175	0.030	0.017: 0.068	0.031	0.032

Table 3-4: Difference in water surface elevations (WSE) between measured flows at the time of the survey and flows modeled in HEC-RAS. The maximum and mean percent of the channel depth at the deepest point that is represented by the differences in WSE is also indicated.

Segment	Discharge at time of survey (m^3/s)	Maximum difference in WSE		Mean difference in WSE (cm)	Max % of depth at deepest point	Mean % of depth at deepest point
		Lower than measured (cm)	Higher than measured (cm)			
1	125	8	4	4	2.4	1.3
2	144	4	6	3	3.8	1.3
3	171	7	7	4	4.0	2.0
4	175	6	11	5	6.5	2.8

Table 3-5: Grain size distribution by weight of sediment from floodplain stratigraphy.

	Lower Floodplain – Abandoned Channel		Lower Floodplain – Channel-Margin					
Phi/Grain	Sample A		Sample A		Sample B		Sample C	
Size (mm)	Weight (g)	% Finer	Weight (g)	% Finer	Weight (g)	% Finer	Weight (g)	% Finer
--/45	0.00	100.00	0.00	100.00	0.00	100.00	0.00	100.00
-5/32	0.00	100.00	0.00	100.00	0.00	100.00	68.77	93.84
-4.5/22.6	0.00	100.00	0.00	100.00	0.00	100.00	215.89	74.50
-4/16	0.00	100.00	0.00	100.00	0.00	100.00	145.97	61.42
-3.5/11.3	0.00	100.00	0.00	100.00	0.00	100.00	106.80	51.85
-3/8	0.00	100.00	0.00	100.00	0.00	100.00	64.66	46.06
-2.5/5.6	0.00	100.00	0.00	100.00	0.00	100.00	68.56	39.92
-2/4	0.00	100.00	0.00	100.00	0.00	100.00	69.40	33.70
-1.5/2.8	0.00	100.00	0.00	100.00	0.00	100.00	75.81	26.91
-1/2	0.03	99.99	0.17	99.86	0.22	99.80	62.40	21.32
-0.5/1.4	0.21	99.89	0.21	99.69	0.30	99.52	42.54	17.51
0/1	1.10	99.41	0.37	99.39	0.64	98.93	26.28	15.15
0.5/0.7	1.41	98.78	0.54	98.96	0.83	98.16	13.98	13.90
1/0.5	2.20	97.80	0.86	98.26	1.25	97.00	9.26	13.07
1.5/0.355	2.78	96.57	1.44	97.09	1.68	95.45	10.22	12.16
2/0.25	3.06	95.21	3.57	94.20	2.52	93.11	24.55	9.96
2.5/0.18	6.46	92.35	14.73	82.28	6.95	86.68	49.84	5.49
3/0.125	24.89	81.31	27.93	59.67	14.59	73.17	30.09	2.80
3.5/0.09	46.48	60.70	26.58	38.15	19.63	55.00	13.50	1.59
4/0.063	45.22	40.64	18.43	23.23	19.34	37.10	6.83	0.97
Pan/<0.063	91.64		28.70		40.08		10.88	
Total	225.48		123.53		108.03		1116.23	

	Upper Floodplain (UFP) – Abandoned Bar						UFP – Abandoned Channel			
	Sample A		Sample B		Sample C		Sample A		Sample B	
Phi/Grain Size (mm)	Weight (g)	% Finer	Weight (g)	% Finer	Weight (g)	% Finer	Weight (g)	% Finer	Weight (g)	% Finer
--/64	0.00	100.00	0.00	100.00	0.00	100.00	0.00	100.00	0.00	100.00
--/45	0.00	100.00	0.00	100.00	918.00	70.01	0.00	100.00	0.00	100.00
-5/32	0.00	100.00	0.00	100.00	351.35	58.54	0.00	100.00	0.00	100.00
-4.5/22.6	0.00	100.00	0.00	100.00	237.82	50.77	0.00	100.00	0.00	100.00
-4/16	0.00	100.00	0.00	100.00	197.06	44.33	0.00	100.00	0.00	100.00
-3.5/11.3	0.00	100.00	0.00	100.00	162.19	39.04	0.00	100.00	0.00	100.00
-3/8	0.00	100.00	0.00	100.00	149.05	34.17	0.00	100.00	0.00	100.00
-2.5/5.6	0.00	100.00	0.00	100.00	126.92	30.02	0.00	100.00	0.00	100.00
-2/4	0.00	100.00	0.00	100.00	113.43	26.32	0.00	100.00	0.00	100.00
-1.5/2.8	0.00	100.00	0.00	100.00	118.86	22.43	0.00	100.00	0.00	100.00
-1/2	2.09	98.52	0.00	100.00	109.11	18.87	0.18	99.77	0.18	99.83
-0.5/1.4	1.55	97.43	0.07	99.92	96.82	15.71	0.22	99.50	0.32	99.52
0/1	3.18	95.18	0.14	99.77	68.95	13.46	0.36	99.05	0.48	99.05
0.5/0.7	3.93	92.40	0.25	99.49	49.68	11.83	0.59	98.31	0.50	98.57
1/0.5	5.64	88.41	0.45	98.99	70.35	9.54	1.37	96.60	0.81	97.79
1.5/0.355	8.27	82.57	1.36	97.49	95.27	6.42	4.04	91.54	1.66	96.19
2/0.25	9.47	75.87	4.65	92.34	78.97	3.84	9.10	80.15	3.36	92.95
2.5/0.18	15.55	64.88	15.50	75.18	61.35	1.84	16.25	59.81	8.64	84.62
3/0.125	20.32	50.52	25.86	46.55	26.72	0.97	16.37	39.32	12.43	72.63
3.5/0.09	20.04	36.35	18.20	26.40	11.72	0.59	11.64	24.76	14.54	58.61
4/0.063	16.36	24.78	9.93	15.41	6.26	0.38	7.66	15.17	16.62	42.58
Pan/<0.063	35.06		13.92		11.65		12.12		44.15	
Total	141.46		90.33		3061.53		79.90		103.69	

Table 3-6: Percent of mapped alluvial valley. "Other water" refers to inactive or discontinuous side channels or pools of water disconnected from the active bankfull channel. Total % is the sum of bankfull channel, other water, lower floodplain, upper floodplain, and lowest terrace; bare gravel bars are included in the bankfull channel values. Total percents do not precisely add up to 100 because of rounding. "NA" = not available.

		Percent of Total Area						
Reach #	Total Area (x 10^4 m^2)	Bare Gravel Bars	Bankfull Channel	Other Water	Lower Floodplain	Upper Floodplain	Lowest Terrace	Total %
1	30.8	0.33	48.1	0.00	3.28	26.3	22.2	99.9
2	43.7	0.94	36.6	2.75	6.96	21.3	32.3	99.9
3	86.5	0.16	29.7	30.2	10.7	15.5	14.0	100.0
4	40.4	0.00	65.1	3.47	8.51	17.4	5.45	99.9
5	3.13	21.0	73.5	14.4	1.88	4.15	6.07	100.0
6*	18.0	8.97	45.2	2.22	2.56	15.2	34.8	99.9
7*	8.37	14.4	40.1	0.00	5.73	32.7	21.4	100.0
8*	106	9.75	30.2	4.62	3.38	50.5	11.5	100.2
9	5.32	0.49	44.0	0.00	0.00	15.3	40.6	99.9
10*	122	4.50	22.2	2.21	3.29	53.1	19.5	100.3
11	11.2	0.12	55.3	0.18	3.13	41.0	0.00	99.6
12	7.47	0.62	20.7	0.00	1.85	75.6	1.79	100.0
13*	134	4.64	17.8	5.45	3.62	58.4	14.9	100.1
14	127	1.86	15.9	3.31	3.48	28.6	48.7	100.0
15*	775	4.56	12.8	1.38	2.63	36.3	47.0	100.1
16	121	3.22	31.0	0.25	1.31	23.1	44.0	99.7
17*	NA	NA	NA	NA	NA	NA	NA	NA
18*	NA	NA	NA	NA	NA	NA	NA	NA
19	17.7	0.71	70.6	0.00	3.08	5.53	20.6	99.9
JLD to Moose	1660	4.11	21.6	3.55	3.47	36.0	35.2	99.9

*Multi-thread reaches.

Table 3-7: The magnitude, recurrence interval (RI), and inundation period (IP) of flows necessary to inundate three deposits in each segment of the Snake River. Inundation discharge was determined using HEC-RAS flow models and RIs and IPs were based on measured mean daily flow data from 1916 to 1958 and 1959 to 2005.

		Based on Measured Flows				Based on Estimated Unregulated Flows			
		1916-1958		1959-2005		1916-1958		1959-2005	
Segment	Inundation Discharge (m^3/s)	RI (years)	IP (% year (# days))	RI (years)	IP (% year (# days))	RI (years)	IP (% year (# days))	RI (years)	IP (% year (# days))
Lower Floodplain									
1	142	1.1	9.8 (36.0)	1.6	3.5 (12.9)	1.0	6.4 (23.4)	1.1	9.7 (35.4)
2	174	1.1	8.2 (29.9)	1.7	3.2 (11.5)	1.0	6.4 (23.4)	1.1	9.6 (35.2)
3	213	1.0	9.6 (35.0)	1.2	4.4 (15.9)	1.0	7.4 (27.1)	1.1	11.1 (40.6)
4	222	1.0	11.8 (43.1)	1.2	6.6 (24.2)	1.0	8.7 (31.8)	1.0	12.5 (45.8)
Upper Floodplain									
1	252	3.2	1.1 (3.9)	16.5	0.2 (0.7)	1.7	1.2 (4.5)	1.6	1.9 (7.0)
2	299	4.1	0.7 (2.7)	12.3	0.2 (0.7)	1.6	1.4 (5.2)	1.6	2.2 (8.1)
3	422	5.3	0.5 (1.8)	10.8	0.2 (0.8)	1.9	1.0 (3.7)	1.9	1.6 (5.8)
4	467	5.0	0.5 (1.9)	10.0	0.2 (0.8)	1.9	1.1 (4.0)	1.9	1.6 (6.0)
Lowest Terrace									
1	--*	--*	--*	--*	--*	--*	--*	--*	--*
2	431	37.0	0.0 (0.1)	121	0.0†	7.7	0.2 (0.7)	5.6	0.3 (1.1)
3	889	330	0.0†	340	0.0†	310	0.0†	240	0.0†
4	795	171	0.0†	171	0.0†	80.9	0.0 (0.1)	45.1	0.0 (0.1)

*Insufficient cross section data to estimate inundating flows.

†Measured or estimated unregulated flows never exceeded the magnitudes necessary for inundation in the period of record in these segments; thus we cannot calculate an inundation period.

Table 3-8: The number of years in which the peak flows in each segment of the Snake River equaled or exceeded the inundation discharge of each floodplain deposit from 1916 to 1958 (43 years) and from 1959 to 2005 (47 years). Based on mean daily flow data.

	Lower Floodplain			Upper Floodplain			
		# of years discharge was equaled or exceeded			# of years discharge was equaled or exceeded		
Segment	Inundation Discharge (m^3/s)	1916-1958	1959-2005	Inundation Discharge (m^3/s)	1916-1958	1959-2005	Years that inundation flows were equaled or exceeded between 1959 and 2005
1	142	41	32	252	14	5	1983, 1984, 1986, 1996, 1997
2	174	42	30	299	12	4	1983, 1986, 1996, 1997
3	213	42	37	422	11	5	1983, 1986, 1996, 1997, 1999
4	222	43	41	467	11	5	1974, 1983, 1986, 1996, 1997

Table 3-9: Floodplain area built in each time period.

Reach #	Ave. Reach Length (km)	Lower Floodplain (x 10^3 m^2)					Upper Floodplain (x 10^3 m^2)				
		Before 1945	1945-1969	1969-1990/1991	1990/1991-2002	Total Area	Before 1945	1945-1969	1969-1990/1991	1990/1991-2002	Total Area
1	1.99	7.6	0	0	0	7.6	81	0	0	0	81
2	1.66	15	2.2	0	0	17.2	88	0	0	1.8	89.8
3	2.39	50	1.8	0	2.6	54.4	130	0	0	0	130
4	2.59	11	0	0.16	0	11.16	70	0	0	0	70
5	0.302	0.40	0.17	0	0	0.57	1.3	0	0	0	1.3
6*	0.761	1.1	0.10	3.0	0.06	4.26	14	1.3	4.3	0	19.6
7*	0.214	0	0	0	0	0	0.77	1.9	0	0	2.67
8*	1.97	7.7	4.3	3.8	11	26.8	230	59	30	26	345
9	0.293	0	0	0	0	0	6.3	0	0	0	6.3
10*	2.59	2.7	0.58	3.2	3.2	9.68	150	35	9.3	7.4	201.7
11	0.826	0.18	0.08	0	0	0.26	14	0.19	0	0	14.19
12	0.213	0.10	0	0	0	0.10	7.1	0.17	0.34	0	7.61
13*	1.81	0.30	0.20	2.4	1.8	4.7	71	32	23	11	137
14	2.15	2.5	4.7	0	0.63	7.83	120	4.5	0	0.56	125.06
15*	5.94	14	50	11	6.6	81.6	860	220	160	120	1360
16	4.34	3.1	11	0.61	0.98	15.69	240	24	3.4	1.9	269.3
17*	NA	NA	NA	NA	NA	NA	NA	NA	NA	NA	NA
18*	NA	NA	NA	NA	NA	NA	NA	NA	NA	NA	NA
19	1.65	1.2	0.24	2.6	0	4.04	5.5	0.73	3.5	0	9.73
JLD to Moose	31.7	120	75	27	27	249	2100	380	230	170	2880

*Multi-thread reaches.

Table 3-10: Annual floodplain construction per km of river during each time period.

		Lower Floodplain (m^2/km-yr)			Upper Floodplain (m^2/km-yr)		
Reach #	Ave Length (km)	1945-1969	1969-1990/1991	1990/1991-2002	1945-1969	1969-1990/1991	1990/1991-2002
1	1.99	0	0	0	0	0	0
2	1.66	60 ± 1	0	0	0	0	90 ± 1
3	2.39	30	0	90 ± 1	0	0	0
4	2.59	0	0	0	0	0	0
5	0.302	20	0	0	0	0	0
6*	0.761	10	180 ± 2	10	50 ± 1	250 ± 3	0
7*	0.214	0	0	0	370 ± 4	0	0
8*	1.97	90 ± 1	90 ± 1	470 ± 5	1100 ± 10	760 ± 8	1000 ± 10
9	0.293	0	0	0	0	0	0
10*	2.59	10	60 ± 1	100 ± 1	560 ± 6	140 ± 1	220 ± 2
11	0.826	0	0	0	10	0	0
12	0.213	0	0	0	40	70 ± 1	0
13*	1.81	0	60 ± 1	80 ± 1	740 ± 7	580 ± 6	510 ± 5
14	2.15	90 ± 1	0	20	90 ± 1	0	10
15*	5.94	350 ± 4	80 ± 1	90 ± 1	1700 ± 20	1200 ± 10	1500 ± 20
16	4.34	110 ± 1	10	160 ± 2	190 ± 2	30	40
17*	--	NA	NA	NA	NA	NA	NA
18*	--	NA	NA	NA	NA	NA	NA
19	1.65	10	70 ± 1	0	30	60 ± 1	0
JLD to Moose	31.7	100 ± 1	40	70 ± 1	500 ± 4	330 ± 2	450 ± 3

*Multi-thread reaches.

Table 3-11: Ratio of upper floodplain to lower floodplain in each time period.

Reach #	1945-1969	1969-1990/1991	1990/1991-2002
1	--	--	--
2	0.00	--	--
3	0.00	--	0.00
4	--	--	--
5	0.00	--	--
6*	5.00	1.39	0.00
7*	--	--	--
8*	12.2	8.44	2.13
9	--	--	--
10*	56.0	2.33	2.20
11	--	--	--
12	--	--	--
13*	--	9.67	6.38
14	1.00	--	0.50
15*	4.86	15.0	16.7
16	1.73	3.00	0.25
17*	NA	NA	NA
18*	NA	NA	NA
19	3.00	0.86	--
JLD to Moose	5.00	8.25	6.43

*Multi-thread reaches.

FIGURES

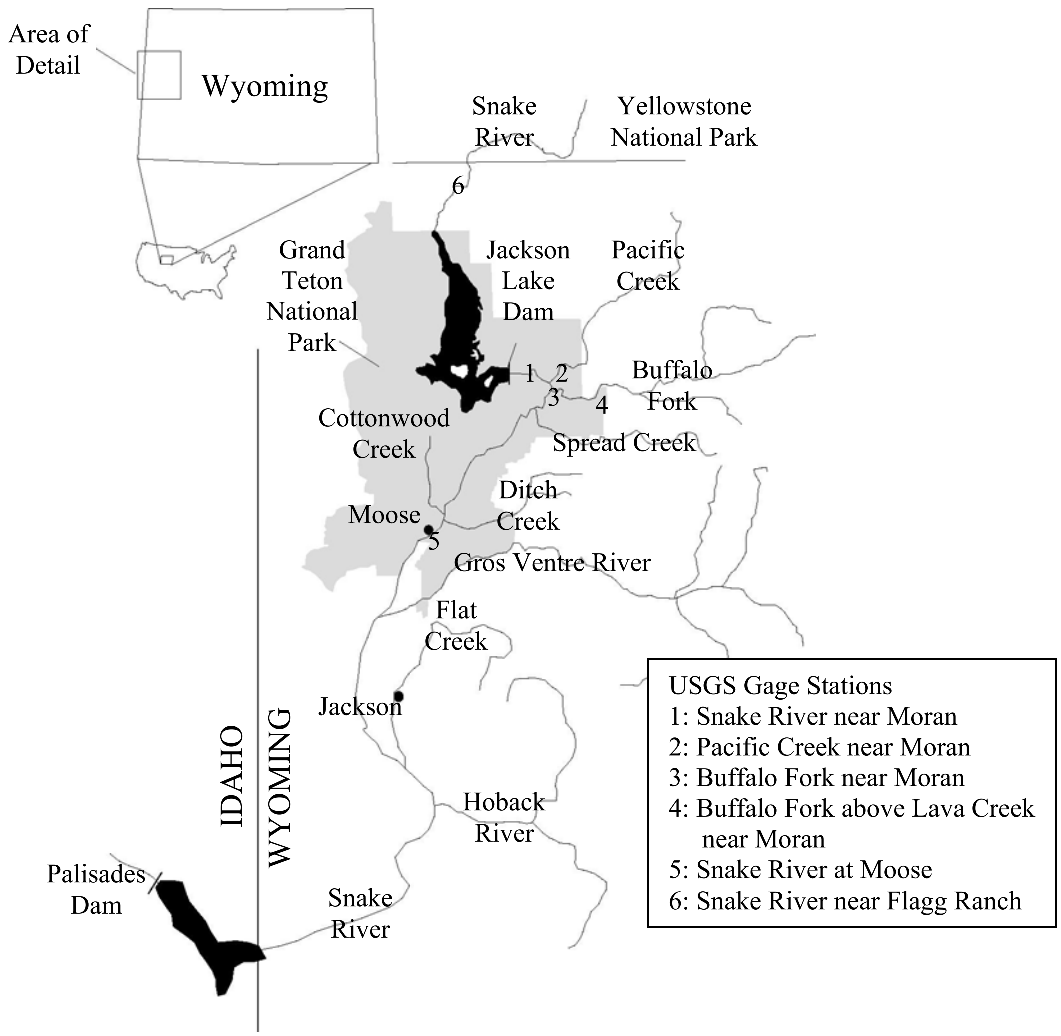

Figure 3-1: The Snake River as it flows from Yellowstone National Park to Palisades Reservoir. The study reach is from Jackson Lake Dam to Moose. Modified from Figure 2-1, Chapter 2 in Nelson (2007).

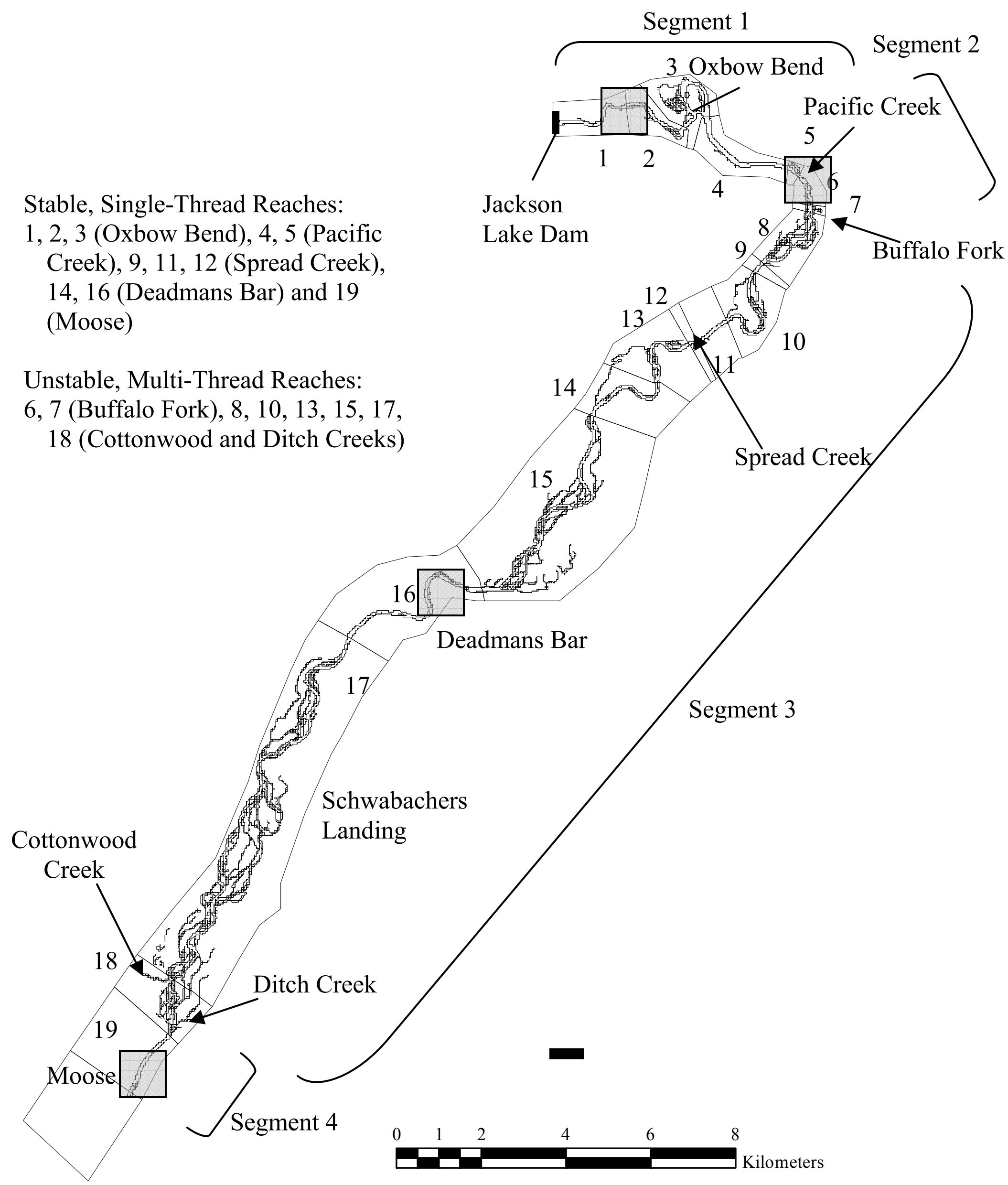

Figure 3-2: Map of the Snake River from JLD to Moose. The four segments are the portions of the river analyzed for hydrologic change; numbers refer to reaches, outlined with thin black lines, analyzed for channel change (Reaches 1-19) and floodplain formation (Reaches 1-16, 19); the shaded boxes are the approximate locations of cross-sectional surveys conducted for flow modeling; the river channel is that of 2002. Modified from Figure 2-3, Chapter 2 in Nelson (2007).

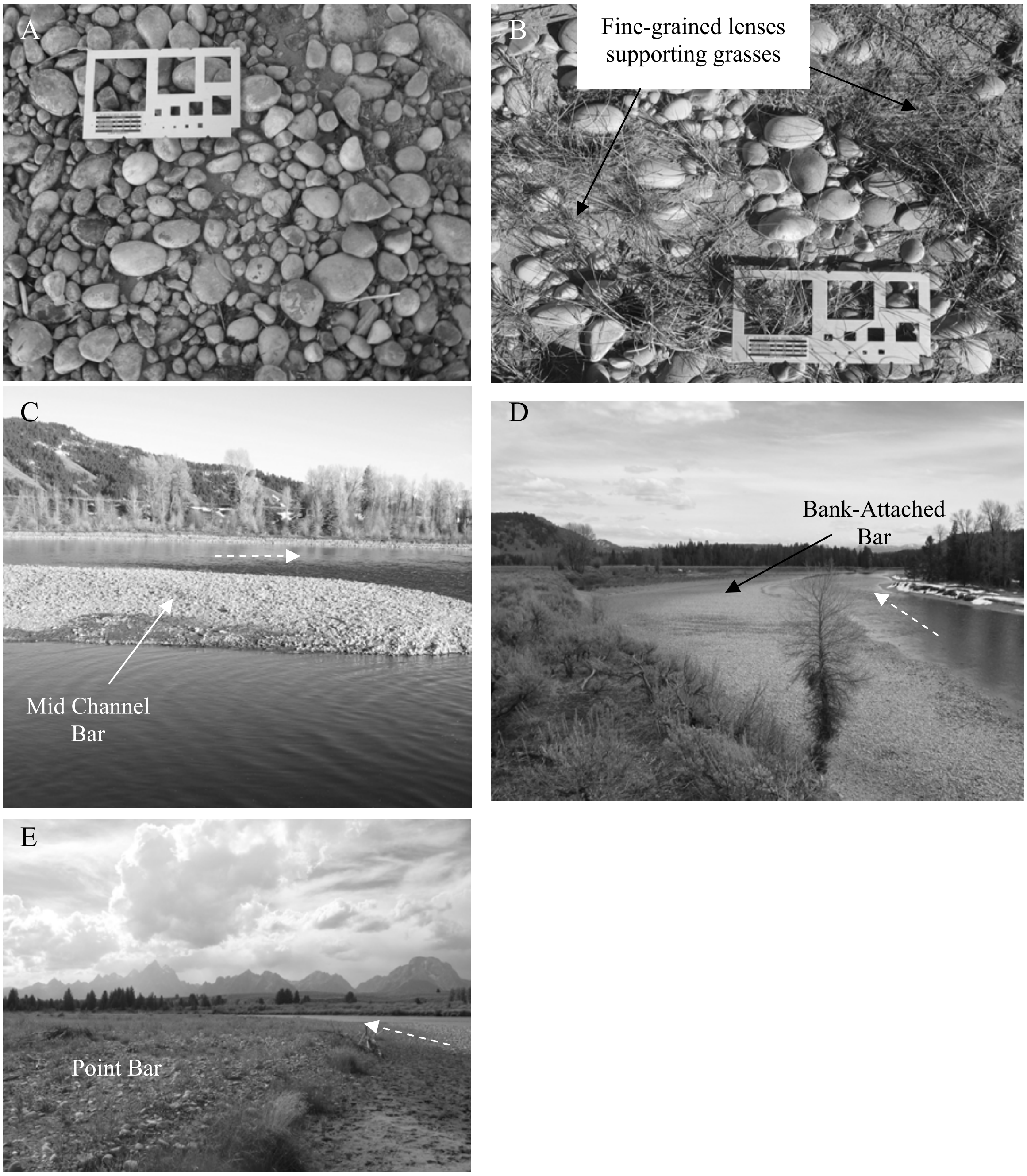

Figure 3-3: Bare gravel bar deposits are (A) clast supported with a fine-grained matrix and occasionally contain (B) surficial fine-grained lenses that support young vegetation. There are three types of bare gravel bars: (C) mid channel bars with active channels separating the bar from both banks, (D) bank-attached bars on the inside of bends, and (E) point bars typically opposite actively eroding cut banks.

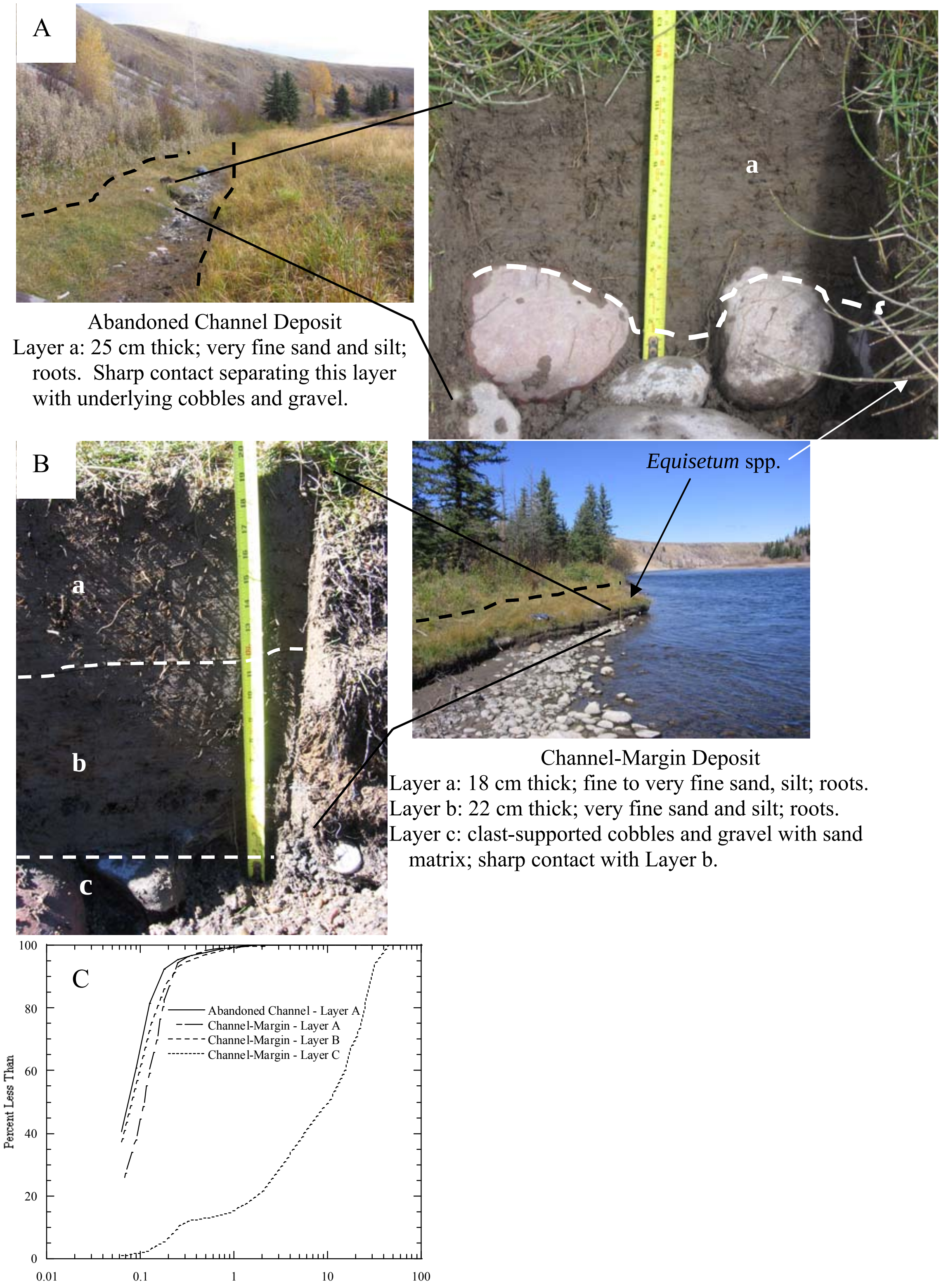

Figure 3-4: (A) Abandoned channel and (B) channel-margin facies of the lower floodplain with (C) the grain size distribution of the stratigraphic layers.

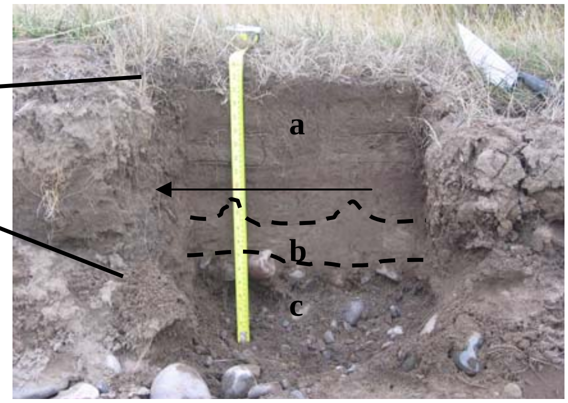

Abandoned Bar Deposit

Layer a: 25 cm thick; silt and fine sand; contains lenses of substrate similar to Layer b.

Layer b: 12 cm thick with isolated lenses in Layer a; fine sand.

Layer c: 122 cm above water surface; coarse sand, fine gravel, cobbles; sharp contact with layer b.

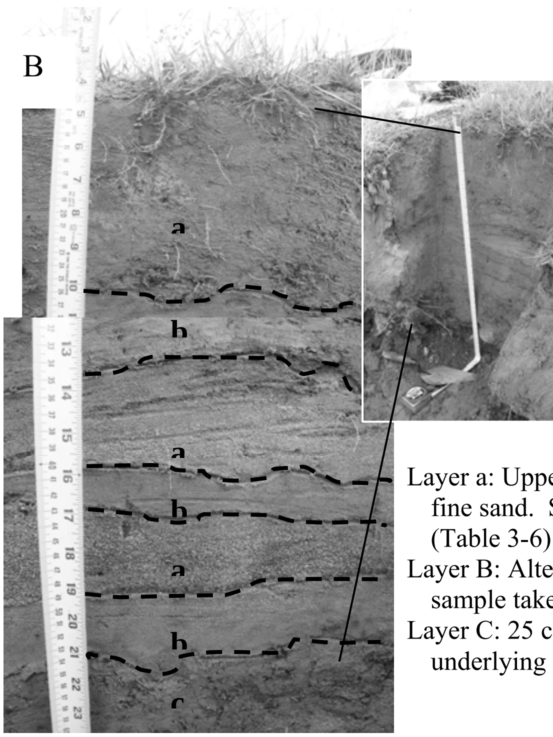

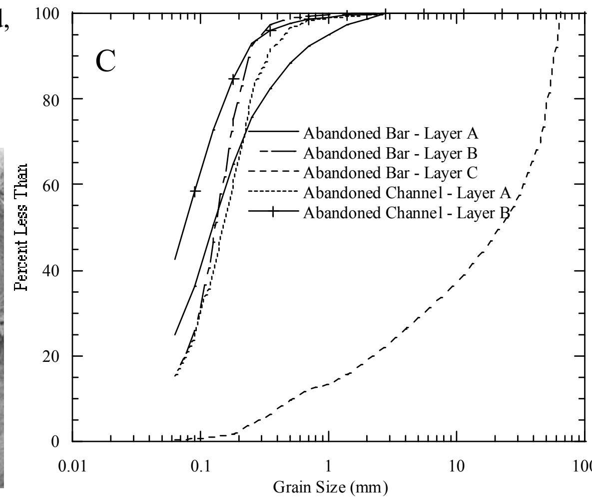

Abandoned Channel Deposit

Layer a: Upper layer is 20 cm thick, others are 5-10 cm thick; fine sand. Sediment sample taken from uppermost Layer a (Table 3-6).

Layer B: Alternates with Layer a; 5-10 cm thick; silt. Sediment sample taken from uppermost Layer b (Table 3-6).

Layer C: 25 cm thick; very fine silt. Sharp contact with underlying cobbles, coarse sand, and gravel.

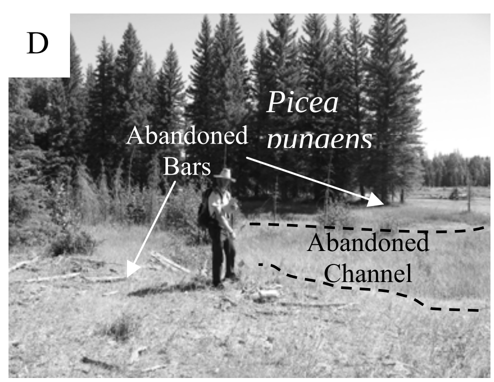

Figure 3-5: Stratigraphy of (A) abandoned bar and (B) abandoned channel facies that make up the upper floodplain with (C) their respective grain size distribution. (D) Upper floodplain deposit showing facies and typical vegetation.

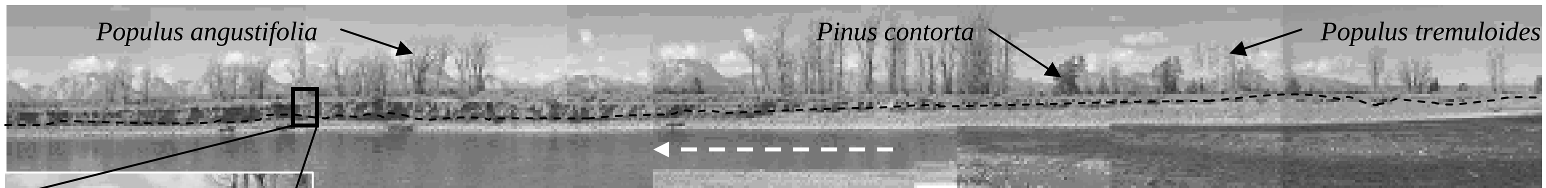

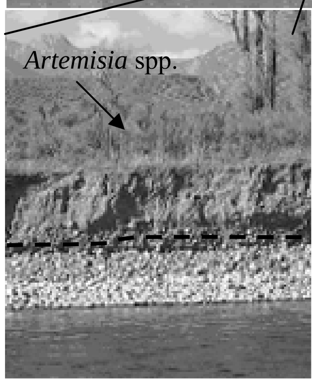

Figure 3-6: Lowest terrace exposed by a cutbank; view is to the west. The dotted black lines in each image separate the finer grained upper layers from the gravel and cobble layer below. Portions of the terrace with greater depths of fine-grained sediments are likely abandoned channels (middle/left side of upper image), whereas portions with thin layers of fine-grained sediments are likely abandoned bars (right side of upper image). The top of the terrace varies from approximately 2.0 to 2.5 m above the water surface and the length of the upper image is approximately 380 m. Typical vegetation species found on the lowest terrace are indicated. White arrow indicates flow direction.

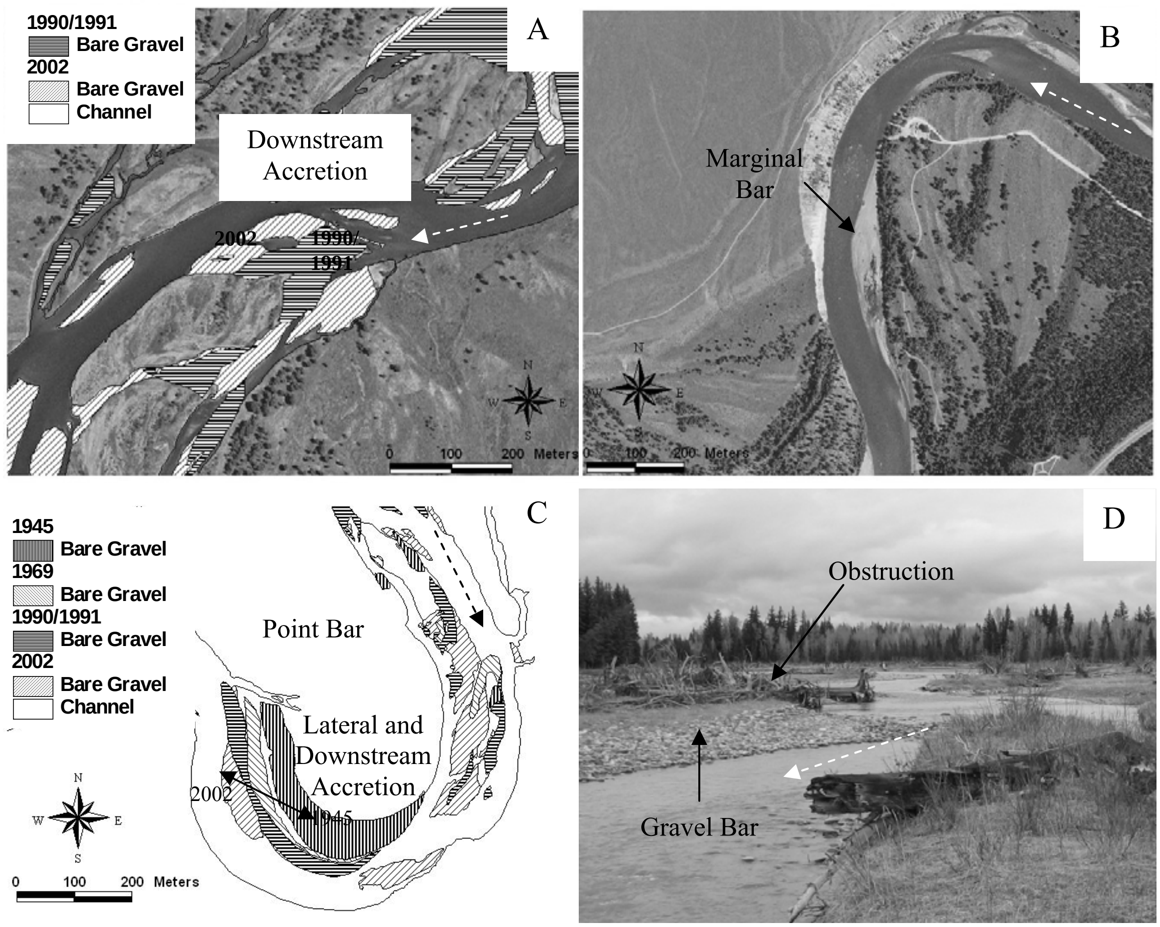

Figure 3-7: Three facies make up the bare gravel bar deposits: (A) mid-channel bars, (B) bank-attached bars, and (C) point bars. These deposits form by lateral and downstream accretion and develop in the low-energy portions of the channel (B) downstream from channel bends, (C) on the inside of channel bends, and (D) downstream from obstructions such as logjams. Dashed arrows indicate flow direction.

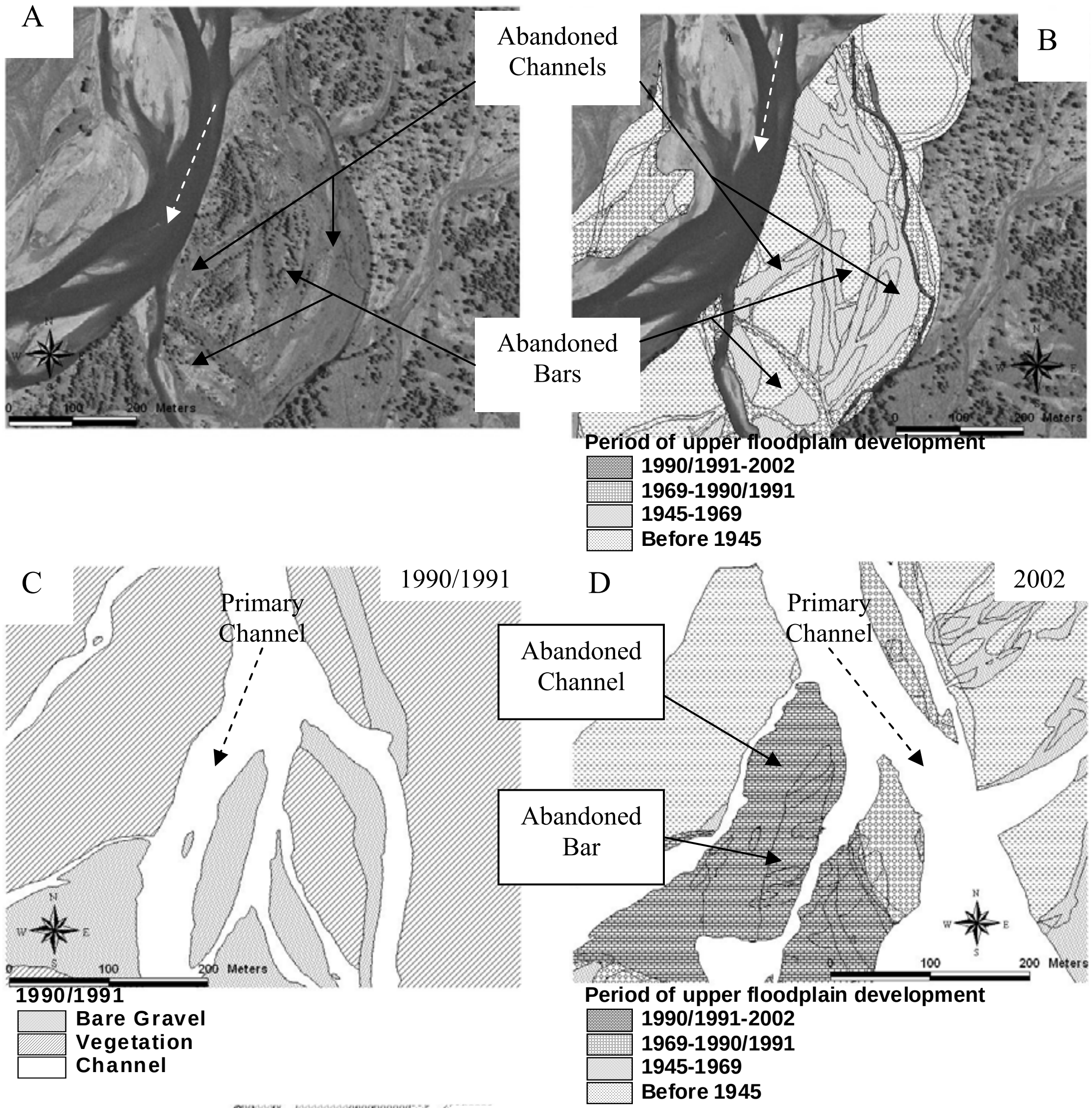

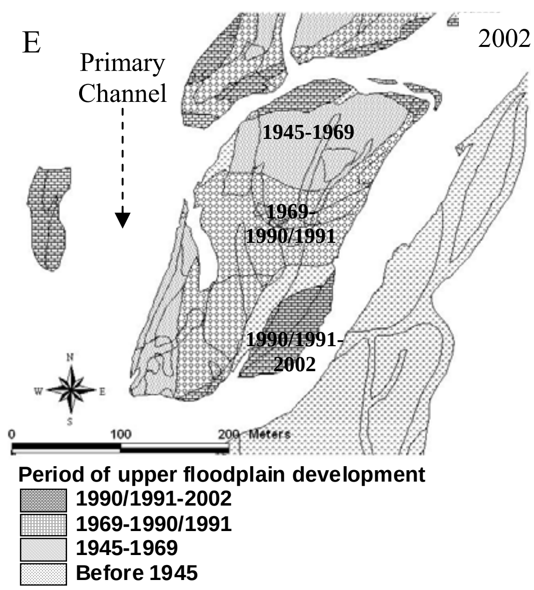

Figure 3-8: The upper floodplain is composed of (A, B) abandoned channels and bars (2002 aerial photographs) which form by (C, D) channel migration or channel avulsion as well as by (E) vertical and downstream accretion. Dashed arrows indicate flow direction.

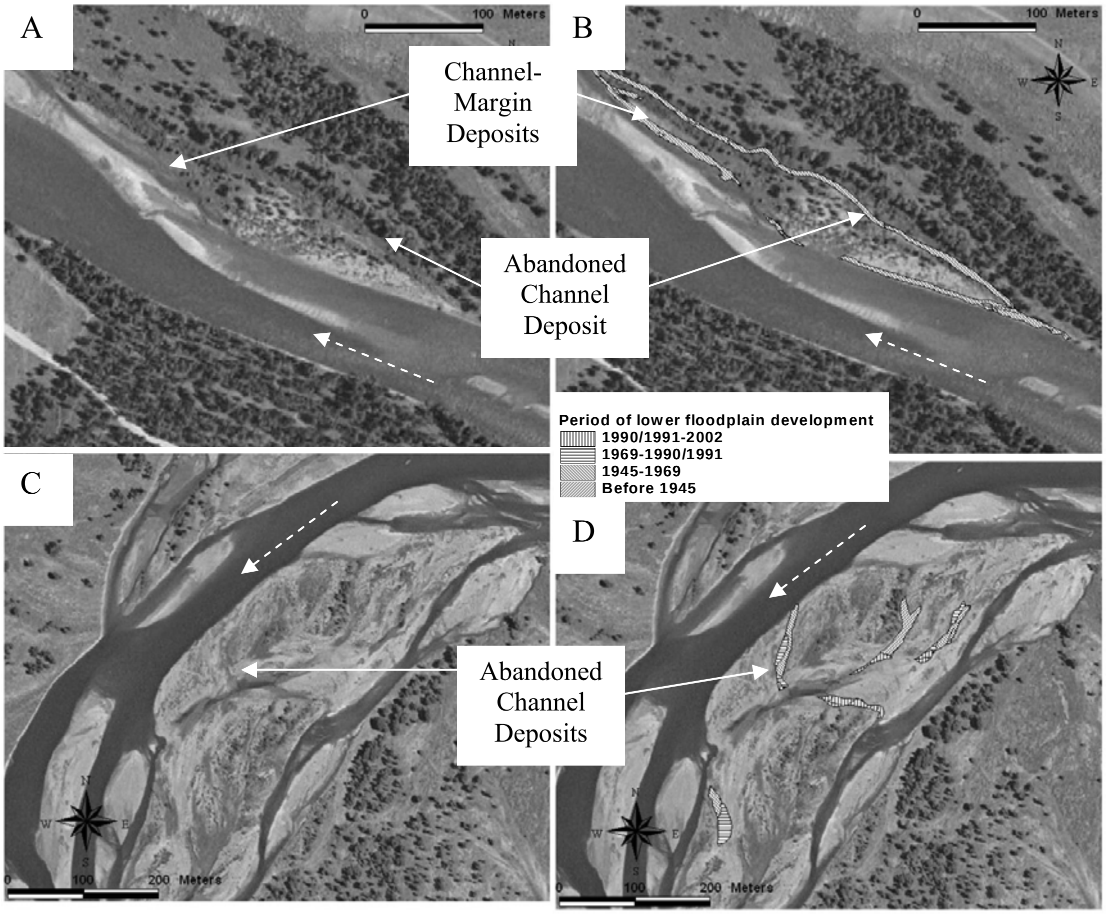

Figure 3-9: The lower floodplain is made up of (A, B) channel-margin and abandoned channel facies, which form (A, B) on the inside of abandoned bank-attached bars or (C, D) within abandoned mid-channel bars. Dashed arrows indicate flow direction.

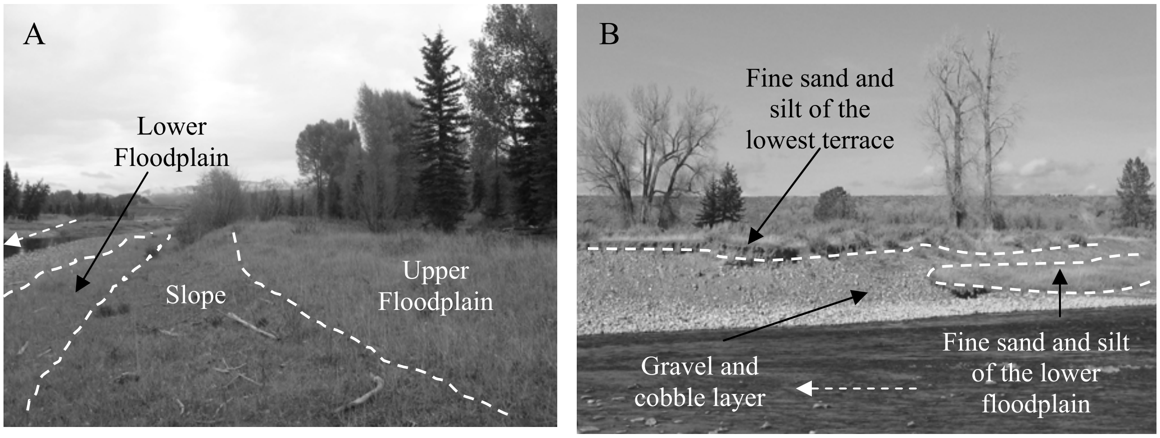

Figure 3-10: The channel margin facies of the lower floodplain adjacent to (A) the upper floodplain and (B) the lowest terrace, showing no distinct contact between the basal gravel layers of the lowest terrace and lower floodplain. Dashed arrows indicate flow direction.

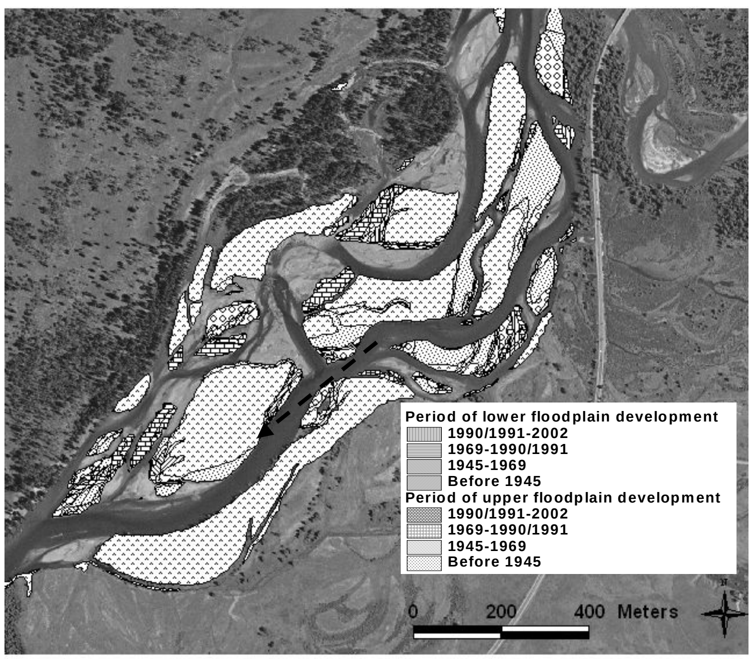

Figure 3-11: Period of lower and upper floodplain development downstream from Buffalo Fork. Dashed arrow indicates flow direction.

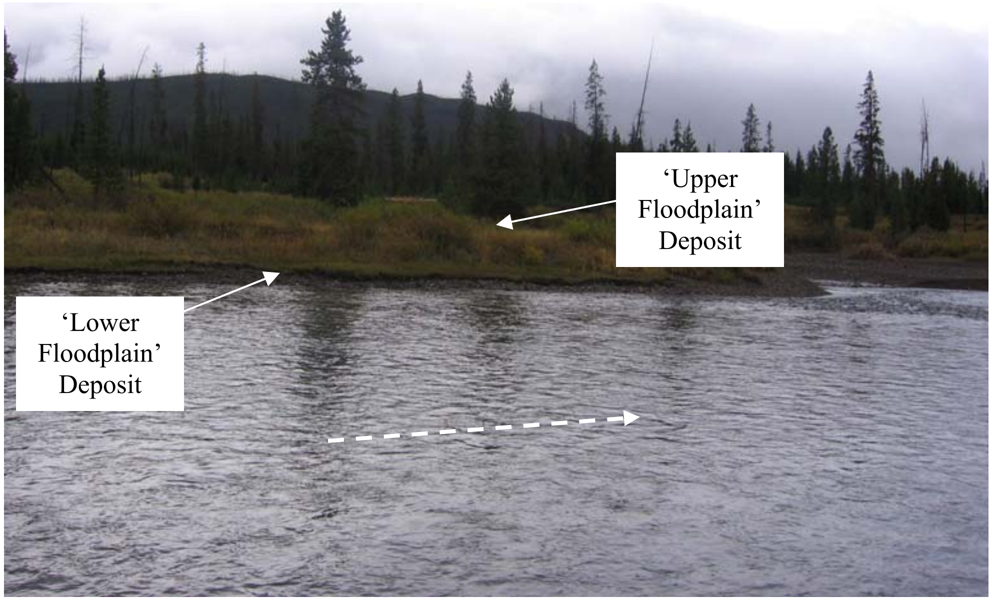

Figure 3-12: Deposits adjacent to the Snake River near Flagg Ranch, upstream from Jackson Lake, that are similar to the lower and upper floodplains of the Snake River downstream from JLD. Dashed arrow indicates flow direction.

CHAPTER 4

CONCLUSIONS

Dam regulation has impacted the flow regime of the Snake River, but these impacts are mitigated downstream from tributaries. Prior to 1958, the tributaries were the primary source of the winter flows in the main stem as releases were nearly non-existent. Peak flows decreased 32% after 1958 in relation to those prior, but because the timing of the peak flows were realigned with tributary flooding, peak flows decreased only 19% downstream from Buffalo Fork.

The influence of tributaries likely resulted in the increased bed mobility with distance downstream from JLD during the 2005 floods. There was little movement of tracers immediately downstream from JLD, suggesting that the segment of the bed between JLD and Pacific Creek is well armored and requires greater magnitude floods than those of 2005 to be fully mobilized. Although the median bed grain size increases downstream, tracer clusters downstream from Pacific Creek and Buffalo Fork were partially and fully mobilized in 2005, suggesting that the influence of tributaries more than compensates for the increase in bed grain size. The change in flow regime downstream from tributaries and the resultant impact on bed mobility emphasizes the importance of analyzing all available flow data within the study area.

There was no long-term progressive channel change resulting from the changes in flow regime. Low magnitude peak flows between 1945 and 1969 resulted in widespread deposition and channel narrowing as well as an increase in braid index in reaches both close to, and far from, tributaries. This trend reversed between 1969 and 2002 with widespread erosion and channel widening, likely a result of the large floods that occurred in the 1980s and 1990s. We found no evidence of progressive decreased stability near tributaries and increased stability far from tributaries as was previously suggested (Marston et al., 2005). There were periods of increased and decreased stability in reaches throughout the study area, regardless of their proximity to tributaries.

We identified two distinct floodplains and a low terrace at different elevations above the water surface along the Snake River. The lower floodplain is a fine-grained deposit approximately 0.2 to 0.7 m above the elevation of the 2005 late-summer flows. This floodplain is made up of abandoned channel and channel-margin facies. Both facies contain fine-grained layers overlying gravel and cobbles and primarily support grasses and *Equisetum* spp. The lower floodplain is inundated by the 1.2-yr recurrence flood under the current flow regime downstream from Buffalo Fork and has been forming during both regulated flow regimes, before and after 1958.

The upper floodplain is approximately 0.7 to 2.0 m above the elevation of the 2005 late-summer flows and is composed of abandoned channels and alluvial bars. The abandoned channels consist of up to 1.5 m of fine-grained sediments overlying gravel and cobbles. This facies is slightly lower in elevation than the surrounding abandoned bars and often supports grasses, small shrubs, and saplings. There are generally greater depths of fine-grained sediments overlying the gravel and cobble layer in the abandoned channels than the abandoned bars. The abandoned bars primarily supported saplings and mature trees. The upper floodplain was built in every time period analyzed and is inundated by the 10.8-yr recurrence flood under the current flow regime downstream from Buffalo Fork. This represents an increase from a recurrence interval of 5.3 years prior to 1958 and 1.9 years based on the estimated unregulated flows.

The lowest terrace is composed of abandoned bars and channels and was likely not inundated during the period of record. No portions of this deposit have formed since 1945. The lowest terrace was the only deposit described that supported large *Artemisia* spp. communities. *Picea pungens*, *Populus angustifolia*, *Populus tremuloides*, and *Pinus contorta* were also located on the lowest terrace.

The most significant finding of this study is that two distinct floodplains at different elevations are currently being formed and have been forming since before the flow regime change in 1958. The greatest impact of regulation on channel and floodplain form along the Snake River is the increase in recurrence interval for floods inundating the upper floodplain. The large floods in the last few decades were likely the primary catalysts for maintaining the channel width and high channel activity throughout the study area. Without these large floods, the deposition and channel narrowing that began after the flow regime change in 1958 may have continued progressively. Rare, high-magnitude floods may maintain the form of the Snake River alluvial valley, but the consequences of the more infrequent inundation of the upper floodplain may be more severe for riparian vegetation and habitat. Portions of the upper floodplain may become further abandoned and later successional plant species may dominate.

REFERENCES

Marston, R.A., Mills, J.D., Wrazien, D.R., Bassett, B., and Splinter, D.K., 2005. Effects of Jackson Lake Dam on the Snake River and its floodplain, Grand Teton National Park, Wyoming, USA. Geomorphology 71, 79-98.

APPENDIX

REPEAT SURVEYS OF TOPOGRAPHY WHERE TRACERS WERE LOCATED CAPTURING THE DEPOSITION AND EROSION THAT OCCURRED THROUGH THE PEAK FLOWS IN MID-JUNE, 2005

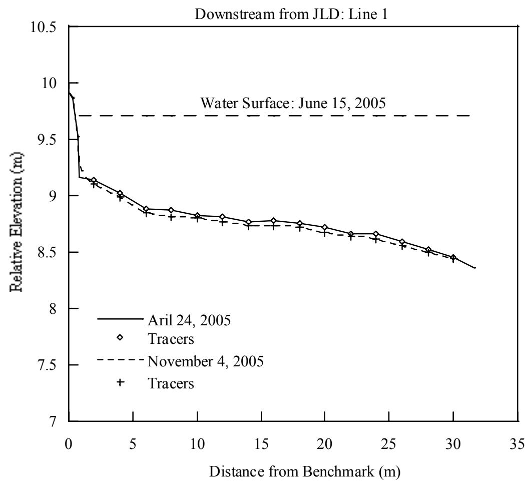
Downstream from JLD: Line 1
Water Surface: June 15, 2005
Relative Elevation (m)
Distance from Benchmark (m)
Aril 24, 2005
Tracers
November 4, 2005
Tracers

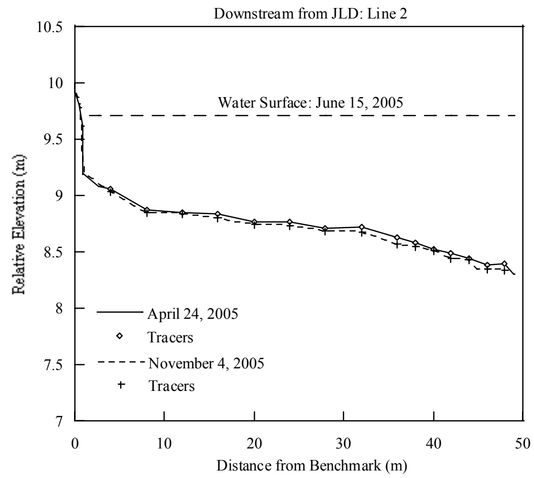
Downstream from JLD: Line 2
Water Surface: June 15, 2005
Relative Elevation (m)
Distance from Benchmark (m)
April 24, 2005
Tracers
November 4, 2005
Tracers

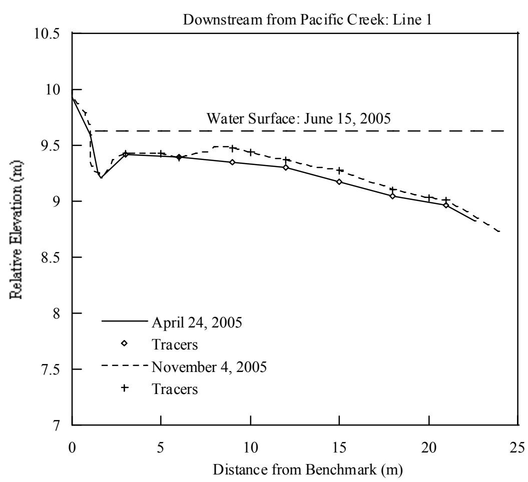
Downstream from Pacific Creek: Line 1
Water Surface: June 15, 2005
Relative Elevation (m)
Distance from Benchmark (m)
April 24, 2005
Tracers
November 4, 2005
Tracers

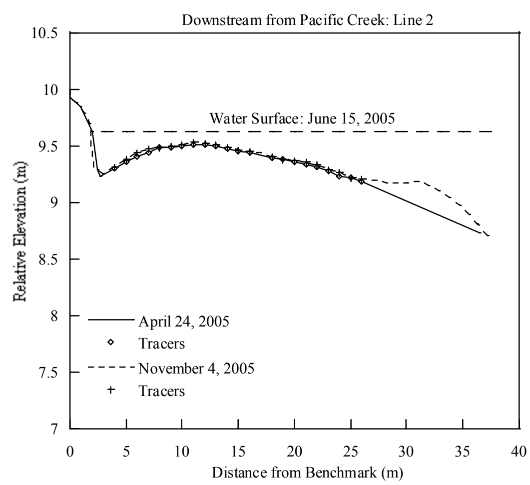
Downstream from Pacific Creek: Line 2
Water Surface: June 15, 2005
Relative Elevation (m)
Distance from Benchmark (m)
April 24, 2005
Tracers
November 4, 2005
Tracers

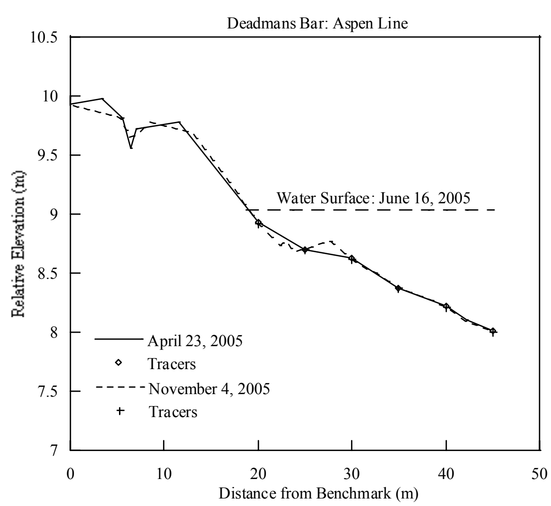
Deadmans Bar: Aspen Line
Water Surface: June 16, 2005
Relative Elevation (m)
Distance from Benchmark (m)
April 23, 2005
Tracers
November 4, 2005
Tracers

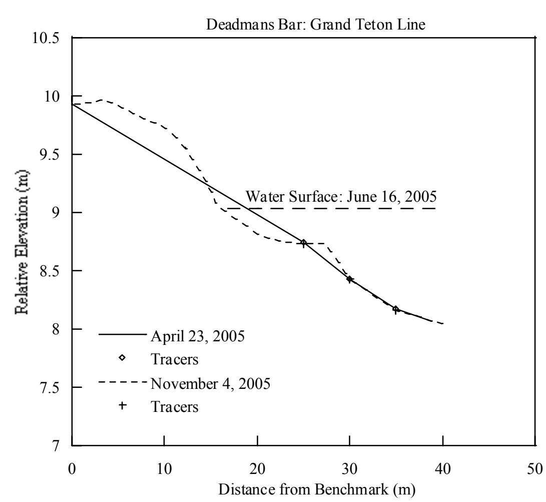
Deadmans Bar: Grand Teton Line
Water Surface: June 16, 2005
Relative Elevation (m)
Distance from Benchmark (m)
April 23, 2005
Tracers
November 4, 2005
Tracers

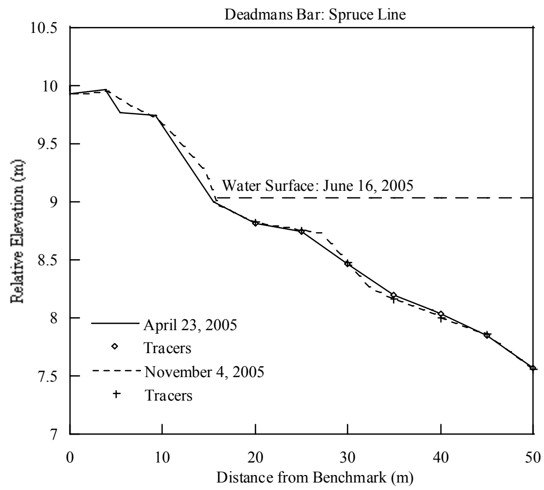
Deadmans Bar: Spruce Line
Relative Elevation (m)
Distance from Benchmark (m)
Water Surface: June 16, 2005
April 23, 2005
Tracers
November 4, 2005
Tracers

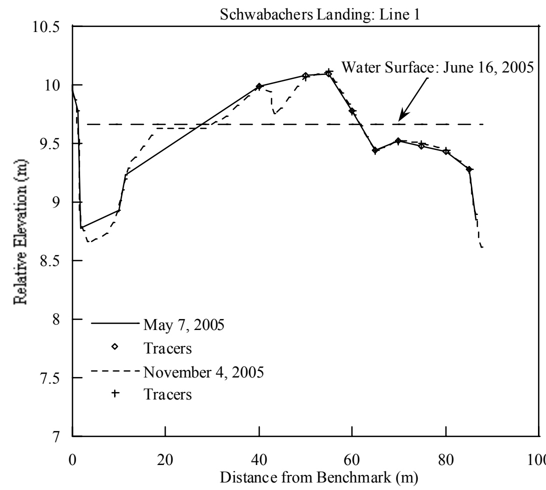
Schwabachers Landing: Line 1
Relative Elevation (m)
Distance from Benchmark (m)
Water Surface: June 16, 2005
May 7, 2005
Tracers
November 4, 2005
Tracers

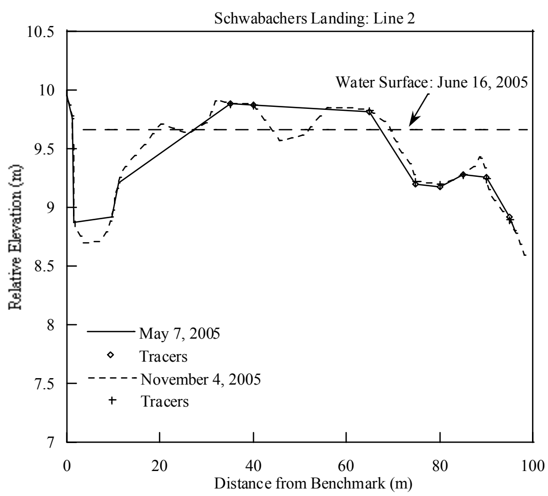
Schwabachers Landing: Line 2
Relative Elevation (m)
Distance from Benchmark (m)
Water Surface: June 16, 2005
May 7, 2005
Tracers
November 4, 2005
Tracers

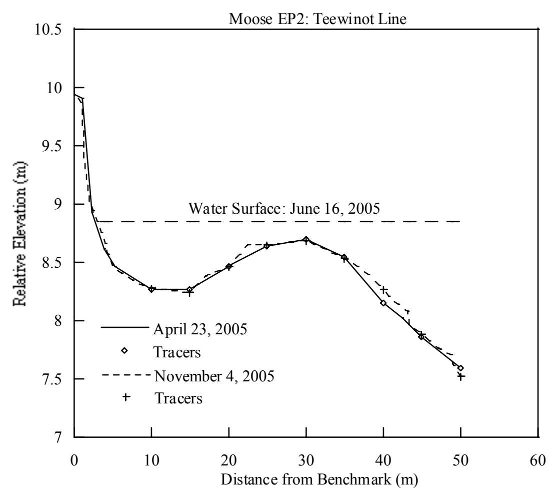
Moose EP2: Teewinot Line
Relative Elevation (m)
Distance from Benchmark (m)
Water Surface: June 16, 2005
April 23, 2005
Tracers
November 4, 2005
Tracers

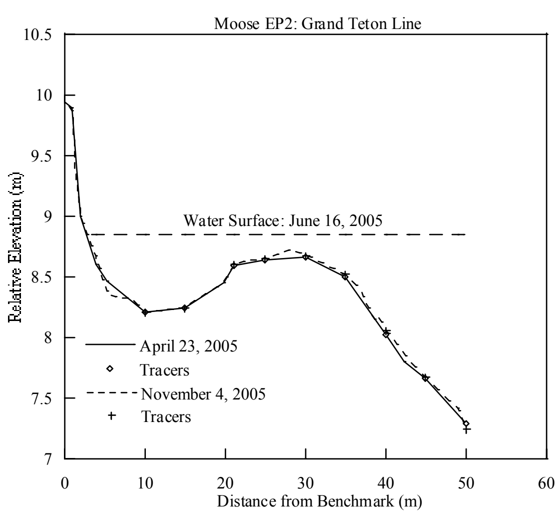
Moose EP2: Grand Teton Line
Relative Elevation (m)
Distance from Benchmark (m)
Water Surface: June 16, 2005
April 23, 2005
Tracers
November 4, 2005
Tracers

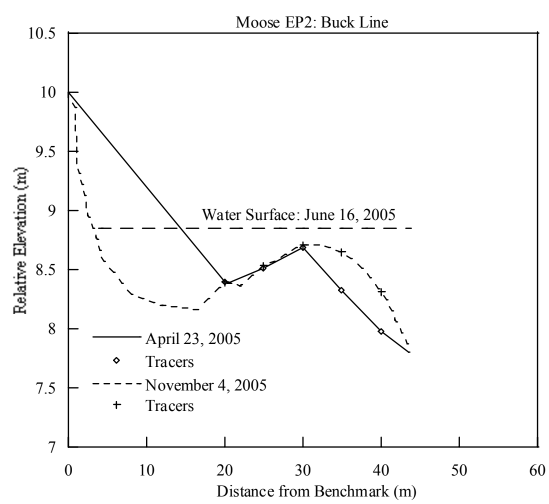
Moose EP2: Buck Line
Relative Elevation (m)
Distance from Benchmark (m)
Water Surface: June 16, 2005
April 23, 2005
Tracers
November 4, 2005
Tracers

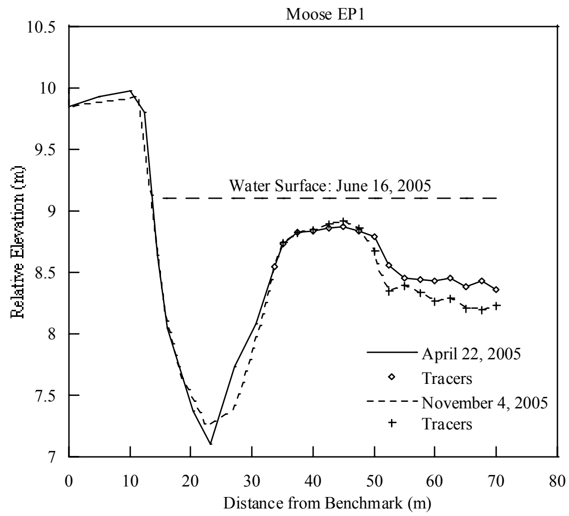
Moose EP1
10.5
10
9.5
9
8.5
8
7.5
7
Relative Elevation (m)
Water Surface: June 16, 2005
April 22, 2005
Tracers
November 4, 2005
Tracers
0
10
20
30
40
50
60
70
80
Distance from Benchmark (m)